Multiplexed simultaneous representations of cognitive and motor features, in the mouse medial prefrontal cortex, during a memory guided behavior

João Afonso

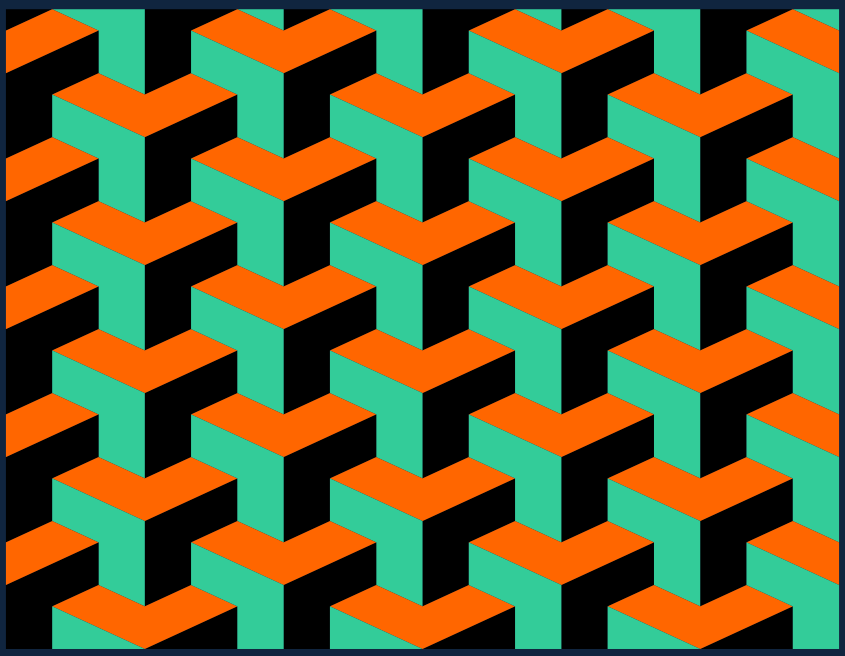

Dissertation presented to obtain the Ph.D degree in Biology | Neuroscience

Instituto de Tecnologia Química e Biológica António Xavier | Universidade Nova de Lisboa

Oeiras,
February, 2019

UNIVERSIDADE NOVA DE LISBOA

Multiplexed simultaneous representations of cognitive and motor features, in the mouse medial prefrontal cortex, during a memory guided behavior

João Afonso

Dissertation presented to obtain the Ph.D degree in Biology | Neuroscience

Instituto de Tecnologia Química e Biológica António Xavier | Universidade Nova de Lisboa

Research work coordinated by: Champalimaud Foundation

Oeiras, February, 2019

UNIVERSIDADE NOVA DE LISBOA

I would like to thank:

My parents and family,
for the unconditional support.

Rita,
for the happiness, patience and love.

Alfonso,
for the trust, idealism and guidance.

The Champalimaud Research community,
for the nurturing and stimulating environment.

Contents

List of Figures

List of Acronyms

AP anterior-posterior. 41, 45, 46, 89, 90, 97–99

AUC area under the curve. 48, 59, 60, 62, 156, 157, 162

dlPFC dorsolateral prefrontal cortex. 2, 4, 5, 7, 14

dPCA demixed principal components analysis. iv, ix, x, xii, 83, 87, 88, 93–96, 106–111, 113, 115, 116, 120, 122, 168, 178–182, 185

DV dorsal-ventral. 40, 41, 90, 98

FR firing rate. iv, 91–93, 102, 103, 105, 112, 113, 118, 138–140, 144, 146, 149, 151–153, 177

IL infralimbic. 6, 87

IR infrared. 40, 41

ITI intra trial interval. 39, 41, 49, 105, 119–121, 181

ML medial-lateral. 45, 98

MO medial orbital. 6, 87

mPFC medial prefrontal cortex. ix, x, 7, 71, 83, 87, 97, 98, 106, 108, 111, 118, 121, 123, 133, 135–137, 143, 148, 151–153, 155, 156, 163–169, 176–179, 182–187

ODR oculomotor delayed response. iii, 10, 11

PBS phosphate-buffered saline solution. 89

PCA principal components analysis. iv, 95, 96, 110, 113–115

PETH Peri-event time histogram. 93, 103–105

PFC prefrontal cortex. iii, ix, 2–7, 9–13, 15–17, 83–85, 120, 121, 133, 134, 177, 182, 184–186

PFI past future index. 139, 151

PRL prelimbic. 6, 87, 97, 98

ROC receiver operating characteristic. 48, 59, 141

SAI speed acceleration index. 140

SD standard deviation. 51, 54, 59, 114, 145, 147, 148

SEM standard error of the mean. 50, 51, 56, 64–69, 102, 147

TSH trial space histogram. 87, 92, 101, 109, 118

WM working memory. ix, x, 4, 8, 9, 11–13, 33, 35, 36, 52, 57, 64, 65, 71, 72, 74, 75, 83–85, 87, 98, 118, 121, 133, 135, 136, 158, 168, 176–179, 181, 185–187

Summary

To develop complex models of the environment, coordinate extended sequences of actions and plane ahead organisms must break free from rigid stimulus response associations and be able to link events and behaviors that are separated in time. Essential to these is the ability of the brain to maintain sustained representations of environmental absent information: a process generally designated as working memory (WM).

Seating at the apex of the cortical hierarchy the prefrontal cortex (PFC) as been strongly implicated, by both lesions and physiology studies, in WM dependent behaviors. Given its integrative nature activity in the area it's a combination of preprocessed sensory and motor inputs with time varying cognitive internal mechanisms, making a complete understanding of its function only possible in the context of a moment to moment comparison with behavior.

To investigate how the joint activity of neurons, in prefrontal regions, encodes task relevant information, during a WM dependent behavior, we developed a head-fixed delayed response task on a treadmill for mice. Our task allowed us to minutely monitor the animals' behavior while acutely recording the simultaneous activity of dozens of cells in the mPFC of the mice. Such features enabled us to have a good understanding of how the animals were solving the task, confirming its WM, and to relate representations encoded in the joint neural activity with the mice's behavior in each trial.

We found that it was possible to demix from the joint activity of the neu-

rons, using a dimensionality reduction technique, demixed principal components analysis (dPCA), retrospective and prospective WM representations of both cue and decision. Also demixable was a trial length stable signal seemingly related to the animals' engagement in the task. dPCA further revealed that the mice's movement strategies on the treadmill had a strong influence in the recorded activity.

Taking advantage of our simultaneously recorded neurons we also discovered that in each trial the mouse mPFC encodes both WM sustained information, during the cue free memory period, and a faithful representation of the mice speed strategy on the treadmill.

Together these results show that the joint activity of neurons in the mPFC of the mice encodes, in a multiplexed way, multimodal representations of informative sensory features, future goals or decisions, speed strategies and the animals' internal state - engagement. All the aforementioned variables are relevant when considering a putative function of the area in organizing context adapted, WM dependent, goal directed behavior.

Resumo

Para conseguirem formar modelos complexos do ambiente, coordenar sequências de acções que se desenrolam no tempo e fazer planos, os organismos não podem depender apenas de associações rígidas entre estímulos e repostas, tendo que ser capazes de ligar eventos e comportamentos que acontecem separados no tempo. Essencial para tal é a possibilidade do cérebro manter e suster representações de informação que já não se encontra presente no exterior, um processo genericamente denominado por memória de trabalho.

Posicionado no cume da hierarquia cortical o córtex pré-frontal tem sido implicado, por estudos baseados em lesões e fisiologia, em comportamentos dependentes da memória de trabalho. Dado a sua natureza integradora a actividade nesta área é uma combinação de estímulos sensoriais e motores com processos cognitivos que variam no tempo, tornando um entendimento completo da sua função apenas possível no contexto de uma comparação, momento a momento, com o comportamento.

De modo a investigar como a actividade conjunta dos neurónios, nas regiões pré-frontais, codifica informação relevante, durante um comportamento dependente da memória de trabalho, desenvolvemos uma tarefa de resposta tardia, numa passadeira rolante, para ratinhos com cabeça imobilizada por um implante. A tarefa permitiu-nos monitorizar com precisão o comportamento dos animais enquanto gravávamos a actividade simultânea de dezenas de células no seu córtex pré-frontal medial. Estas características permitiram-nos perceber bem como é que os animais resolviam a tarefa, con-

firmando a sua dependência na manutenção de uma memória de trabalho, e relacionar as representações codificadas pela totalidade da actividade neuronal com o comportamento dos ratinhos em cada ensaio.

Usando uma técnica de redução dimensional, dPCA, descobrimos que era possível separar da actividade conjunta dos neurónios representações de memória de trabalho, retrospectivas e prospectivas, das pistas e decisões implicadas na tarefa. Também separável foi um sinal estável, presente durante todo o ensaio, aparentemente relacionado com o envolvimento dos animais na tarefa. Para além destes o dPCA também revelou que a estratégia de movimento dos ratinhos na passadeira tinha uma grande influência na actividade que gravámos.

Tirando partido das nossas gravações simultâneas da actividade neuronal também percebemos que, em cada ensaio, o córtex pré-frontal medial do ratinho codifica informação em memória de trabalho, durante um período de memória livre de pistas, juntamente com uma representação fiel da estratégia de velocidade dos animais na passadeira.

Juntos estes resultados demonstram que a actividade conjunta dos neurónios no córtex pré-frontal dos ratinhos codifica, de uma maneira multiplexada, representações multi-modais de variáveis sensoriais informativas, objectivos futuros ou decisões, estratégias de velocidade e estados internos dos animais. Todas estas variáveis são relevantes para uma possível função da área em organizar comportamento deliberado, e adaptado ao contexto, dependente de memória de trabalho.

Chapter 1

General Introduction

1.1 The Prefrontal Cortex

Measured by our success in adapting, prospering and becoming dominant in almost all environments there seems to be something strikingly different between humans and the other species. We are not the most adapted of animals, when considering the relation with a specific habitat, but we seem to be the more flexible in creating new maps between our possible repertoire of behaviors and the specific challenges imposed by different or evolving contexts. When looking into the brain in search for what endows us with this particular ability the spotlight has been historically centered on the PFC. A set of features seems to point to the distinctive character of the area: the PFC attained maximum relative growth in the human brain (29% of the total cortical surface against 17% in the chimpanzee and 3.5% in the cat, for instance) also, in the timeline of brain evolution, it was one of the last cortical regions to develop [37], a pattern mimicked by ontogeny, with it maturing late, in humans [36] and monkeys [29], and not attaining full maturity until adolescence [70].

The PFC is located at the anterior pole of the mammalian brain and is generally considered to be formed by three main regions: dorsolateral, medial and orbital prefrontal cortices. The boundaries between these (and respective subdivisions not mentioned here) have been traced in different ways, dependent on the applied methodologies and followed criteria, and despite the existence of common motifs (the dorsolateral prefrontal cortex (dlPFC) is usually associated with cognitive functions supporting behavior and the medial and orbital with regulating emotional behavior and basic

drives) there are no strong evidences to consider the whole area, or its subdivisions, as structural entities with unitary functions [25].

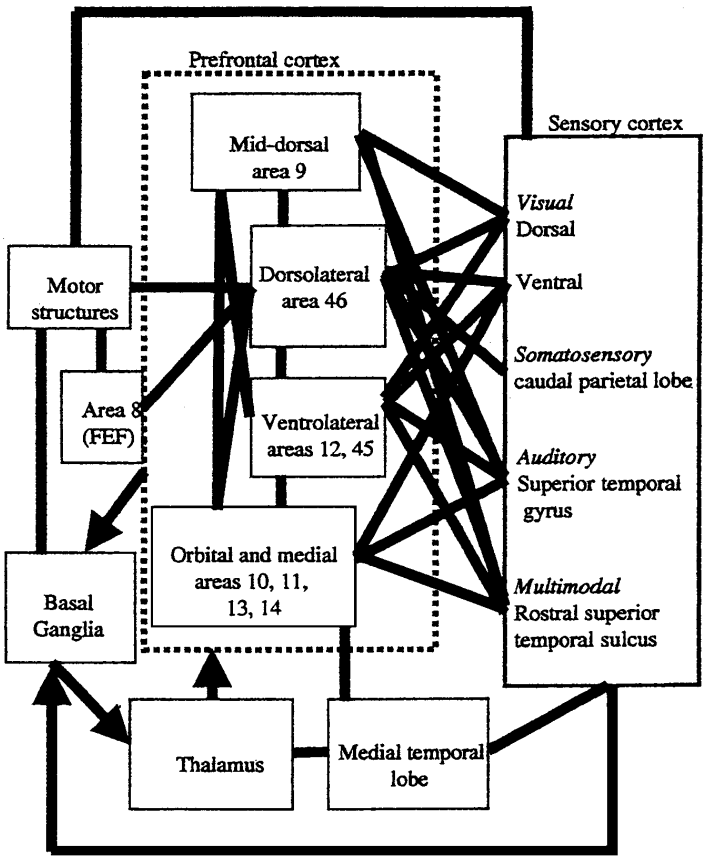

Figure 1.1: Schematic Diagram of Some PFC's Connections: Inputs from several brain systems converge in the interconnected PFC. Most connections are reciprocal with the exceptions indicated by arrows. Figure from Miller and Cohen, 2001 [53].

Determinant for the understanding and description of PFC function and organization are its profuse and reciprocal connection with virtually all sensory and motor systems and many subcortical structures [53] (*Figure 1.1*). The diversity of information streams that converge in it imply that complex

sensory and motor landscapes, as well as the cognitive mechanisms to operate on them, can be found in the PFC. The neural networks underlying these, however, are not confined to topographically demarcated areas, and the computations they perform are many times concomitant in the context of the same behavior and common across several behaviors. Such is one of the main reasons why it as been historically difficult to reconcile a wide collection of, many times, seemingly unrelated facts into a coherent whole.

General theories put forward to bound prefrontal function (particularly the dlPFC) have tried to frame its involvement in disparate cognitive mechanisms (e.g attention [10], WM [21], planning [84], decision making [43] and inhibitory control [2]) in the broader context of executive function [22] and cognitive control [52] responsible for context adapted organization of goal-directed behavior [19]. Such idea is supported by its aforementioned connections as well as hierarchical position on top of the motor oriented frontal half of the brain, which highlights his role as, in essence, an action and execution cortex [26].

The PFC is not critical for performing simple, automatic forms of behavior [52][53], it may be involved in learning them, but, with sufficient training, they are automatized and completely implemented by lower hierarchical areas. The PFC is, however, particularly necessary in situations and contexts that because of their novelty, ambiguity, complexity or extension in time demand for top-down control of behavior. The area, in a position where its representations encapsulate goals and schemes of actions containing in themselves subordinate actions and subgoals, can then be said to have a central part in integrating cross-temporal contingencies, percepts and actions,

by maintaining time sustained representations and monitoring their progress against a general plan.

1.2 The Rodent Prefrontal Cortex

Even if the PFC, and PFC related behaviors, attain their maximal expression in primates, and in particular in humans, such doesn't mean that other species don't have a PFC or exhibit prefrontal mediated behaviors. There has been then, since long, a strong practical interest in being able to study the area in more cost and manipulation amenable model animals, with rodents being strong candidates.

Establishing parallels between the prefrontal function in primates and rodents is not easy [78]. First, the area general role and regional specializations are not well understood in both model animals, creating a base problem about what exactly is being compared; second, there are enormous cross-species variations in the cortical cytoarchitectonics and connections[57]; third, a wide array of criteria and nomenclatures has been used, seemingly ad-hoc, in both species [46].

Combining anatomical with functional information to address the issue different authors proposed that, even if not possessing a granular structure directly equivalent to the human and monkey dlPFC [61] [79], rodents have behaviors that engage functional mechanisms akin to the ones normally ascribed to that area, mechanisms that are shared among several regions of their own PFC [8][40]. The rodent prefrontal is, for sure, not as differentiated as the primates' one, with later specializations likely to have occurred, but dorsolateral-like features, both anatomical and functional, are present

and can be revealed by the use of assays probing species-relevant executive functions [79] [8].

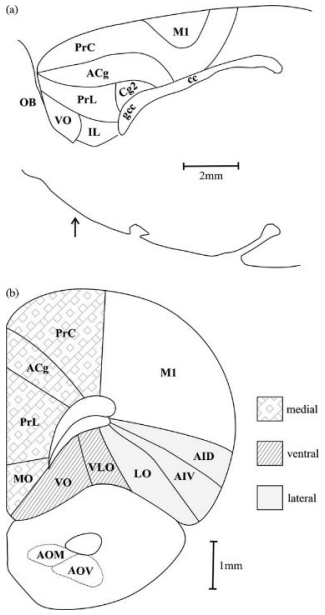

Figure 1.2: Schematic Diagram of the Rat Prefrontal Cortex: (a) Lateral view, 0.9 mm from the midline. (b) Unilateral coronal section, AP location depicted by the arrow above. The different shadings represent the three major sub- divisions of the prefrontal cortex (medial, ventral and lateral). Abbreviations: ACg, anterior cingulate cortex; AID, dorsal agranular insular cortex; AIV, ventral agranular insular cortex; AOM, medial anterior olfactory nucleus; AOV, ventral anterior olfactory nucleus; cc, corpus callosum; Cg2, cingulate cortex area 2; gcc, genu of corpus callosum; IL, infralimbic cortex; LO, lateral orbital cortex; M1, primary motor area; MO, medial orbital cortex; OB, olfactory bulb; PrL, prelimbic cortex; PrC, precentral cortex; VLO, ventrolateral orbital cortex; VO, ventral orbital cortex. Figure from Dalley et.al, 2004 [15].

The rodent PFC can be organized in medial, lateral and ventral areas (see [79] and [40] for variations on this arrangement). The medial can be subdivided in a dorsal region, with precentral and anterior cingulate cortices, and a ventral with the prelimbic (PRL), infralimbic (IL) and medial orbital (MO) cortices. The lateral includes the ventral agranular, insular and lateral

orbital cortices. The ventral region encompasses the ventral orbital and ventral lateral orbital cortices (*Figure 2*) [15].

Based on its anatomical connections, in particular the reciprocal ones with the mediodorsal thalamus [68], and involvement in specific behaviors, the rodent mPFC as long been considered to take part in cognitive processes analogous to some of the ones ascribed to the primate dlPFC [40]. Some authors have investigated and pointed to the existence of functional heterogeneity within the area, particularly between its dorsal and ventral parts [15][40][19][69], but such differences, and its reasons, are many times difficult to interpret out of the context of specific tasks and in the broader spectrum of prefrontal function.

Hence, as with the PFC (especially dorsolateral) of humans and non-human primates, and even if in the scope of less differentiated forms of behavior, the rodent mPFC can be said to be implicated in a set of cognitive control processes needed for the optimal scheduling of complex sequences of behavior including decision making [76], attentional selection [39], monitoring [30], behavioral inhibition [44] and task switching[60]. Crucially, it has also been systematically considered critical for the online maintenance of memory representations necessary for the organization of actions over time [35][33][63].

1.3 Prefrontal Cortex and Working Memory

To go from simple, but inflexible, bottom up determined behaviors, including reflexes and habits, to complex and versatile streams of actions, animals need to be able to integrate context relevant information and fu-

ture plans, over variable periods of time, and use them to generate adapted conducts.

The recognition of such need, different from the long term storage of information in reference memory, led researchers to come up with the concept of WM, a mechanism by which the brain would be able to sustain and manipulate, for a short period of time, representations that could provide the backbone to high level cognitive operations such as thinking, planning, reasoning and decision-making [21]. Given this central role in goal-directed behavior, establishing the neural basis of WM has been a primary focus of neuroscience research.

The terminologies working and short-term memory have been used largely interchangeably when scientists want to refer, at the behavioral or mechanistic level, to something that needs to be remembered for a short period of time. There is no general consensus about the terms [1] and whether they refer to distinct mechanisms or qualitative levels within the same general mechanism. The more accepted distinction, though, implies a complexity difference, with short-term memory referring to the passive maintenance of information and WM also to the processes through which that information is manipulated [22]. In what relates to our work here, even taking in consideration the complexity arguments and the heavy assumptions loaded on the term by human and primate research, we'll use the designation WM. Our decision is mainly based on the fact that it is the more generally used by the field and that to go back and forth between terminologies, when referring to our or others' work, would result confusing. It should be clear, though, that, despite using the term WM, we interpret it as the basic mechanism

through which information is maintained active in the brain and imply no distinction with short-term memory.

Based on psychological evidence several conceptual WM models were developed [54], but the more well-known and influential is the one proposed by Baddeley and Hitch [3]. Badelley's model includes one master component (the central executive) and three slave components, responsible for processing and maintaining information from several modalities: the visuospatial sketchpad (visuospatial information), the phonological loop (speech perception and language comprehension) and the episodic buffer (integrating chunks of information from a different variety of sources). The central executive supervises the performance of the slave components and it's considered to be an attentional system with a limited memory capability. Baddeley's proposal is an abstract, not mechanistic, model and establishing a comparison between its components and particular brain structures it's difficult and of limited usefulness. Despite, and in a loose sense, it's central executive component has been related to the function played in the brain by the PFC [16].

The PFC involvement in WM supported behaviors has been consistently established by lesion studies, both in primates [25][59] and other mammalian species [35], and non-invasive brain activation experiments in humans [75], but it was the finding of neurons with elevated activity throughout a short WM dependent period that, by providing a simple explanation for the mechanism of information storage, contributed the most for the association of the area with the process.

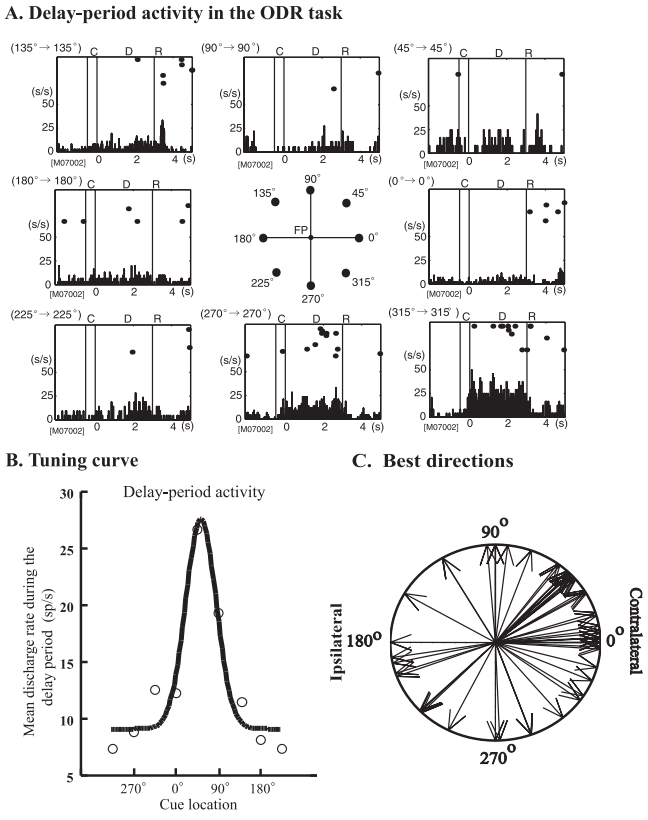

Figure 1.3: Delay Period Activity in ODR Task: (A) An example of directional delay-period activity. (B) An example of a tuning curve of directional delay-period activity. (C) Polar distribution of the best directions of delay-period activity. A majority of the best directions were directed toward the contralateral visual field. Figure from Funahashi, 2006 [15].

Neurons in the PFC with firing rate higher than the baseline, between the presentation of a cue and the response of the subject, were first found in delayed response tasks [45] [27] [56], where the former and the later were separated by a time interval (delay). Their hypothetical role as the mechanism for temporal active maintenance of information was, however, decisively established and investigated in the context of the oculomotor delayed

response (ODR) task[23]. In it monkeys had to fixate a central point on a screen. After fixation an image was shown for some time and then disappeared, marking the beginning of a delay period. During the delay animals had to keep fixating the central point, controlling for movement related neural activity. With the subsequent disappearance of the central point the monkey had to make a saccade to the location where the image had been initially displayed.

Neural activity, during the delay period of the ODR task, showed characteristics that made it an ideal candidate mechanism for the maintenance of information in WM: it was prolonged or shortened depending on the duration of the delay period [42], was only present when the animals performed correct responses, being truncated or absent in error trials [27] and, importantly, exhibited directional preference, with specific neurons firing only when the visual cue was presented at one or a few adjacent positions [64] (*Figure 1.3*). Also, and curiously, the neurons seemed to encode preferentially the location of the cue and not the direction of the saccade [77]. The clarity of the results and the seeming simplicity of the mechanism, PFC neurons, or neuronal populations, selectively tuned to the to-be-remembered information, hold it in an active state through persistent activation [32], made this the predominant model in the WM field, inspiring several proposed theoretical mechanisms [17] [11].

Recently, however, several lines of evidence have questioned the role of the PFC, and stable persistent neural activity, in WM related behaviors [71]. Following the ODR task results, subsequent studies, and tasks, revealed PFC neurons with activity that showed selectivity regarding a varied panoply of

information (e.g. tactile [67], auditory [41], task rules [83] and temporal order of stimuli [24]). This led to a progressively compartmentalized view of the area in which it apparently contained specialized neurons for every type of potentially useful information. Such idea seems rather implausible, and not parsimonious, if one thinks that the same information is already being represented, and processed, in lower hierarchical areas and that these also possess the hypothetical requisites to maintain it over short periods of time, with cells with sustained activity having been observed throughout the brain (e.g. parietal cortex [31], primary visual cortex [28], superior colliculus [6], thalamus [82] and even the spinal cord[62]).

Adding to such, and more revealing, temporal and occipital areas were shown to also encode, during the entire memory period, task relevant representations[80] that were tied to WM precision and the behavior of the subjects [18]. Moreover, information in sensory areas seems to better represent the characteristics of the remembered item during the delay period than activity in the PFC [47], where representations were shown to be more categorical in nature [50]. Together, these led to an alternative view according to which the PFC's primary function, in WM, is not to store but rather to influence representations stored in hierarchically lower areas[51] [20] through top-down signals [12][53].

The relevance of the PFC's fixed selectivity persistent neural activity has also been questioned. This type of activity in the PFC as practically become a symbol for WM, but, as before mentioned, sustained activity can be found nearly everywhere in the brain, questioning any privileged status of the area. Also, despite its recognized importance in forming temporal links [26] [14],

short-term lived representations can be stored in different ways and are not dependent on selective sustained activity, as proved by works in which information could still be decoded, during the delay period, despite the removal of cells with selective elevated activity [4] [66] [72], or the observation of relatively silent periods, between encoding and response preparation, where, despite the inexistence of overt sustained activity, memory is still maintained [5].

Because of the before mentioned arguments, and following developments on brain monitoring technologies and data analysis capabilities, the focus of research has been shifting from information encoded by neurons, or groups of neurons, with delay period selective elevated activity, to WM encoding based on the joint activity of neuron ensembles (*Figure 4*). Indeed, an increasing number of studies reports that, rather than utilizing distinct populations to encode each task variable, activity in the PFC encodes multiple task parameters within a single neuronal population [38] [74]. Further, researchers have also discovered that the encoding is often done through dynamic spatiotemporal patterns (*Figure 1.4 3*) [50][74][4], which evolve through state space trajectories and in which the encoding might be entirely different in distinct time points. Although the precise mechanisms underlying dynamic population coding are still not well understood, recent works have highlighted its possible coupling with functional and short term synaptic plasticity [55][73].

Dynamic coding is certainly not limited to the PFC, but the area's hierarchical location and temporal integration role, allow it to fully explore a general principle of WM dynamic coding in organizing flexible cognition and behavior.

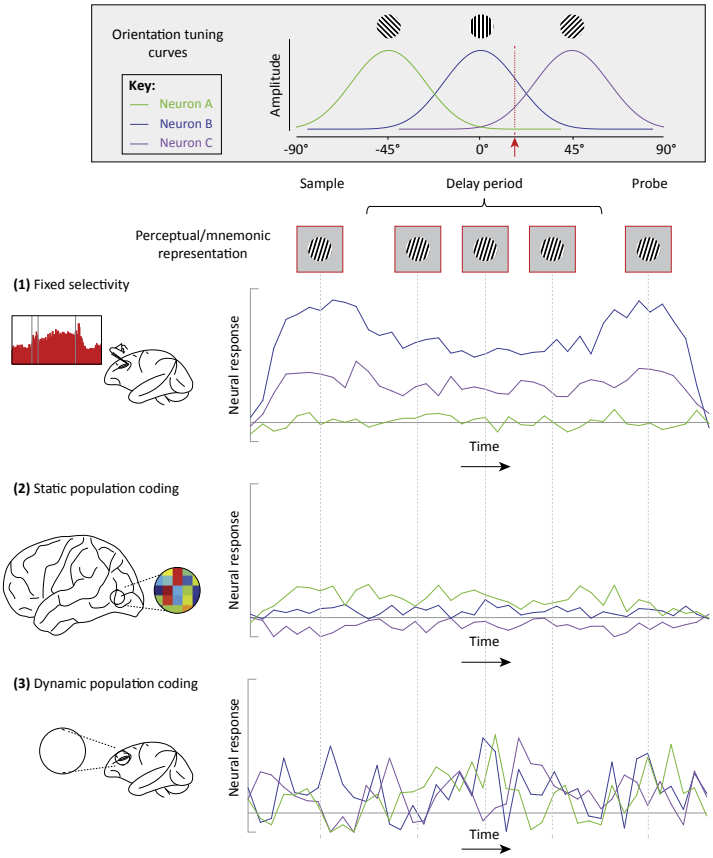

Figure 1.4: Neural Mechanisms of WM: A simplified schematic comparing and contrasting the fixed-selectivity model with population coding models involving static and dynamic temporal codes. Orientation tuning curves for three hypothetical neurons, A, B, and C, are shown in the top inset. Below this are schematics for three different potential neural models of WM. Top row: The fixed-selectivity model, primarily derived from single-unit recordings in monkey dlPFC. Middle row: Evidence for static population coding comes primarily from fMRI decoding and forward encoding studies of visual cortex. Here the pattern of activity across neurons can encode stimulus orientation in the absence of highly selective neural responses. This pattern is sustained throughout maintenance. Bottom row: Dynamic population coding has been demonstrated largely in monkey lPFC. Despite time-varying activity in all three neurons, the representation of orientation remains stable. The relevant orientation is encoded by a different combination of neural responses at each point in time. Figure from Sreenivasan et.al, 2014 [71].

1.4 Heterogeneous Representations in the Prefrontal Cortex

An interpretation of the neural activity mediating the perception-action cycle solely based on a function that takes us from stimuli to behavior is made difficult by the fact that the brain doesn't simple represent the world in a different way. Personal significant preexistant attributions modulate the primary representations of sensory stimuli and motor implementations through a collection of cognitive mechanisms. At any given moment, thus, what is being encoded by the neurons are representations of environmental and behavioral features coloured and contextualized according to an organism's interpretation, based on its world model and future goals [9]. Such fact is more and more evident when moving away from the periphery, with the activity of each neuron being less and less determined by external drivers and more a reflection of activity in lower information processing levels. In its position at the apex of a hierarchy through which feedforward information ascends, being processed in the way by multiple intermediate loops [26], the PFC deals essentially with representations that are already highly abstracted, filtered and integrated for task relevance[58].

A direct consequence of what as been described is that neurons in the PFC often have complex responses that are not organized anatomically and may reflect multiple parameters such as stimuli, rules, responses or combinations of these [48] [42] [7]. Traditionally this heterogeneity was neglected and considered a difficulty in understanding the mechanistic roles of certain neurons and brain regions. Consequently, in an effort to identify the com-

ponents involved in the processes they were interested in, scientists tended to handpick cells that could be directly related with features of interest, or average the activity of a given neuron over repetitions of the same feature, blurring all other information its response might also contain.

Recently though, this mixed selectivity, common characteristic of neurons in high order areas, as been associated to high-dimensional neural representations and the way PFC encodes information. *Rigotti et.al, 2013* [66] showed that activity in a population of neurons, in the PFC of monkeys, simultaneously encoded all task relevant variables, in an object sequence memory task, even when classic neural selectivity was artificially abolished. The authors propose nonlinear mixed selectivity as the crucial characteristic that allows for high-dimensional neural representations (*Figure 1.5*) and show that artificially abolishing it reduces the representations dimensionality. High-dimensionality seemingly allows task relevant aspects to be accessible to linear classifiers, such as simple neuron models, that can only separate representations through planes, which would be impossible, for instance, in the case of the pure and linear mixed selective neurons in *Figure 1.5 b.*

The characteristic response profile of neurons found in the PFC, with its heterogeneity and mixed selectivity, might thus be at the core of the mechanisms responsible for the adaptability of the area and its seemingly limitless capacity to represent a multiplicity of information. Riding the wave of technological and computational power development, both at the level of brain activity recording and data analysis, scientists have been discovering that the joint activity of neural ensembles in high order areas encode, simul-

taneously and without the need for feature selectivity, multiple task relevant variables. Findings, both in the primate [65] and rodent PFC [49], revealed evidence for multiplexed encoding, in diverse task moments, of contextually relevant information concerning stimuli, goals, rules and strategies [81] [48] [4] [34], the basic necessary ingredients to orchestrate behavior.

Recording population activity allows a shift of focus from cells with easily interpretable response tuning to the information contained in mixed selectivity neurons. Leveraging statistical power from simultaneously recorded activity [13] researchers can move away from trial averaging and extract meaningful representations from the activity in individual trials, something particularly important if the questions being addressed involves brain areas where neurons are not directly, and reliable, driven by external stimuli or actions. As said before, in the PFC the observed activity results from a combination of external influences with the brain appraisal of these and ensembles in the area, working at multiple temporal and spatial scales, reflect a panoply of internal processing mechanisms taking place in networks at several hierarchical levels. Hence, even if the contingencies of a given trial type are kept constant, the time course of relevant internal mechanisms may differ substantially, making them only fully intelligible when analyzed trial by trial, the importance of such increasing with the cognitive complexity of task or problem.

It seems so that to fully understand the mechanisms behind the functional role of an highly integrative area, like the PFC, one needs to combine, and contrast, an understanding of the moment to moment neural activity, with a thorough description, and comprehension, of the synchronous behav-

ior.

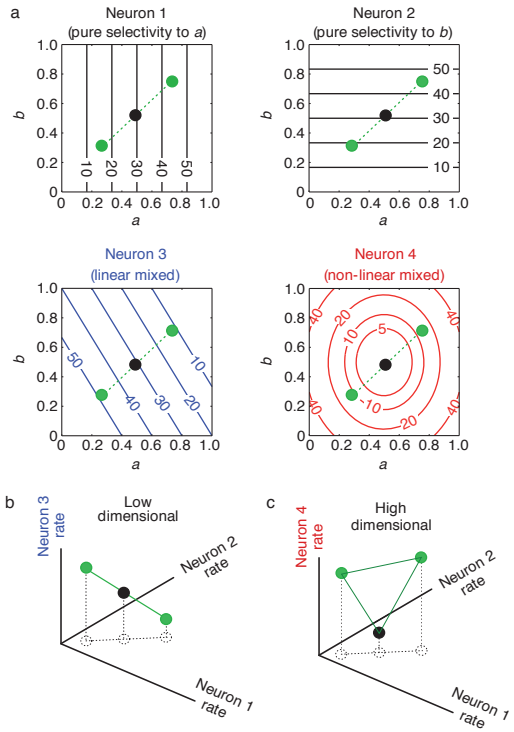

*Figure 1.5: Low and High Dimensional Representations and Mixed Selectivity: (a), Contour plots of the responses (spikes per s) of four hypothetical neurons to two continuous parameters that characterize two task-relevant aspects (**a**,**b**, varying between 0 and 1) corresponding to relevant stimulus features. Neurons 1,2 are pure selectivity neurons, selective to individual parameters (**a** and **b**, respectively). Neuron 3 is a linear mixed selectivity neuron: its response is a linear combination of the responses to parameters **a** and **b**. Neuron 4 is a nonlinear mixed selectivity neuron: its response cannot be explained by a linear superposition of responses to the individual parameters. The green circles indicate the responses to three sensory stimuli parameterized by three **a**,**b** combinations. (b), The responses of the pure and linear mixed selectivity neurons from a in the space of activity patterns elicited by the three stimuli indicated by the green circles in **a** lie on a line, therefore spanning a low-dimensional space. (c), As in (b), with the third neuron being the nonlinear mixed selectivity Neuron 4 in **a**.The representations of the stimuli lie on a plane, no longer being confined on a line . Figure from Rigotti et.al, 2013 [66].*

References

[1] B. Aben, S. Stapert, and A. Blokland. "About the Distinction between Working Memory and Short-Term Memory." In: *Frontiers in psychology* 3 (2012), p. 301 (cit. on p. 8).

[2] A. R. Aron, Trevor W. Robbins, and R. A. Poldrack. "Inhibition and the right inferior frontal cortex." In: *Trends in cognitive sciences* 8 (4 Apr. 2004), pp. 170–177 (cit. on p. 4).

[3] A. Baddeley. "Working memory: theories, models, and controversies." In: *Annual review of psychology* 63 (2012), pp. 1–29 (cit. on p. 9).

[4] E. H. Baeg et al. "Dynamics of population code for working memory in the prefrontal cortex." In: *Neuron* 40 (1 Sept. 2003), pp. 177–188 (cit. on pp. 13, 17).

[5] O. Barak, M. Tsodyks, and R. Romo. "Neuronal Population Coding of Parametric Working Memory". In: *Journal of Neuroscience* 30.28 (July 2010), pp. 9424–9430 (cit. on p. 13).

[6] M. A. Basso and R. H. Wurtz. "Modulation of neuronal activity in superior colliculus by changes in target probability." In: *The Journal of neuroscience* 18 (18 Sept. 1998), pp. 7519–7534 (cit. on p. 12).

[7] C. D. Brody et al. "Timing and neural encoding of somatosensory parametric working memory in macaque prefrontal cortex." In: *Cerebral cortex (New York, N.Y. : 1991)* 13 (11 Nov. 2003), pp. 1196–1207 (cit. on p. 15).

[8] V. J. Brown and E. M. Bowman. "Rodent models of prefrontal cortical function." In: *Trends in neurosciences* 25 (7 July 2002), pp. 340–343 (cit. on pp. 5, 6).

[9] G. Buzsáki. "Large-scale recording of neuronal ensembles." In: *Nature neuroscience* 7 (5 May 2004), pp. 446–451 (cit. on p. 15).

[10] L. L. Chao and R. T. Knight. "Human prefrontal lesions increase distractibility to irrelevant sensory inputs." In: *Neuroreport* 6 (12 Aug. 1995), pp. 1605–1610 (cit. on p. 4).

[11] A. Compte et al. "Synaptic mechanisms and network dynamics underlying spatial working memory in a cortical network model." In: *Cerebral cortex (New York, N.Y. : 1991)* 10 (9 Sept. 2000), pp. 910–923 (cit. on p. 11).

[12] D. A. Crowe et al. "Prefrontal neurons transmit signals to parietal neurons that reflect executive control of cognition." In: *Nature neuroscience* 16 (10 Oct. 2013), pp. 1484–1491 (cit. on p. 12).

[13] J. P. Cunningham and B. M. Yu. "Dimensionality reduction for large-scale neural recordings." In: *Nature neuroscience* 17 (11 Nov. 2014), pp. 1500–1509 (cit. on p. 17).

[14] C. E. Curtis and D. Lee. "Beyond working memory: the role of persistent activity in decision making." In: *Trends in cognitive sciences* 14 (5 May 2010), pp. 216–222 (cit. on p. 12).

[15] J. W. Dalley, R. N. Cardinal, and T. W. Robbins. "Prefrontal executive and cognitive functions in rodents: neural and neurochemical sub-

strates." In: *Neuroscience and biobehavioral reviews* 28 (7 Nov. 2004), pp. 771–784 (cit. on pp. 6, 7, 10).

[16] M. D'Esposito et al. "The neural basis of the central executive system of working memory." In: *Nature* 378 (6554 Nov. 1995), pp. 279–281 (cit. on p. 9).

[17] D. Durstewitz, J. K. Seamans, and T. J. Sejnowski. "Neurocomputational models of working memory." In: *Nature neuroscience* 3 Suppl (Nov. 2000), pp. 1184–1191 (cit. on p. 11).

[18] E. F. Ester et al. "A Neural Measure of Precision in Visual Working Memory". In: *Journal of Cognitive Neuroscience* 25.5 (May 2013), pp. 754–761 (cit. on p. 12).

[19] D. R. Euston, A. J. Gruber, and B. L. McNaughton. "The role of medial prefrontal cortex in memory and decision making." In: *Neuron* 76 (6 Dec. 2012), pp. 1057–1070 (cit. on pp. 4, 7).

[20] E. Feredoes et al. "Causal evidence for frontal involvement in memory target maintenance by posterior brain areas during distracter interference of visual working memory." In: *Proceedings of the National Academy of Sciences of the United States of America* 108 (42 Oct. 2011), pp. 17510–17515 (cit. on p. 12).

[21] S. Funahashi. "Prefrontal cortex and working memory processes." In: *Neuroscience* 139 (1 Apr. 2006), pp. 251–261 (cit. on pp. 4, 8).

[22] S. Funahashi and J. M. Andreau. "Prefrontal cortex and neural mechanisms of executive function." In: *Journal of physiology, Paris* 107 (6 Dec. 2013), pp. 471–482 (cit. on pp. 4, 8).

[23] S. Funahashi, C. J. Bruce, and P. S. Goldman-Rakic. "Mnemonic coding of visual space in the monkey's dorsolateral prefrontal cortex." In: *Journal of neurophysiology* 61 (2 Feb. 1989), pp. 331–349 (cit. on p. 11).

[24] S. Funahashi, M. Inoue, and K. Kubota. "Delay-period activity in the primate prefrontal cortex encoding multiple spatial positions and their order of presentation." In: *Behavioural brain research* 84 (1-2 Mar. 1997), pp. 203–223 (cit. on p. 12).

[25] J. M. Fuster. *The Prefrontal Cortex*. Academic Press, 2008 (cit. on pp. 3, 9).

[26] J. M. Fuster. "The Prefrontal Cortex—An Update". In: *Neuron* 30.2 (May 2001), pp. 319–333 (cit. on pp. 4, 12, 15).

[27] J. M. Fuster. "Unit activity in prefrontal cortex during delayed-response performance: neuronal correlates of transient memory." In: *Journal of neurophysiology* 36 (1 Jan. 1973), pp. 61–78 (cit. on pp. 10, 11).

[28] J. R. Gibson and J. H. Maunsell. "Sensory modality specificity of neural activity related to memory in visual cortex." In: *Journal of neurophysiology* 78 (3 Sept. 1997), pp. 1263–1275 (cit. on p. 12).

[29] K. R. Gibson. "Myelination and behavioral development: a comparative perspective on questions of neoteny, altriciality and intelligence." In: *Brain Maturation and Cognitive Development*. 1991 (cit. on p. 2).

[30] P. Gisquet-Verrier and B. Delatour. "The role of the rat prelimbic/infralimbic cortex in working memory: not involved in the short-term maintenance

but in monitoring and processing functions." In: *Neuroscience* 141 (2 Aug. 2006), pp. 585–596 (cit. on p. 7).

[31] J. W. Gnadt and R. A. Andersen. "Memory related motor planning activity in posterior parietal cortex of macaque." In: *Experimental brain research* 70 (1 1988), pp. 216–220 (cit. on p. 12).

[32] P. S. Goldman-Rakic. "Cellular basis of working memory." In: *Neuron* 14 (3 Mar. 1995), pp. 477–485 (cit. on p. 11).

[33] S. Granon et al. "Working memory, response selection, and effortful processing in rats with medial prefrontal lesions." In: *Behavioral neuroscience* 108 (5 Oct. 1994), pp. 883–891 (cit. on p. 7).

[34] V. Hok et al. "Coding for spatial goals in the prelimbic/infralimbic area of the rat frontal cortex." In: *Proceedings of the National Academy of Sciences of the United States of America* 102 (12 Mar. 2005), pp. 4602–4607 (cit. on p. 17).

[35] N. K. Horst and M. Laubach. "The role of rat dorsomedial prefrontal cortex in spatial working memory." In: *Neuroscience* 164 (2 Dec. 2009), pp. 444–456 (cit. on pp. 7, 9).

[36] P. R. Huttenlocher. "Morphometric study of human cerebral cortex development." In: *Neuropsychologia* 28 (6 1990), pp. 517–527 (cit. on p. 2).

[37] H. J. Jerison. "Evolution of the brain". In: *Neuropsychology*. 1994 (cit. on p. 2).

[38] J. K. Jun et al. "Heterogenous population coding of a short-term memory and decision task." In: *The Journal of neuroscience : the official journal of the Society for Neuroscience* 30 (3 Jan. 2010), pp. 916–929 (cit. on p. 13).

[39] J. B. Kahn et al. "Medial prefrontal lesions in mice impair sustained attention but spare maintenance of information in working memory." In: *Learning & memory (Cold Spring Harbor, N.Y.)* 19 (11 Oct. 2012), pp. 513–517 (cit. on p. 7).

[40] R. P. Kesner and J. C. Churchwell. "An analysis of rat prefrontal cortex in mediating executive function." In: *Neurobiology of learning and memory* 96 (3 Oct. 2011), pp. 417–431 (cit. on pp. 5–7).

[41] Y. Kikuchi-Yorioka and T. Sawaguchi. "Parallel visuospatial and audiospatial working memory processes in the monkey dorsolateral prefrontal cortex." In: *Nature neuroscience* 3 (11 Nov. 2000), pp. 1075–1076 (cit. on p. 12).

[42] S. Kojima and P. S. Goldman-Rakic. "Delay-related activity of prefrontal neurons in rhesus monkeys performing delayed response." In: *Brain research* 248 (1 Sept. 1982), pp. 43–49 (cit. on pp. 11, 15).

[43] D. C. Krawczyk. "Contributions of the prefrontal cortex to the neural basis of human decision making." In: *Neuroscience and biobehavioral reviews* 26 (6 Oct. 2002), pp. 631–664 (cit. on p. 4).

[44] U. M. Krfffdfffdmer et al. "The role of the lateral prefrontal cortex in inhibitory motor control." In: *Cortex; a journal devoted to the study of*

the nervous system and behavior 49 (3 Mar. 2013), pp. 837–849 (cit. on p. 7).

[45] K. Kubota and H. Niki. "Prefrontal cortical unit activity and delayed alternation performance in monkeys." In: *Journal of Neurophysiology* 34.3 (May 1971), pp. 337–347 (cit. on p. 10).

[46] M. Laubach et al. "What, If Anything, Is Rodent Prefrontal Cortex?" In: *eNeuro* 5 (5 2018) (cit. on p. 5).

[47] S. Lee, D. J. Kravitz, and C. I. Baker. "Goal-dependent dissociation of visual and prefrontal cortices during working memory." In: *Nature neuroscience* 16 (8 Aug. 2013), pp. 997–999 (cit. on p. 12).

[48] C. K. Machens, R. Romo, and C. D. Brody. "Functional, But Not Anatomical, Separation of "What" and "When" in Prefrontal Cortex". In: *Journal of Neuroscience* 30.1 (Jan. 2010), pp. 350–360 (cit. on pp. 15, 17).

[49] S. Maggi, A. Peyrache, and M. D. Humphries. "An ensemble code in medial prefrontal cortex links prior events to outcomes during learning". In: *Nature Communications* 9.1 (June 2018) (cit. on p. 17).

[50] E. M. Meyers et al. "Dynamic Population Coding of Category Information in Inferior Temporal and Prefrontal Cortex". In: *Journal of Neurophysiology* 100.3 (Sept. 2008), pp. 1407–1419 (cit. on pp. 12, 13).

[51] B. T. Miller et al. "The prefrontal cortex modulates category selectivity in human extrastriate cortex." In: *Journal of cognitive neuroscience* 23 (1 Jan. 2011), pp. 1–10 (cit. on p. 12).

[52] E. K. Miller. "The prefrontal cortex and cognitive control." In: *Nature reviews. Neuroscience* 1 (1 Oct. 2000), pp. 59–65 (cit. on p. 4).

[53] E. K. Miller and J. D. Cohen. "An integrative theory of prefrontal cortex function." In: *Annual review of neuroscience* 24 (2001), pp. 167–202 (cit. on pp. 3, 4, 12).

[54] A. Miyake and P. Shah. *Models of Working Memory*. Ed. by Akira Miyake and Priti Shah. Cambridge University Press, 1999 (cit. on p. 9).

[55] G. Mongillo, O. Barak, and M. Tsodyks. "Synaptic Theory of Working Memory". In: *Science* 319.5869 (Mar. 2008), pp. 1543–1546 (cit. on p. 13).

[56] H. Niki. "Differential activity of prefrontal units during right and left delayed response trials". In: *Brain Research* 70.2 (Apr. 1974), pp. 346–349 (cit. on p. 10).

[57] D. Ongfffdfffdr and J. L. Price. "The organization of networks within the orbital and medial prefrontal cortex of rats, monkeys and humans." In: *Cerebral cortex (New York, N.Y. : 1991)* 10 (3 Mar. 2000), pp. 206–219 (cit. on p. 5).

[58] D. Passingham and K. Sakai. "The prefrontal cortex and working memory: physiology and brain imaging". In: *Current Opinion in Neurobiology* 14.2 (Apr. 2004), pp. 163–168 (cit. on p. 15).

[59] M. Petrides. "Frontal lobes and working memory: evidence from investigations of the effects of cortical excisions in nonhuman primates". In: *Handbook of neuropsychology, Vol. 9 (Boller*. 1994 (cit. on p. 9).

[60] N. J. Powell and A. D. Redish. "Complex neural codes in rat prelimbic cortex are stable across days on a spatial decision task." In: *Frontiers in behavioral neuroscience* 8 (2014), p. 120 (cit. on p. 7).

[61] T. M. Preuss. "Do rats have prefrontal cortex? The rose-woolsey-akert program reconsidered." In: *Journal of cognitive neuroscience* 7 (1 1995), pp. 1–24 (cit. on p. 5).

[62] Y. Prut and E. E. Fetz. "Primate spinal interneurons show pre-movement instructed delay activity." In: *Nature* 401 (6753 Oct. 1999), pp. 590–594 (cit. on p. 12).

[63] M. E. Ragozzino, S. Adams, and R. P. Kesner. "Differential involvement of the dorsal anterior cingulate and prelimbic-infralimbic areas of the rodent prefrontal cortex in spatial working memory." In: *Behavioral neuroscience* 112 (2 Apr. 1998), pp. 293–303 (cit. on p. 7).

[64] G. Rainer, S. C. Rao, and E. K. Miller. "Prospective coding for objects in primate prefrontal cortex." In: *The Journal of neuroscience : the official journal of the Society for Neuroscience* 19 (13 July 1999), pp. 5493–5505 (cit. on p. 11).

[65] M. Rigotti et al. "Internal representation of task rules by recurrent dynamics: the importance of the diversity of neural responses." In: *Frontiers in computational neuroscience* 4 (2010), p. 24 (cit. on p. 17).

[66] M. Rigotti et al. "The importance of mixed selectivity in complex cognitive tasks". In: *Nature* 497.7451 (May 2013), pp. 585–590 (cit. on pp. 13, 16, 18).

[67] R. Romo et al. "Neuronal correlates of parametric working memory in the prefrontal cortex." In: *Nature* 399 (6735 June 1999), pp. 470–473 (cit. on p. 12).

[68] J. E. Rose and C. N. Woolsey. "The orbitofrontal cortex and its connections with the mediodorsal nucleus in rabbit, sheep and cat." In: *Research publications - Association for Research in Nervous and Mental Disease* 27 (1 vol.) (1948), pp. 210–232 (cit. on p. 7).

[69] J. K. Seamans, S. B. Floresco, and A. G. Phillips. "Functional differences between the prelimbic and anterior cingulate regions of the rat prefrontal cortex." In: *Behavioral neuroscience* 109 (6 Dec. 1995), pp. 1063–1073 (cit. on p. 7).

[70] E. R. Sowel et al. "In vivo evidence for post-adolescent brain maturation in frontal and striatal regions". In: *Nature neuroscience* 2.10 (Oct. 1999), pp. 859–861 (cit. on p. 2).

[71] K. K. Sreenivasan, E. K. Curtis, and M. D'Esposito. "Revisiting the role of persistent neural activity during working memory". In: *Trends in Cognitive Sciences* 18.2 (Feb. 2014), pp. 82–89 (cit. on pp. 11, 14).

[72] K. K. Sreenivasan, J. Vytlacil, and M. D'Esposito. "Distributed and dynamic storage of working memory stimulus information in extrastriate cortex." In: *Journal of cognitive neuroscience* 26 (5 May 2014), pp. 1141–1153 (cit. on p. 13).

[73] M. G. Stokes. "'Activity-silent' working memory in prefrontal cortex: a dynamic coding framework." In: *Trends in cognitive sciences* 19 (7 July 2015), pp. 394–405 (cit. on p. 13).

[74] M. G. Stokes et al. "Dynamic coding for cognitive control in prefrontal cortex." In: *Neuron* 78 (2 Apr. 2013), pp. 364–375 (cit. on p. 13).

[75] D. T. Stuss and R. T. Knight. *Principles of Frontal Lobe Function*. Oxford University Press, 2002 (cit. on p. 9).

[76] J. H. Sul et al. "Distinct roles of rodent orbitofrontal and medial prefrontal cortex in decision making." In: *Neuron* 66 (3 May 2010), pp. 449–460 (cit. on p. 7).

[77] K. Takeda and S. Funahashi. "Prefrontal task-related activity representing visual cue location or saccade direction in spatial working memory tasks." In: *Journal of neurophysiology* 87 (1 Jan. 2002), pp. 567–588 (cit. on p. 11).

[78] H. B. Uylings and C. G. van Eden. "Qualitative and quantitative comparison of the prefrontal cortex in rat and in primates, including humans." In: *Progress in brain research* 85 (1990), pp. 31–62 (cit. on p. 5).

[79] H. B. Uylings, H. J. Groenewegen, and B. Kolb. "Do rats have a prefrontal cortex?" In: *Behavioural brain research* 146 (1-2 Nov. 2003), pp. 3–17 (cit. on pp. 5, 6).

[80] E. K. Vogel, A. W. McCollough, and M. G. Machizawa. "Neural measures reveal individual differences in controlling access to working memory." In: *Nature* 438 (7067 Nov. 2005), pp. 500–503 (cit. on p. 12).

[81] M. R. Warden and E. K. Miller. "The representation of multiple objects in prefrontal neuronal delay activity." In: *Cerebral cortex (New York, N.Y. : 1991)* 17 Suppl 1 (Sept. 2007), pp. i41–i50 (cit. on p. 17).

[82] Y. Watanabe and S. Funahashi. "Neuronal activity throughout the primate mediodorsal nucleus of the thalamus during oculomotor delayed-responses. I. Cue-, delay-, and response-period activity." In: *Journal of neurophysiology* 92 (3 Sept. 2004), pp. 1738–1755 (cit. on p. 12).

[83] K. G. White, A. C. Ruske, and M. Colombo. "Memory procedures, performance and processes in pigeons." In: *Brain research. Cognitive brain research* 3 (3-4 June 1996), pp. 309–317 (cit. on p. 12).

[84] T. Zalla et al. "Action planning in a virtual context after prefrontal cortex damage." In: *Neuropsychologia* 39 (8 2001), pp. 759–770 (cit. on p. 4).

Chapter 2

Head-Fixed Delayed Response Task on a Treadmill

Chapter Authors

João Afonso, André Monteiro, Sebastien Royer and Alfonso Renart

Authors' Contributions

Built and designed the experimental setups: *João Afonso and Sebastien Royer*

Conceived and designed the behavior protocol, analysis and controls: *João Afonso and Alfonso Renart*

Performed the surgical procedures: *João Afonso*

Trained the animals: *João Afonso and André Monteiro*

Analysed the behavioral data: *João Afonso*

Acknowledgements

We thank the staff of the Champalimaud Centre for the Unknown Vivarium for assistance and support in mice care related issues. We are also in debt to the Hardware Platform for building dedicated electronics for our setups and assisting us on all matters of electronics related issues.

2.1 Abstract

When using behavioral paradigms to investigate the neural basis of certain behaviors, or cognitive processes, one must first make sure to completely understand how the subjects are solving them. Delayed response tasks have been successfully used in investigating WM at the behavioral and neural level, but, given their design, with the cue immediately giving away the future response, subjects have been found to use behavioral strategies to avoid the need of keeping a memory during their cue absent period. Here we present an head-fixed delayed response task on a treadmill, for mice, that allows us to precisely monitor the behavior of the animals while simultaneously performing multi-electrode acute recordings. Mice perform consistently well in the task and, through a combination of analysis and behavior based controls, we show that a WM representation is effectively needed for correct performance, paving the way for a meaningful interpretation of the neural activity.

2.2 Introduction

Behavior is one of those pervasive concepts for which seemingly simple and clear intuitions become suddenly muddled when a formal definition is attempted. Nevertheless, from Tinbergen's "The total movements made by the intact animal" [26], to a more recent definition that emerged from a survey performed in the behavioral biologists' community: "Behavior is the internally coordinated responses (actions or inactions) of whole living organisms (individuals or groups) to internal and/or external stimuli, excluding responses more easily understood as developmental changes"[15], the idea that behavior is something that organisms perform, their way to interact, respond and intervene in the environment, appears as a common theme. It's through behavior that organisms, single or collective, thrive or perish and so it was through behavior that natural selection shaped the evolution of nervous systems.

It should thus be clear that it's not possible to truly understand brain function in isolation from the behaviors it evolved to generate and control, and that only by systematically connecting the dots between this two spaces will it be feasible to uncover how the first gives rise to the second. Because behavior is a complex and high-dimensional phenomenon, changing dynamically in space and time in the context of a particular environment, this is more easily said than done [10].

There is an inherent conflict between the need to simplify and constrain animal behavior, in order to isolate particular phenomenons of interest and facilitate the interpretation of always complex neural signals, the reduction-

ist approach neuroscience tends to follow, and the notion that animals will only fully express their behavioral repertoire, and that this will only be fully understandable, in the context of more naturalistic environments [14] [24]. Even if no definitive solution to this conflict is still foreseeable, it should stand out that behavioral tasks mustn't totally ignore each animals' natural repertoire and that minutely monitoring and controlling how the subjects are actually solving the problems imposed on them by the experimenter is probably as important to understanding the brain as recording the biggest number of neurons or being able to perturb their activity [8].

In an attempt to understand and describe particular behaviors, cognitive functions and the neural activity underlying these, scientists have tried to isolate them through the use of specifically designed behavioral assays - the previously mentioned reductionist approach. The defining characteristic of WM probing tasks is the existence of a delay, or memory, period over which animals have to remember some piece of information that will allow them to correctly perform the task. During the memory period there should be no external cue about the memorized item: forcing the subject to store and use an internal representation of it.

In general terms these tasks can be organized in two groups: delayed response and delayed comparison tasks[21]. In delayed response tasks all the information needed to correctly solve the task is already present at the onset of the memory period and the subject only has to withhold its response until the appropriate moment. In delayed comparison tasks the correct response can only be determined at the end of the memory period by comparing the previously presented cue with a new one. From this follows that wile in

a delayed response context it's not possible to know what information the subjects are actually storing during the delay, the cue previously presented or the action to be performed, in delayed comparison tasks the cue presented before the memory period is necessarily the memorized item.

A variety of tasks, falling in one of these categories, have been used interchangeably to study WM in rodents [4]. From widely popular maze based approaches, taking advantage of the rodents' spatial navigation skills and natural preference for narrow passages (e.g. the radial arms maze [19], t-maze [25], Morris [18] and other water mazes [2]), to non automated delay comparison tasks, probing match and non match conditions (e.g. with objects [23] and odours [20]), and automated freely moving delayed orienting [13] or head-fixed delayed response [16], and comparison [17], licking tasks. If it's true that the same cognitive mechanisms are involved and combined in different behavioral manifestations it is also true that different tasks will pose different challenges to the animals, making it difficult to disentangle general from task-specific behavioral, or neural, observations.

Understanding what a task is asking from the subjects and controlling for how they are solving it is crucial for a meaningful interpretation of the obtained observations. In the case of WM guided behaviors, as it became clear since very early [27], to make claims about the actual use of a memory it's necessary to guarantee that the animals are not "bridging" the memory period through any kind of non-mnemonic embodied strategy. Only such certainty will make possible to correctly characterize the subjects' performance dependence on the memory period duration, interpret deficits caused by behavioral or neural perturbations and identify related neural activity.

The use of behavioral strategies during the memory period is prevented by design in delayed comparison protocols, but although these have been successful taught to other non primate species, like pigeons [28], and rodents can perform them in more naturalistic type of paradigms [6],training true delayed comparison tasks, with both rats and mice, has proved to be difficult and time-consuming in the context of high-throughput automated tasks (see [17] for a recent exception). If the question of interest depends fully in knowing or determining the identity of the to be remembered item then a delayed comparison task seems essential, but if that is not the case and one just needs to guarantee that a memory is needed for the subjects to correctly perform the behavior, delayed response tasks can and have been used with great success throughout the years [9], providing that the appropriate efforts and controls are put in place to monitor and understand how is the task being solved.

Here we developed a fully automated, head-fixed, delayed response task on a treadmill with a long belt that, given its self-initiation and spatial features, was very engaging and easy to learn for the mice which performed a high number of trials per session with a very good performance. Moreover, our setups allowed us to closely monitor animal behavior, namely licks and movement on the treadmill, giving us access to how the mice were solving the task and guidance in designing the appropriate controls to guarantee that a behavioral strategy was not being used to eliminate the need for keeping a memory through the memory period. These made us confident that, like desired, upon the presentation of an auditory cue, mice kept, throughout the memory period, an active representation that allowed them to perform

the correct action when presented with trigger stimulus at the end of it.

2.3 Methods and Materials

2.3.1 Behavioral Apparatus

The results here presented were obtained using three behavioral setups: two of them, used only for behavior, were identical and the third differed only in what was necessary to perform the electrophysiological recordings, namely the possibility of attaching to it a stereotaxic arm, a microscope connected via a flexible moving arm and a light-source - all essential to the insertion of the recording probe. The first two setups were inside the same custom made sound-proof box which was split in two by an internal division, the electrophysiology setup had a dedicated sound-proof box. Each setup was connected to its own dedicated computer with the task being programmed and controlled via Matlab. All setups sensors (rotary encoder, lick detector, belt lap detector) and effectors (speakers, reward valve, intra trial interval (ITI) lights) were controlled via a in-house developed input-output board with a sampling rate of 2082 Hz .

The basic component of each setup was a treadmill formed by two 3D printed wheels and a fabric belt running loosely around both. The back wheel, on top of which the head-fixed mice were placed, had 20 cm of diameter and 5 of width; the front wheel was smaller with 10 cm of diameter and the same width. The axes of both wheels were fitted to ball bearings, mounted on laser cut pieces of acrylic, that were fixed, roughly 30 cm apart, on two 50 x 4 x 4 cm parallel aluminum rails. These two rails were fixed centered on the top face of a hollow cube also made with the same 50 x 4 x

4 cm rails. The belt, with 130 x 5 cm, which covered the top of both wheels and hanged towards the ground, had glued on its surface, approximately 100 cm from one of its ends, a set of bands with a rough texture. The textured surface covered a 15 cm stretch and was used to signal the place where the mice could get reward in the task. To make the animals more comfortable while running a half tube, tunnel like, plastic piece was placed around their body during the task. This was fixed to the setup by a set of optical posts and clamps (Thorlabs) that allowed it to be easily put in place and adapted to each animal position.

To monitor the position of the mice on the treadmill an absolute magnetic encoder (US Digital, MAE3) was fitted to one end of the big wheel axis. A pair of infrared (IR) LED emitter and logic detector were used to monitor each complete lap of the belt. For that they were installed, facing each other, on a custom made piece of acrylic, fixed to one of the top aluminum rails just after the front wheel, that extended towards the floor. In its lower end this piece had the shape of a rectangular prism with approximately 5.2 x 2 x 2 cm with the top and bottom sides open to allow the belt to run through the middle. A 0.4 cm hole was punctured in the belt aligned with the IR emitter and detector. The rectangular prism also served the purpose of maintaining the belt aligned with the wheels.

Mice were head-fixed in the setup to a custom made, 0.2 cm thick, aluminum head-plate. The head-plate was situated on top of the back wheel with each of its lateral edges connected to one of the parallel rails by two optical posts. The posts in each side were connected in a 90° angle allowing to change the position of the head-plate both in the dorsal-ventral (DV)

and anterior-posterior (AP) axis relative to the wheel. The head-plate had a hole that, when the mice were head-fixed, gave direct access to the center of the head-implant allowing for the easy insertion of the recording probes. It also allowed the fixation, on its lower face, of speakers in several different positions and on its upper face, facing the animal, of the reward delivery system - lick-port.

To deliver reward to the mice during the task and monitor their licking lick-ports were custom built out of a 3D printed plastic body to which a water delivery spout and a IR LED emitter and logic detector were fitted. For the delivery spout we used an 18 gauge metal needle with the tip cut and polished. The emitter and detector were fitted and glued to specific parts of the plastic body so that the IR beam crossed the front of the delivery spout allowing us to monitor when the animals licked. The lick-port was fixed to the anterior upper face of the head-plate through a set of mini optical posts and clamps (Thorlabs) allowing for a precise positioning by moving it in the AP and DV axis relative to mice's mouth.

To signal ITI, and illuminate the setups while off-task, two boards of white LED stripes, with adjustable intensity, were attached to the lateral rails of the base cube at the height of the mice when running on the treadmill.

2.3.2 Behavioral Task

2.3.2.1 Experimental Subjects

All mice used in the experiments here presented were male from the C57BL/6 strain. Mice selected to be implanted, and start the training protocol, were typically 3 months old with a weight around 24 gr.

2.3.2.2 Habituation Period and First Time in the Setup

Circa one week before the beginning of the actual training protocol animals started to be water deprived and habituated to being handled. Once a day they were moved to the behavioral room, taken out of their home-cage, given water from a 1 ml syringe and allowed to explore the experimenters' arms and upper torso. This was the only water the animals were allowed to drink during the day.

When accustomed to be handled mice were ready to be placed on the wheel and head-fixed for the first time. To make them feel more comfortable and less stressed the head-plate position was adjusted so that their body was closer to the surface of the wheel and more to the back relative to its apex. The half tunnel was then lowered to cover the body from neck to beginning of the tail. After a few minutes, when the animals had already calmed down, the lick-port was slowly moved towards their mouth until the spout almost touched it.

The first session had a maximum length of 10 minutes, with each session after being increased by 5 minutes until a maximum length of 40 minutes. In each session mice were allowed to drink a maximum of 220 rewards, if this value was reached the session ended. Session by session the head-plate position was progressively shifted upper and towards the apex of the wheel so that the animals reached an ideal running configuration.

2.3.2.3 Training Procedure

All training phases described below were performed in the dark inside the sound-proof boxes. The only exception was the white light signaling the

ITIs.

Phase 1 *Learn to drink* - A 0.3 μl drop of water was delivered to the reward spout, when the mouse licked it another was delivered after 0.5 seconds. Mice moved to the next phase when they managed to get 100 rewards in one session. This happened, typically, within the first 3 sessions.

Phase 2 *Learn to run* - In this phase animals were asked to move a given amount of centimeters, on the wheel without the belt, before a reward was delivered. The initial reward distance was 20 cm and it was increased by 5 cm for each 20 rewards collected until a maximum of 100 cm. Mice were allowed to move to the next phase when totally comfortable running on the wheel, in which situation they would typically collect the maximum amount of reward allowed in 20 to 30 minutes.

Phase 3 *Running on the belt* - The fabric belt was installed on the treadmill. Mice had to run but now reward was delivered 1 cm inside the reward area each time they cross it. Again, mice were allowed to move phase once running comfortable on the belt and collecting a large number of rewards per session.

Phase 4 *Passive association of sound with reward* - Same as in the previous phase but now one of two sounds (5 or 12 kHz pure tones) was played between 8 cm before the start of the textured area and 1 cm inside it. If the sound played was the rewarded one a drop of water was delivered immediately after it ended, if it was the non rewarded sound nothing happened. For animals with an even number the rewarded sound was 5 kHz; for animals with an odd number the rewarded sound was 12 kHz. To keep the animals motivated the probability of the rewarded sound being the one played was

0.8. For both sounds no more than 3 repetitions were allowed. Animals were kept in this phase until getting 1000 rewards across several sessions, which typically happened in the fourth.

Phase 5 *Learn to stop* - As in the previous phase but now mice had to stop for 0.1 seconds to receive a reward. After 3 sessions in this phase, if their hit rate was higher than 0.9 in a 40 trials running window, mice were allowed to progress. The probability for both types of trials was leveled to 0.5.

Phase 6 *Learn to discriminate between sounds* - In this phase the stop criterion was increased to 0.2 seconds, also, to progress to the next phase, mice had now to continue to run when the no stop sound was played. Probability of both sounds was 0.5 but, to discourage the animals from stopping indiscriminately, if the false alarms rate was higher than 0.6 the probability of a no stop sound being played was increased to 0.8. Mice were allowed to progress, after 3 sessions in this phase, when the proportion of correct trials over a 50 trials running window was higher that 0.9.

Phase 7 *Imposing a memory period* - The sound start and end positions were shifted back, relative to the area, by 5 cm each time the mice reached a 0.85 performance over a 40 trials running window. When the sound start location reached the centimeter 25 from trial start the sound was set to randomly begin in the positions 20, 25 and 30 cm. With each successfully completed running window the possible sound start locations increased by 5 cm in each direction until the 11 final possible sound start locations (1,5,10,15,20,25,30,35,40,45 and 50 cm) were reached.

The training procedure (from a habituation to stable performance) lasted

typically two to two and half months. From the originally implanted animals around 60% normally reached stable performance with 30% never learning to run and 10% loosing motivation during the remaining training process.

2.3.3 Head-Implant Surgery

2.3.3.1 Head-Implant

The head-fixing implants were custom designed and 3D printed. The implants were bowl shaped, bottomless and when in position covered the top of the skull of the mice with the edges seating on the interparietal plates, the lateral extremes of the parietal plates and just before the animals' eyes. Being bottomless the implants allowed access to the top part of the mice's skull from a little before bregma to the anterior extreme of the frontal plate. On its most posterior dorsal part the implant allowed for the insertion of two screws, used to attach it to the head-plate. Also on the back, two hollow tubes raising 1.5 cm from the upper surface of the implant and connected to it in a 80° angle, allowed for the protection of ground wires, to be used during electrophysiology, while the mice were being trained.

2.3.3.2 Surgical Procedure

In the surgery day mice were taken from their home-cage and put in an induction chamber connected to the isoflurane delivery system (RWD Life Sciences). When stably anesthetized they were moved to the stereotaxic apparatus (RWD Life Sciences), their snout covered by the isoflurane delivery mask, their eyes protected with eye ointment and the skull immobilized with ear bars. An intracutaneous injection of local anesthetic (Lidocaine)

was then applied on top of the skull, after what a roughly round patch of skin was cut, with surgical scissors, exposing the surface of the skull from the intraparietal plate above the cerebellum to just before the eyes, in the AP axis, and from the lateral edge of one parietal plate to the other in the medial-lateral (ML) axis. The exposed skull surface was then cleaned of any connective tissue and aligned in all three axis.

Two holes were drilled above the cerebellum, each roughly centered in the interparietal plate of one hemisphere and custom made ground pins, to be used during electrophysiology, were screwed to them. A needle tip was then used to gently scratch the skull's surface in a grid pattern and a thin layer of "superglue" was applied covering the entire exposed skull surface and the edges of cut skin around it. After the glue dried out a very thin layer of dental cement was applied over covering the same surface. The location of bregma and two positions just after and before the AP extremities of the coordinates we wanted to target were marked, on the surface of the dental cement, with a bone marker pen, for future reference.

A half a pea chunk of viscous dental cement was then placed on top of the cerebellum, where the screw heads were, and the most posterior part of the implant was lowered, aligned in all three axis, with help of the stereotaxic arm, and pressed onto it. When the hat was solidly glued on its position, dental cement was used to fill the remaining gap between the edges of the implant and the cement covered skull surface. While the cement was allowed to dry, the wires of the recording pins were tuck into their position inside the head implant tubes.

The dental cement covered skull surface was then protected with a layer

of silicone adhesive (World Precision Instruments - Kwik Sil) and the animal was given one intraperitoneal (IP) injection of antibiotic (Enrofloxacin) and one of analgesic (Buprenorphine). With the surgery finished the mouse was gently returned to its homecage and allowed to wake up in an heated environment. Animals were allowed to recover for one week before initiating the training protocol.

2.3.4 Modeling Stop Probability

2.3.4.1 Model Fitting

We used logistic regression to model the probability of the mice stopping upon reaching the reward area. To fit the model we used the Glmnet package [22] that employs cyclical gradient descent to, in the case of logistic regression, minimize

$$-\frac{1}{N}\sum_{i=1}^{N} y_i * (\beta_0 + x_i^T\beta) + \log(1 + e^{(\beta_0 + x_i^T\beta)}) + \lambda[(1-\alpha)||\beta||_2^2/2 + \alpha||\beta||_1],$$

with $\lambda \geq 0$ as a complexity parameter and $0 \leq \alpha \leq 1$ as a compromise between ridge and lasso (ridge:$\alpha = 0$; lasso: $\alpha = 1$).

For all the models in this section we used an elasticnet mixing parameter α of 0.5 ($\alpha = 1$ is the lasso and $\alpha = 0$ is the ridge). Also, all predictions were made on data not used for training, using 10 fold cross validation and the regularization parameter λ was fitted by the algorithm using an inner nest of cross validation again with 10 folds.

2.3.4.2 Model With All Positions Speed Predictors

In *Figures 2.9* and *2.10* two models were fitted to the trials with same sound start location: one using just the sound played as predictor and the other using both the sound and the speed of the mouse in 19 bins linearly spaced between sound start location and reward area start.

2.3.4.3 Model With Single Position Speed Predictors

In *Figures 2.11* and *2.12* one model was fitted per individual bin speed in trials grouped by sound start location. In each model the sound played and the speed of the mouse in one of the 19 memory period's bins were used as predictors.

2.3.4.4 Model Performance

The performance of the models (how well were we able to predict if the animals stopped or not) was accessed via the area under the receiver operating characteristic (ROC) curve (AUC). The ROC curve is created by plotting the hit rate (true positives) of a model against the false alarm rate (false positives) at various threshold settings. Our thresholds went from 0 to 1 in 0.001 increments.

2.3.4.5 Fraction of Variance Calculation

To evaluate how both predictors, sound and speed, were contributing to the predictions being made by the models we calculated the fraction of variance associated with each when multiplied by its respective model

coefficient. For each predictor i of n:

$$Fraction\,of\,Variance = \frac{Var(P_{:i} * B_i)}{\sum_{j=1}^{n \neq i} Var(P_{:j} * B_j)},$$

where each column of P is the set of values of 1 of n predictors and B is an array with the coefficients atributed by the model to each predictor.

2.4 Results

2.4.1 Performance in the Task

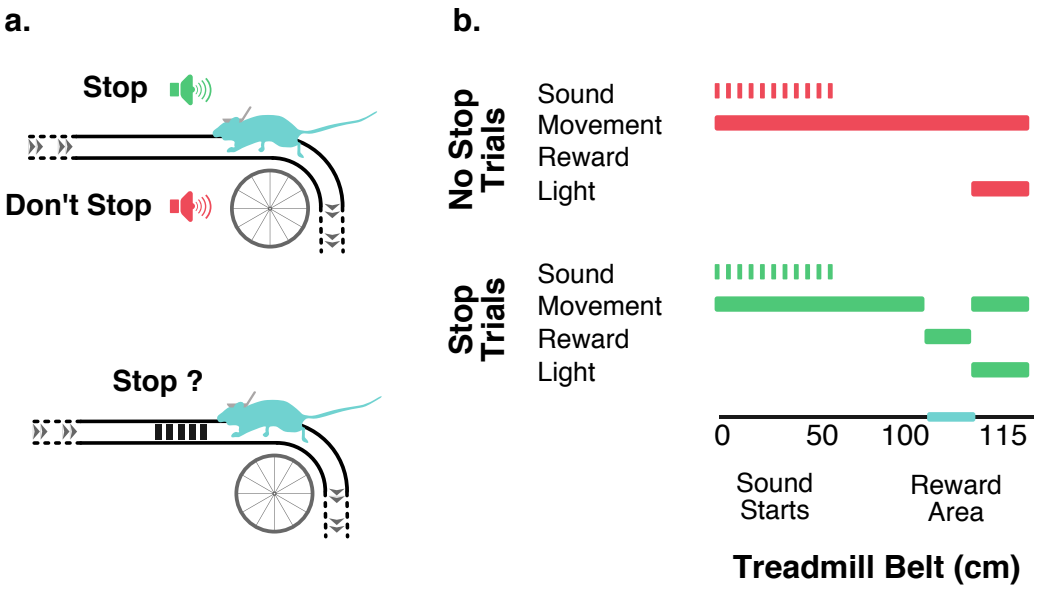

Figure 2.1: Head-fixed Delayed Response Task on a Treadmill: (a) Head-fixed mice running on a passive treadmill with a long belt had to decide to stop, or not, on a textured area depending on the identity of a sound (5 or 12 KHz pure tone) played a given distance before. (b) All task contingencies were dependent on the position of the mouse in the belt. In each trial one of two sounds started randomly in one of 11 possible locations (1, 5, 10, 15, 20, 25, 30, 35, 40, 45 and 50 cm from trial start) and ended 8 cm after. At centimeter 100 from trial start the animals encountered the 15 cm long stopping area, where they could express (or not) the reward triggering behavior: stopping. If the stop meaning sound had been played and the animal stopped it received a drop of water (hit trials). If the no stop meaning sound had been played the animal had to continue running and received no reward (correct rejection trial). No punishments were used in both types of incorrect rials (false alarm and miss trials). When the animals left the textured area a light was turned on for a 15 cm ITI interval.

In our task, head-fixed mice, running on a passive treadmill with a long belt (130 cm), had to decide to stop (or not), upon reaching an area marked

with a textured fabric, depending on the identity of a sound (5 or 12 KHz pure tone) heard some centimeters before, but not present at the final decision moment (*Figure 2.1 a*). Unlike what is more common in automated behavioral assays used in the neuroscience field the events of our task were not set in time but in space (*Figure 2.1 b*). This meant that the mice's movement on the treadmill determined if and when would they initiate a new trial and encounter a new event, as well as the duration, in time, of events and inter-event intervals.

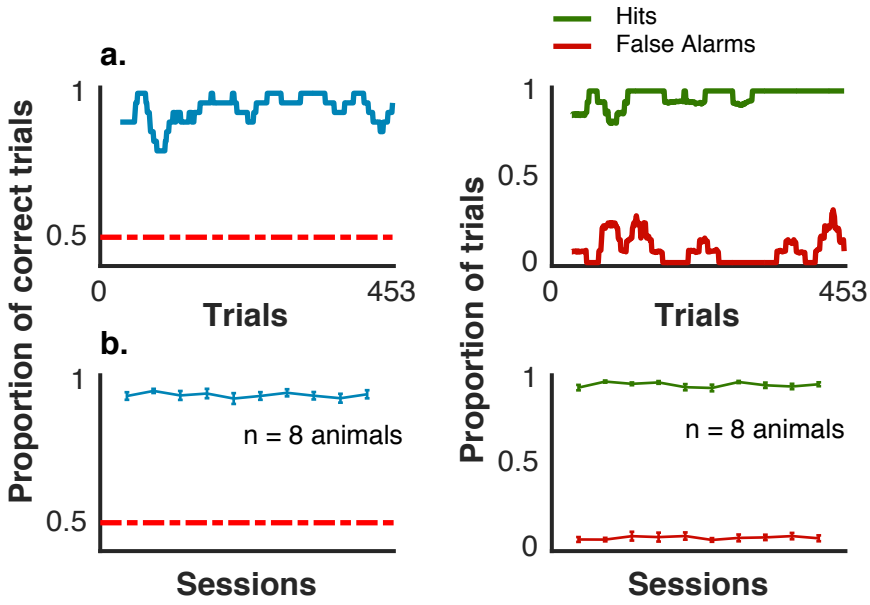

Figure 2.2: Mice Performance: (a) Left: running performance of one animal in a single session (30 trials window). Right: running hit and false alarm rates in the same session (30 trials window). (b) Left: mean performance of 8 animals across 10 sessions (error bars are for standard error of the mean (SEM)). Right: hit and false alarm rates for 8 animals across 10 sessions (error bars are for SEM).

Mice performance in the task was very good and robust both within a single session (*Figure 2.2 a*) and across different sessions (overall mean

performance of 0.95 with performance > 0.85 for all sessions of the 8 animals; overall mean hit rate of 0.96 with hit rate > 0.90 for all sessions of the 8 animals; overall mean false alarm rate of 0.05 with false alarms < 0.2 for all sessions of the 8 animals) (*Figure 2.2 b*). The natural time penalty associated with stopping was enough for the mice to refrain from doing it when not necessary. Also, within session, we didn't normally observe slow performance oscillations related to motivation: the running aspect of the task, which seemed to be engaging for the animals, together with it being self initiated probably contributed to this.

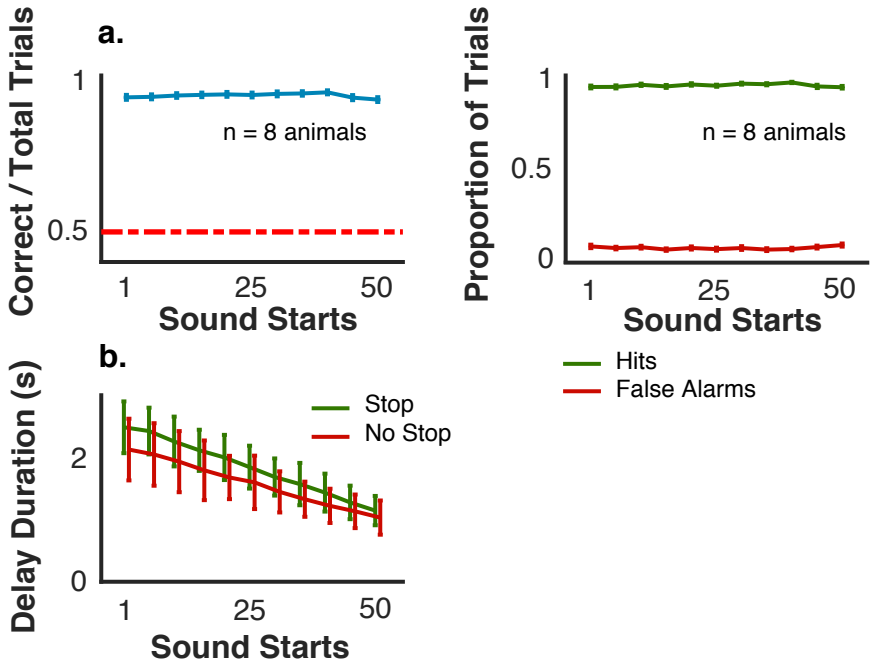

Figure 2.3: Performance Across Sound Start Locations: (a) Left: performance of the animals in trials grouped by sound start location (error bars are for SEM). Right: hit and false alarm rates in trials grouped by sound start location (error bars are for SEM). (b) Mean memory period duration in time, across sound start locations, for stop and no stop trials (error bars are for standard deviation (SD)). 8 animals and 10 session per animal for all the above.

The difficulty component of behavioral tasks aimed at probing WM is traditionally placed on the amount of time the subject needs to sustain the memory representation before using it. Unlike in other tasks, where mice report their choices by licking, the reward triggering behavior in ours, stopping, was different from the reward consumption behavior, a fact that allowed us to avoid impulsivity confounds and establish longer memory periods. The mean duration, in time, of the memory period varied in quasi-linear fashion with its length: mean hit trials delay duration 2.5 and 1.15 seconds for the longest and shortest memory period; mean correct rejection trials delay duration 2.14 and 1.03 seconds for the longest and shortest memory period (*Figure 2.3 b*). Mice took, in mean, more time to cross the memory period in stop than in no stop trials. Such happened because they tended to slow down before stopping, a feature more visible in the longest memory periods where the two behaviors had more space to diverge. Contrary to what might have been expected, memory period duration had no significant visible effect on the mice's performance in the task (*Figure 2.3 a and b*). If something performance was even a little worst in the two shortest memory periods (performance = 0.947,0.955 and 0.939 for the longest middle and shortest delays), what might have been related with the speed dynamics of the animals while solving the task.

2.4.2 Speed Behavior in the Task

Our setups allowed us to monitor the movement of the mice on the treadmill giving us access to their speed, throughout the trials, while solving the task. Being head-fixed, moving on the wheel was the primary way mice

had to manifest their behavior and the only that allowed them to achieve their goal. Animals had to close the distance between sound and stopping area location to collect their reward or continue running to the next trial, the speed at which they did it was the manifestation of a personal strategy and not determined by the task itself. Also, despite the fact of it being a one dimension variable, the observed speed was the result of a coordinate process that engaged the full body of the animals.

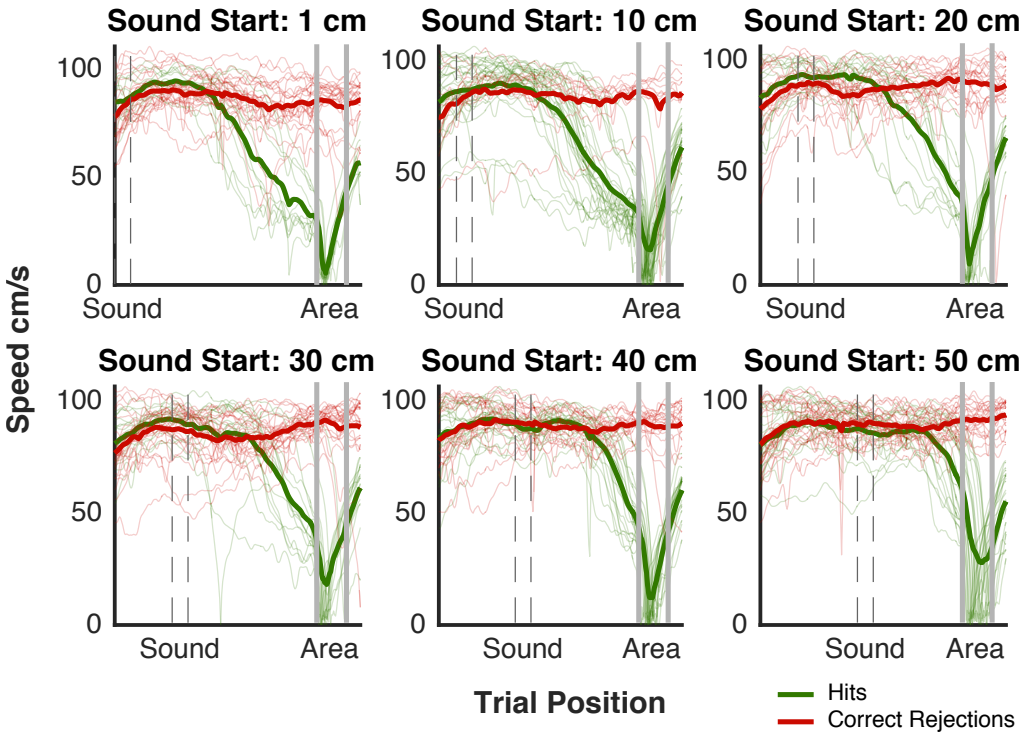

Figure 2.4: Mice's Speed Behavior: Individual trials and mean (thick lines) speeds of one example animal in hit and correct rejection trials across 6 of the 11 possible sound start locations.

We found that in our task, regardless of a fair degree of variability from

trial to trial, animals adopted characteristically different speed strategies in hit and correct rejection trials. These strategies were consistent across the different sound start locations, with mice seemingly employing a general strategy posteriorly modulated by the different lengths of the memory periods: "stretched" in the longer "compressed" in the shortest ones (*Figure 2.4*). Moreover, they were not a single session epiphenomenon being used by the mice across days to navigate the task (*Figure 2.5*). Different animals adopted different behaviors, but common themes existed (*Figure 2.6*). All

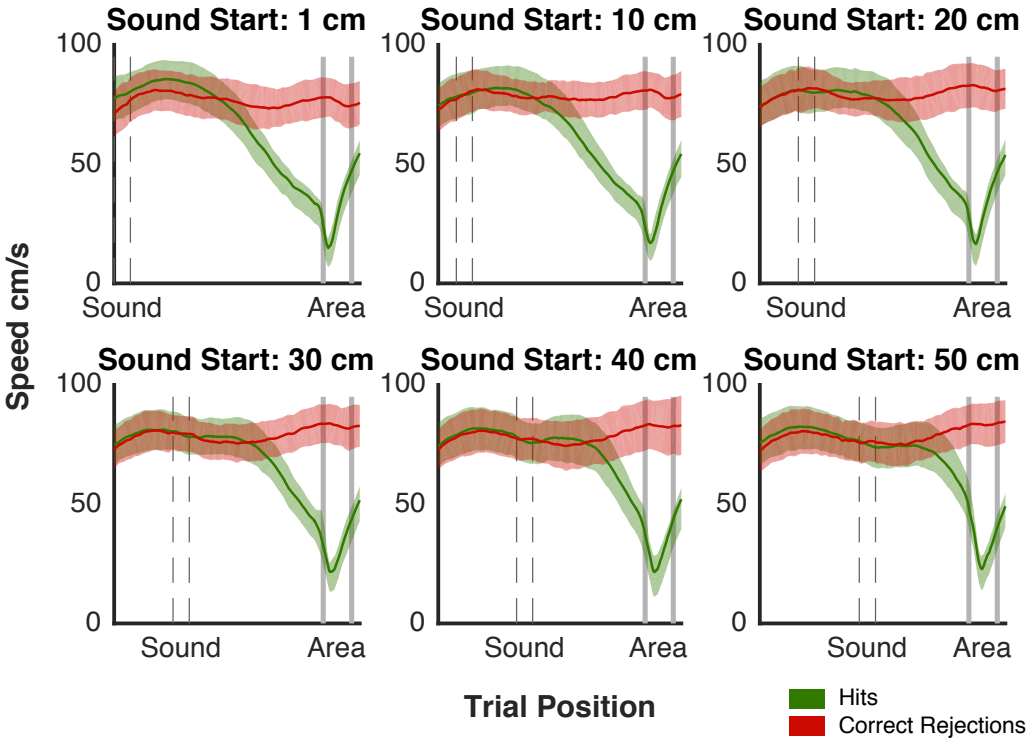

Figure 2.5: Mean Speed Behavior: Mean speeds of 10 sessions, for one animal, across sound 6 of the 11 possible start locations, for hit and correct rejection trials. Error bands are for the SD.

except one animal (bM71) slowed down after trial start, waiting for a cue to tell them what to do, until reaching the sound start position. If the rewarded/stop sound was played mice (again except bM71) executed a parabolic like speed trajectory accelerating and then decelerating before stopping in the area. If the no stop sound was played 5 of the 8 animals accelerated after sound onset until reaching a plateau speed and crossing the area into the next trial. Interestingly three of the animals (bM59,71,73) only accelerated around or after the last possible sound start position. Given that, except for trials with that specific sound start, nothing marked that position, this shows that mice had a good notion of the task rules and their position on the treadmill belt. It also hints to the possibility that, for these animals, the task was effectively a stop sound detection task with the no stop sound having no meaning attached to it.

In theory, looking at the speeds of the mice in incorrect trials might have offered us insights about the reasons behind the mistakes. In practice this was made difficult by the small number of miss and false alarm trials. Inspecting the same sound start mean speeds of incorrect trials (*Figure 2.7*) sugests, for instance, that in bM59, bM67 and, less clear, in bM73 and bM61, false alarm trials there is no acceleration after the sound, as there is in the same mice hit trials, which could indicate that the mistakes were committed because the animals failed to hear or didn't identify the sound correctly. In bM69's false alarm trials it seems that the animal misidentified the sounds, accelerating after sound onset as if the tone played was the one meaning stop. Again, due to the short number of incorrect trials, this is just anecdotal evidence. For more concrete conclusions one would need to

go deeper on noisy single trial speed analysis, we don't pursue that question here.

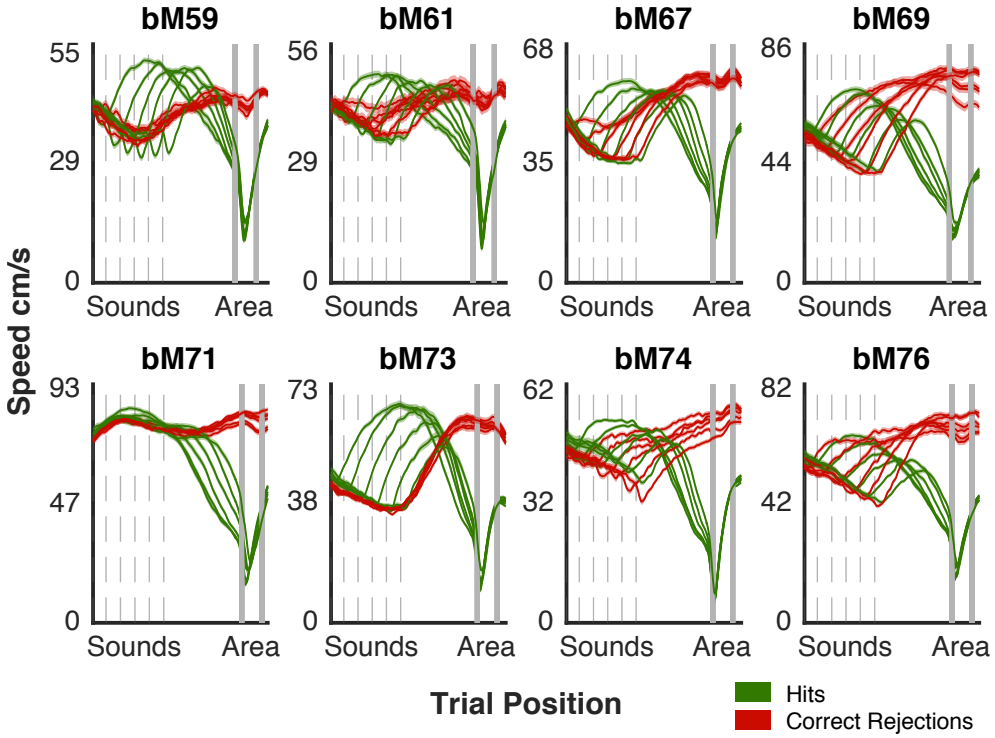

Figure 2.6: Mean Speed Behavior All Animals: Mean speeds of 10 sessions, for all animals, across sound start locations, for hit and correct rejection trials. Error bands are for the SEM.

Collectively, and even with across mice nuances, the speed data collected during the task revealed the existence of mean stereotyped behavioral strategies that were visibly different between the two trial types. This observation raised two concerns:

- Mice could be using the speed difference between hit and correct rejection trials as a cue to solve the task, this way avoiding the cognitive

effort associated with keeping a memory.

- The stereotyped strategies observed during the memory period might be the sign of an automatic, ballistic like, type of behavior in which, upon sound presentation, mice would engage in a predetermined motor plan with no need of cognitive guidance.

To address these issues and guarantee that our task was, in fact, forcing the animals to use a WM while solving it, we designed and implemented a set of data and behavior based controls presented in the next two sections.

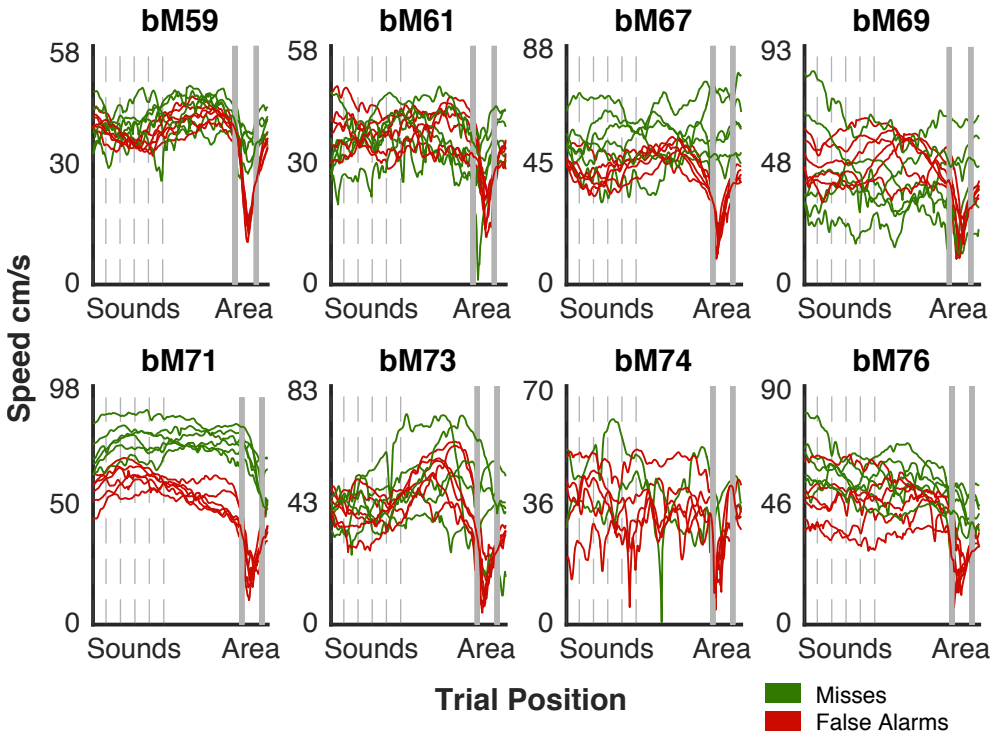

Figure 2.7: Mean Speed Behavior in Incorrect Trials: Mean speeds of 10 sessions, for all animals, across sound start locations, for misses and false alarm trials.

2.4.3 Predicting Stop Behavior

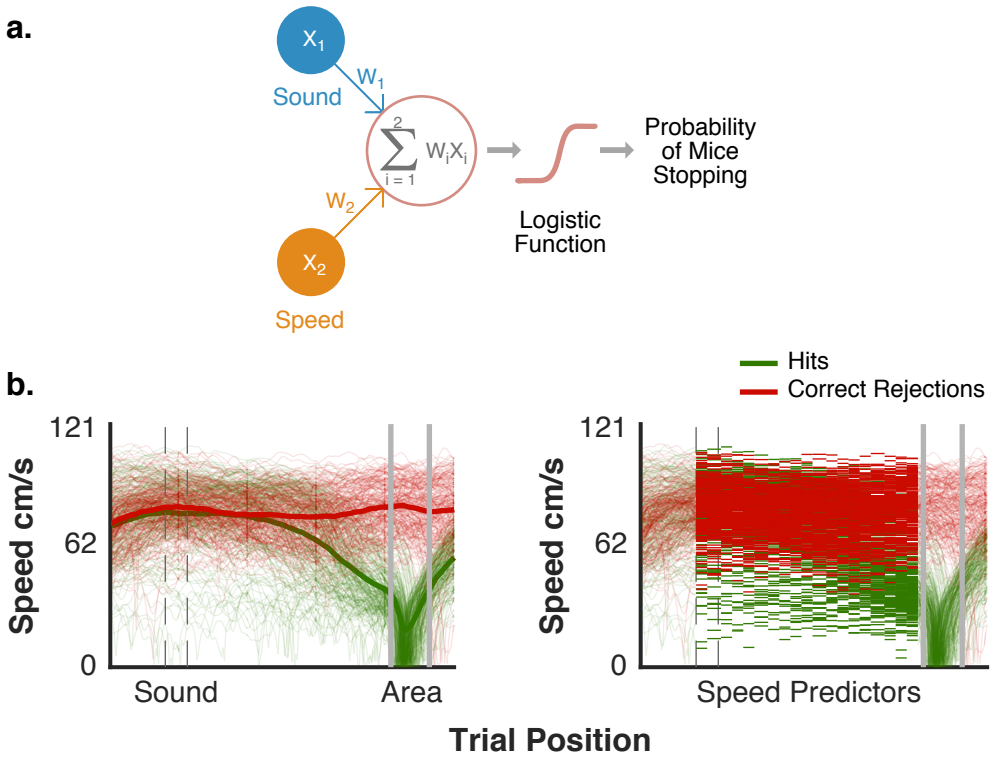

Figure 2.8: Predicting Stop Behavior: (a) Using speed and the sound played as predictors we applied logistic regression to predict the probability of the mice stopping in the reward area in any given trial. (b) As predictors to the model we used the sound played and speed calculated in 19 bins of the same size between sound start and area start.

Despite the different mean speed trajectories individual trials showed a fair degree of variability among same trial type speeds and of overlap between different trial type speeds (*Figure 2.4* and *Figure 2.8 b*). We took advantage of these facts to quantify how well we could predict the probability of the mice stopping (*Figure 2.8 a*), when reaching the reward area, based on the sound played and the speed at which they were running in several

discrete positions of the memory period (*Figure 2.8 c*). Doing so provided us with a notion of how predictive of the animal behavior, at the reward area, speed actually was and of its relative importance, compared with the sound identity, when both were used as inputs to the model.

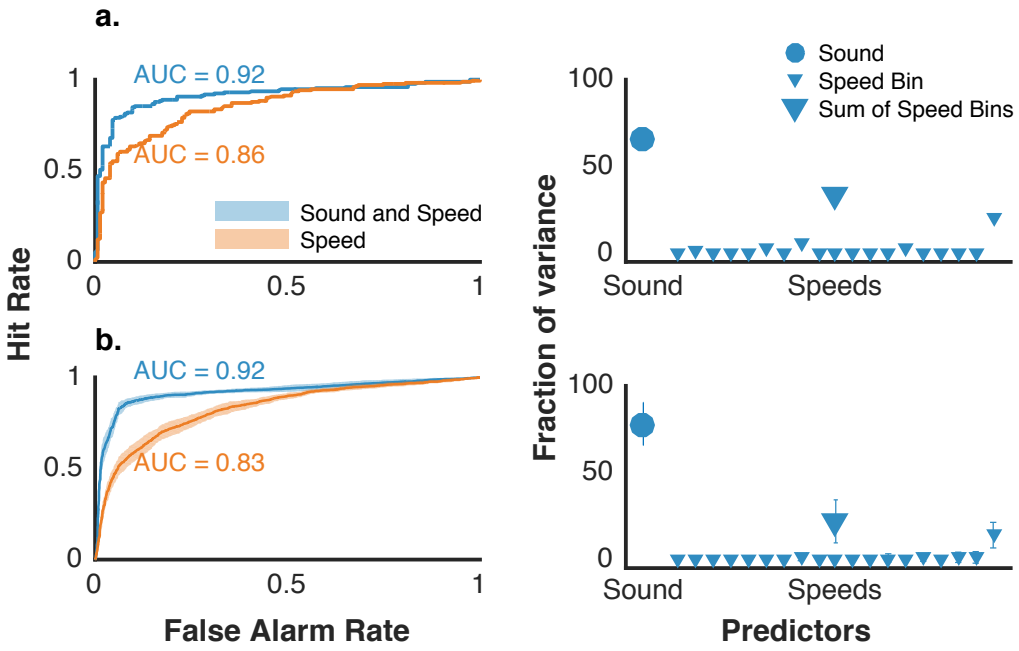

Figure 2.9: Predicting the Stopping Behavior of One Animal: (a) Left: ROC curves and performance measured as AUC of models using sound and speed (blue) or just speed (orange) to predict one animal behavior (stop or not stop) in trials with the same example sound start location. Right: Fraction of variance associated with the predictors of the model in which both sound and speeds were used as inputs and which performance is showed in the left. (b) Left: same as above but now for the mean ROC and AUC of models fitted separately in trials grouped by sound start location. Error bands are for SD. Right: Same as above but now for the fraction of variance means of models fitted separately in trials grouped by sound start location. Error bars are for SD.

As expected, given the mice's extremely good performance in the task, a model using sound and speed at all positions in the memory period was able to predict very well (AUC $>$ 0.9 for all animals in all sound start locations)

the stopping behavior of the mice - blue curves in *Figure 2.9 a,b left* and blue bars in *Figure 2.10*. Interestingly, though not totally surprising given the knowledge that mice tended to slow down before stopping, speed alone was also very predictive: a model fitted using speed in all 19 positions as the only input was able to predict stopping behavior also quite well (AUC > 0.75 for all animals in all sound starts) - orange curves in *Figure 2.9 a,b left* and orange bars in *Figure 2.10*.

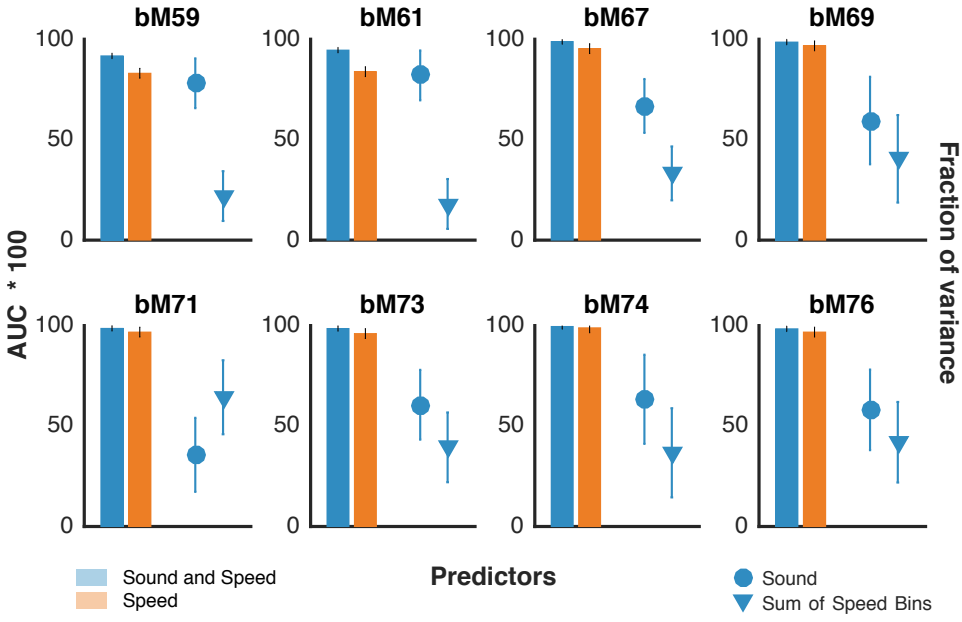

Figure 2.10: Predicting the Stopping Behavior of All Animals: Performance (AUC) of a model using sound and speed (blue) or just speed (orange) as predictors (left of subplots), and fraction of variance associated with the each of the predictors (sound and speed) in the model using both (right of subplots). Error bars are for standard deviation.

The adopted speed behavior was correlated with the auditory cue presented to the animals, especially closer to the area, so it was possible that

speed's predictive power was inherited through its association with sound. To disambiguate this we calculated the fraction of variance (*see methods section*) associated with both sound and speed when used together as inputs to the model. As showed in *Figure 2.9 a,b right* and *Figure 2.10 right*, sound was more informative of the behavior of animal in all but one mouse (bM71).

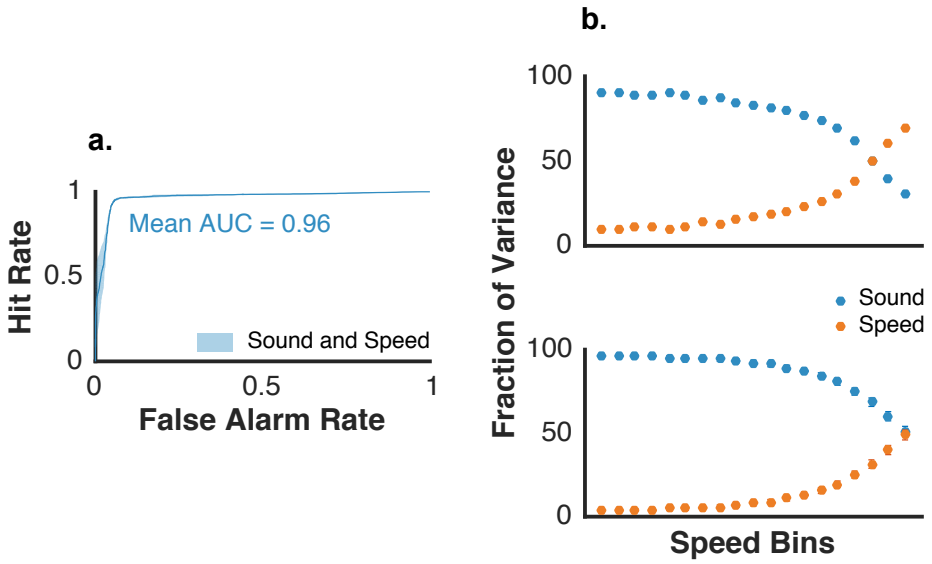

Figure 2.11: Predicting Stop at Different Memory Period Positions : (a) Mean performance, in the 19 speed bins of a single memory period length, of a model using both sound and the speed in each bin as predictors. Error bands are for standard deviation. (b) Top: fraction of variance associated with each predictor in the models run for each of the 19 speed bins for the same memory period length and animal as in (a). Bottom: Same as above but with the mean fraction of variance per speed bin across all 11 sound start locations. Error bars are for standard deviation.

Comparing the plots in *Figure 2.10 right* with the ones in *Figure 2.6* we can see that the relative importance of speed as predictor varies together with the difference, close to the stopping area, of hit and false alarm trials' speeds, also, as shown in *Figure 2.9 a,b right*, the speed information used

by the model in the prediction came, almost exclusively, from these bins where the difference in speed between trials where mice stopped and didn't was bigger. The information of immediate previous positions was correlated with the one from the last bins and thus largely redundant. This was a poor description of the mice behavior, because it was just using, to predict the probability of a mouse stopping, speed information from where the animal was already very close to do it, and not telling us anything about how predictive speed was throughout the complete memory period.

To address this issue we ran a different model per speed position bin to determine how well could we predict the mice stopping behavior, along the entire memory period, based on the sound and the speed at each specific position. All the different position models were able to classify very well (mean AUC > 0.9 for all animals in all positions of all sound start trials) if the animals were in a trial where they were going to stop or not (*Figure 2.11 a*), but now the fraction of variance associated with each predictor in each of the models gave us a more realistic view of their relative importance in the different segments of the memory period (*Figure 2.11 b*).

As the animals got closer to the area, and their speeds diverged more and more depending on if they were going, or not, to stop, speed's predictive power increased and sound's decreased (because, though few, animals made mistakes). The magnitude of this change was related with the magnitude of the speed difference, in those positions, between trials in which the mice stopped or didn't. In longer memory periods speeds diverged more and so the fraction of variance associated with the speed predictor was higher than for shorter memory periods where individual trial speeds from both trial

types overlapped considerably. This can be seen by comparing the fraction of variance associated with each predictor in the longest memory period of one animal sessions (*Figure 2.11 b top*) with the mean fraction of variance across all memory periods of the same animal (*Figure 2.11 b bottom*).

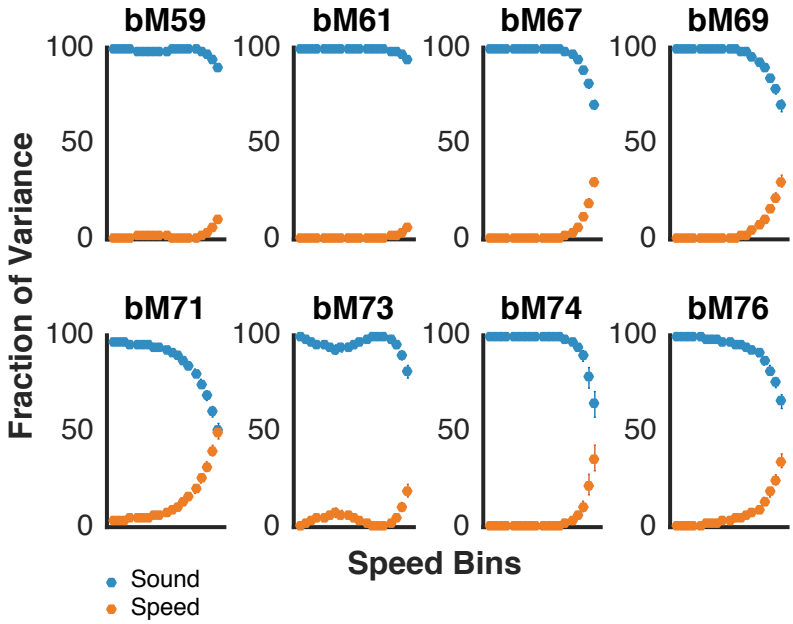

Figure 2.12: Predicting Stop at Different Memory Period Positions in All Animals : Mean fraction of variance associated to each predictor in the models ran for each of the 19 speed bins across all sound start locations. Error bars are for standard deviation.

For all animals (*Figure 2.12*), even in the memory period position closest to the stopping area, only in one (bM71) was the mean fraction of variance, across sound starts, associated with speed equal to the one associated with sound. For all the other mice sound was a more reliable predictor of the stopping behavior than speed. Taking all positions, from sound to stopping area, in all animals, speed is almost not predictive of the stopping behavior

throughout the majority of the memory period.

Together these results show that, at the single trial level, despite the visible mean differences between conditions, speed, by itself, does not allow the unambiguous identification of trial type afforded by sound, making it thus unlikely that it could be used by the animals to distinguish between conditions during the memory period, this way preventing the need for the use of a WM representation in guiding behavior.

2.4.4 Probing Behavioral Strategy Flexibility

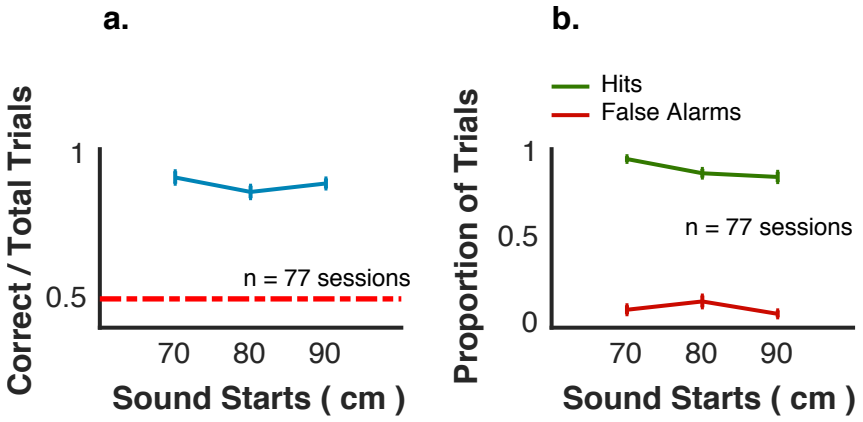

Figure 2.13: Performance in Catch Trials: (a) Performance of 7 animals in trials with 1 of 3 extra sound start locations presented infrequently throughout a session. (b) Hit and false alarm rates on the same trials. Error bars are for SEM for both (a) and (b).

The other concern raised by the observed mean speed trajectories was that their apparent stereotypy could signal an automatic motor plan. In such scenario, to solve the task, mice wouldn't need a WM or to make a decision upon reaching the stopping area. After the sound, an automatic, "reach" like, motor plan would kick in, taking control of behavior without

the need for any cognitive intervention. To test if this was how our animals were solving the task or if, as we intended, the mice were actually making a WM guided decision when reaching the stopping area, we devised a set of behavioral controls. These were aimed at probing the automaticity of the behavior and the role of the physically marked stopping area in the task.

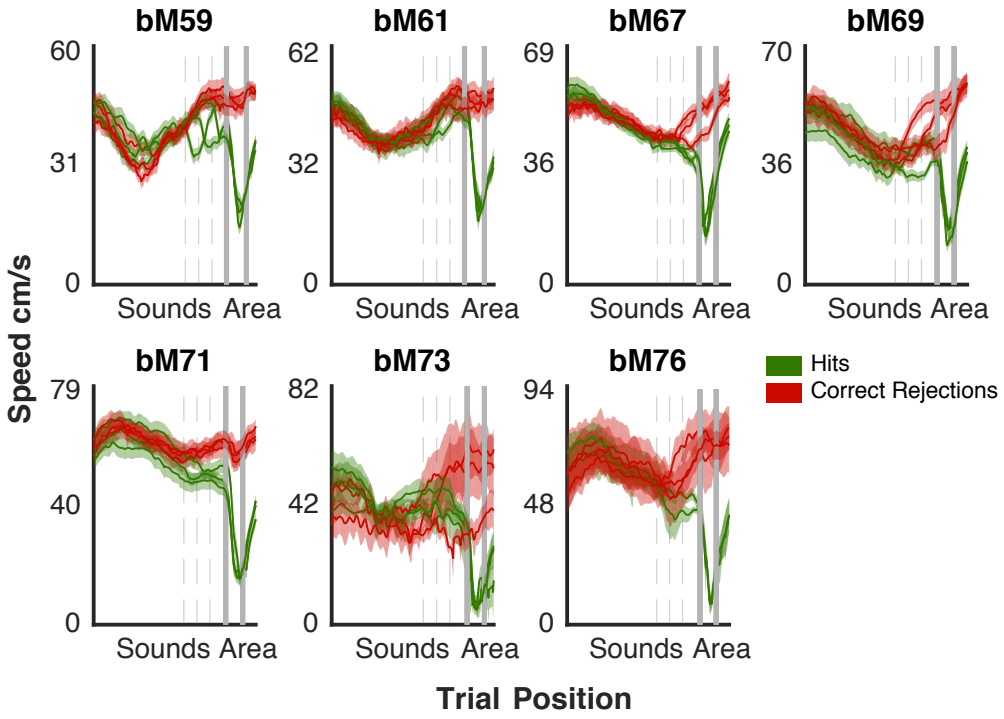

Figure 2.14: Mean Speed Behavior Catch Trials : Mean speed for 7 animals, across sound start locations, for hit and correct rejection trials. Error bands are for the SEM.

The brain tends to automatize frequent and repetitive behaviors, alleviating the need for effortful cognitive control, and making them faster, but also less flexible. We wanted our mice to know the rules and contingencies of the task and then to be able to adapt their behavior in order to meet

them.

One way we used to test the mice's behavioral flexibility was to introduce infrequent trials (1 in 100) with a unusual sound start location (70, 80 or 90 cm), which we called catch trials. Despite the sound start location in these trials being considerably closer to the stopping area than normal, leading to different speed behaviors (*Figure 2.14*) from the ones observed in the frequent sound start location trials (*Figure 2.6*), mice were able to adapt and perform very well in the task (mean performance = 0.92, 0.87 and 0.90 for sound starts 70,80 and 90 respectively) (*Figure 2.13*).

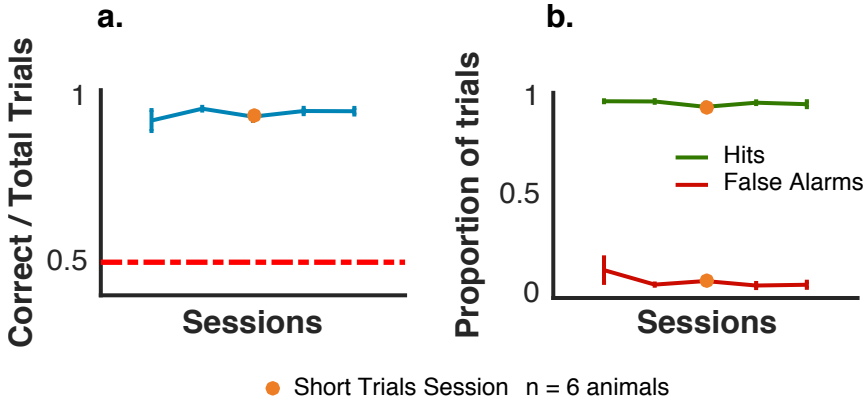

Figure 2.15: Performance in Session with Stopping Area in Different Location: (a) Performance of 6 animals in a session where the distance between the reward area and the trial start was shortened and in two sessions before and after. (b) hit and false alarm rates on the same sessions. Error bars are for SEM for both (a) and (b).

Another way to test behavioral adaptability was to change the environment animals knew and where they had learned the rules of the task. To achieve that we changed the position of the stopping area in a single session, moving it closer to the trial start. Again animals were able to adapt, both in terms of their performance (mean performance = 0.94 with all the six

sessions from different mice above 0.9) and the speed strategy used in that particular session (*Figure 2.15* and *Figure 2.16*).

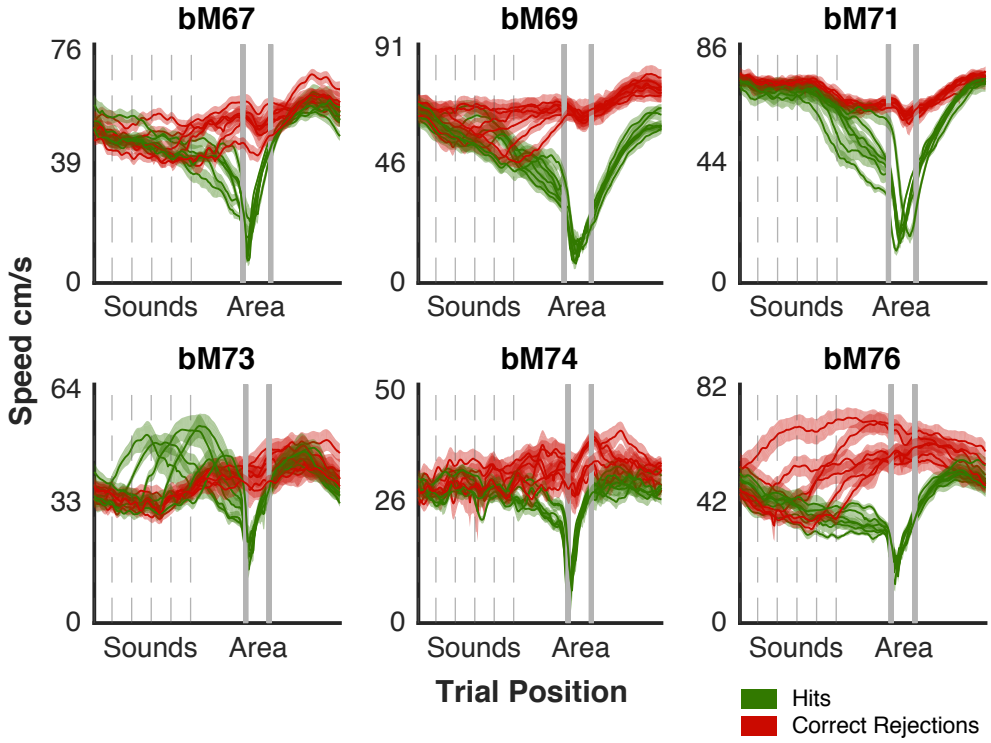

Figure 2.16: Mean Speed Behavior in Session with Stopping Area in Different Location: Mean speed for 6 animals, across sound starts, for hits and false alarm trials in a session where the distance between the reward area and trial start was shortened. Error bands are for the SEM.

In a situation where the animals didn't need the physical presence of the area to commit to a stop, or no stop, response, having a predetermined motor plan that, reacting to the sound, would take them to or through the stopping position, the removal of the texture that signaled the area wouldn't, or would just partially, impair their performance. To probe the role of the stopping area in the task, we completely removed the physical cues that signaled it

for one isolated session. For all task purposes the area still existed and all contingencies associated with it were valid, there was just nothing signaling it.

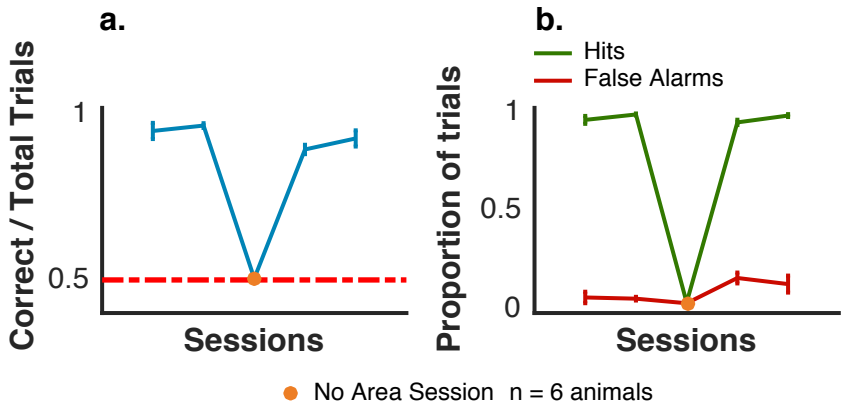

Figure 2.17: Performance in No Area Session: (a) Performance of 6 animals in a session where the texture marking the stopping area was removed and in two sessions before and after. (b) hit and false alarm rates on the same sessions. Error bars are for SEM for both (a) and (b).

Performance of all animals in the no area session dropped to chance level (mean performance = 0.505 with all sessions within 0.49 and 0.51) (*Figure 2.17*) with the hit and false alarm rates going virtually to 0 (mean hit rate = 0.031 with all sessions < 0.04; mean false alarm rate = 0.029 with all sessions < 0.045). Without a physical cue to mark where they had to stop mice just continuously ran through all trials in the session (*Figure 2.17*). Removing the area was a drastic change, it might have happened that mice tried to stop in the first trials of the session, failed by little the exact area location and then disengaged for the remaining session's trials. In *Figure 2.19* we can see that the mean speed of the first 5 trials of the no area session doesn't reveal evidence for that. Across the stopping area the mean speed

trajectory in these trials is essentially as flat as in the remaining session trials, and different from the mean of the first 5 trials in the sessions before and after, where a clear dip is seen. Mean speeds of the first trials in the sessions before and after are noisy because the beginning of the session is when animals tend to make more mistakes.

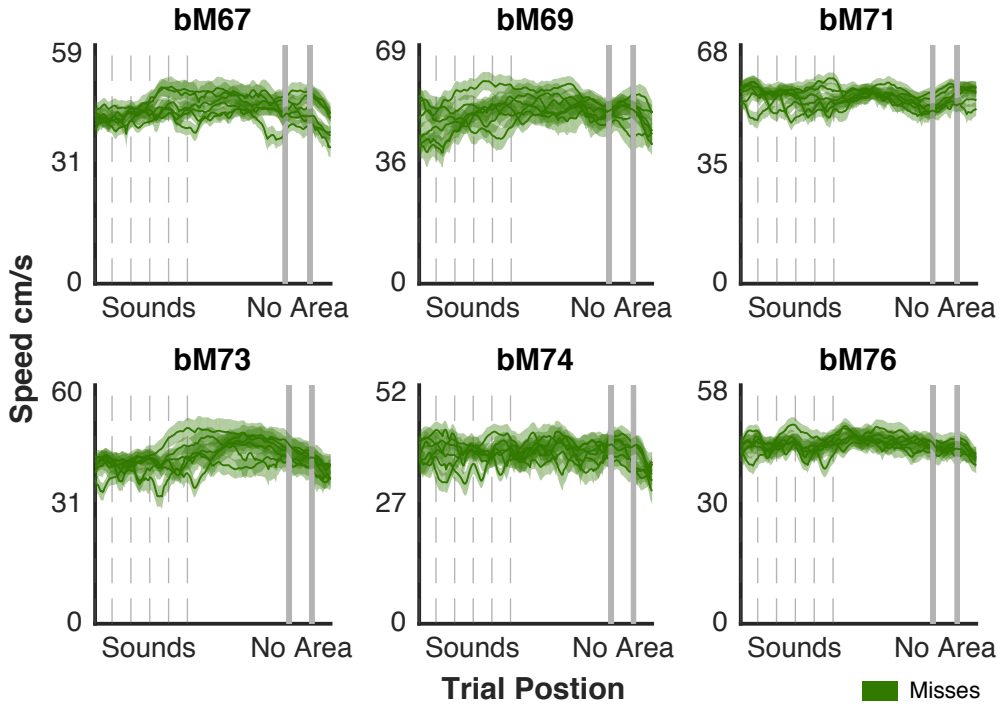

Figure 2.18: Mean Speed Behavior No Area Session: Mean speed for 6 animals, across sound start locations, for miss trials in a session where the texture marking the reward area was removed. Error bands are for the SEM.

Together these controls showed us that the speed trajectories we observed were not the result of automatic and inflexible motor plans, but rather a manifestation of the way the animals chose to perform the task, depending on the sound played and their position in the treadmill. Accordingly, they

showed to be flexible and changed when the mice had to adapt to perturbations in the regularities of the task, like the ones imposed by our two first controls. The no area control proved us that the stopping area actually acts as trigger, or go signal, for the animals to express, or not, the reward associated behavior: stop. To do so correctly, as they mostly do, a memory was necessary to guide they're behavior during the the cue free memory period.

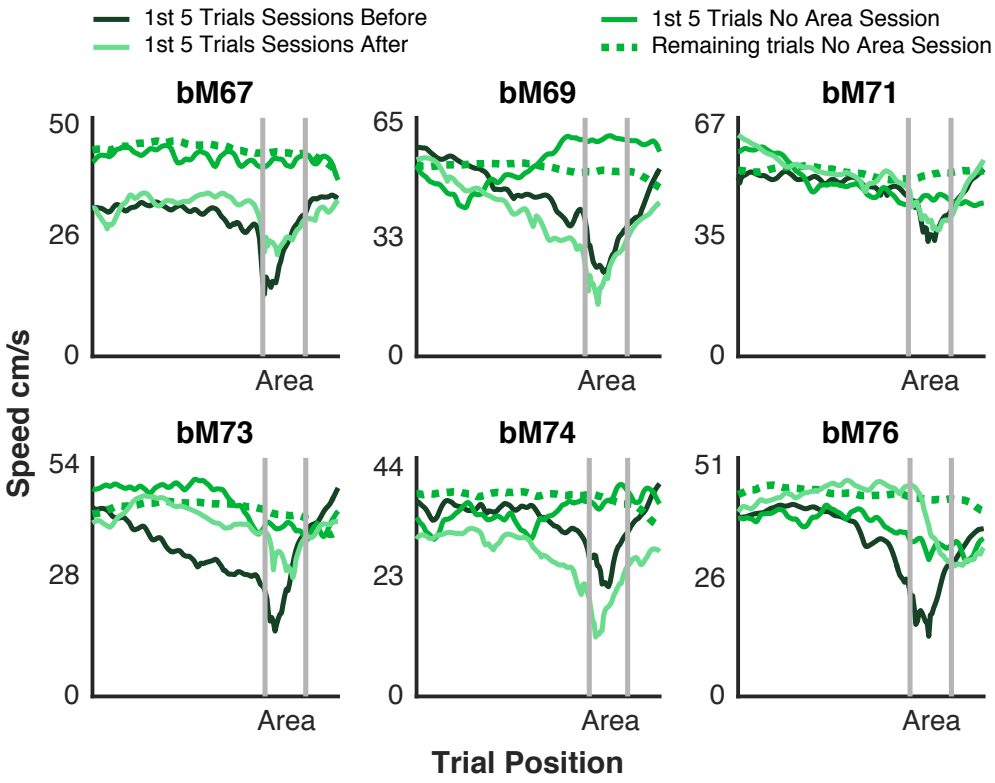

Figure 2.19: Mean Speed Behavior First Trials of No Area Session: Mean speeds of the first 5 stop trials in the no area session compared wit the means of the first 5 trials of one session before and after, and with the mean of the remaining stop trials of the no area session.

2.5 Discussion

To investigate WM related activity in the mPFC we developed a head-fixed spatial response task on a treadmill. The task combined the two interesting aspects of being head-fixed, which allowed for acute multi-electrode silicone probe recordings, and involving spatial and running competences which, combined with the timing of events being determined by the movement of the mice, made it engaging to perform and easy to learn, presumably tapping on natural behavioral competences. As a consequence mice performed typically around 400 trials per session with a very good and consistent performance in one session, along several consecutive sessions and for all sound start positions (*Figure 2.2* and *Figure 2.3)*. All these had obvious positive features, but the almost absence of error trials also had its drawbacks and conditioned our analysis at several steps of the work (e.g. by impeding a detailed investigation of the motifs behind the mistakes and being detrimental to the possibility of disentangling cue from decision related neural activity). One desirable improvement of the task would thus be to make it more difficult. Such could be achieved by using, as cue, a range of different frequencies, with a category boundary defining which should be associated with either stopping or not.

Other relevant feature of our task was the fact that the animals could not immediately perform the response behavior, stopping, unlike in other common head-fixed paradigms [11]. This made it easier to introduce comparatively longer delay periods by avoiding anxiety driven early responses. Separating decision and consumatory behaviors also benefits the interpreta-

tion of task related neural activity.

In our results there were no apparent effects of delay period duration on the animals' behavior. This was contrary to the common observation that performance decreases with delay period duration increase, presumably due to a degradation of the WM content. It is worth noting that in our task the mean duration, in time, for the stop trials with the longest memory period, in distance, was 2.5 seconds, very distant from the 10 minutes it took for performance to drop to chance level in a previous t-maze study [5] or the 120 minutes in a radial-arm maze one [1], for instance. It seems thus that memory maintenance per se is not the factor that most contributes to the difficulty of this types of task.

One noteworthy caveat of the task is the fact that only one of the conditions (auditory cues) gives the mice the possibility of obtaining a reward, putting the task in the universe of Go/No Go tasks. The fact that the animals decide when to progress in the task eliminates the confusion, in no go trials, between correct responses and omissions, a regular caveat associated with these types of task. Nevertheless, the unbalanced nature of the conditions is still a problem with the significance of both sounds varying not only in terms of the associated behaviors (stop or not) but also of their value to the animals. Such fact might contribute to behavioral differences, like the higher acceleration seen in almost all animals after the presentation of the rewarded sound, but also change completely the way some animals solve the task, such as in animals bM59 and bM73 that don't show any behavioral indication of attributing meaning to the non-rewarded sound, which might indicate that their just detecting the reward one. The unbalance between

conditions also makes it more difficult to separate reward from decision related neural activity and interpret observed trial type specific differences. One possibility to deal with this problem would be to add a second stopping area and have each of the sounds correspond to one, making the task more similar to a T-maze navigation [12] [29]. Another, more radical, possible transformation would be to get rid of the physical stopping area and use a second set of sensory cues to signal a period during which the animals could stop to receive reward. This option would introduce a better control and bigger flexibility of the task conditions (e.g being able to precisely determine and vary the exact duration of the memory period), but would also probably devoid it of some of its more naturalistic aspects.

Our setups allowed us to monitor the speed of the animals running on the treadmill, which gave us access to their behavior throughout the trial and in particular during the memory period. This information is particularly important because: 1. moving was the way mice had to progress in the task and reach the intended goals and 2. high speed running in the treadmill engages the entire body in a synchronous activity that, given the fact that the animals were head-fixed, left no visible degrees of freedom for other behaviors that could be used to bridge the memory period.

Monitoring speed showed us that the animals were using different, seemingly stereotyped, speed strategies in hit and correct rejection trials (*Figures 2.4 - 2.6*) and led to the design of a set of behavior controls (*Figures 2.13 - 2.19*) that proved us that those were a consequence of the way mice chose to solve the task rather than a condition for them to perform it correctly. Measuring speed also allowed us to conclude that, despite the mean trajec-

tories, trial to trial variability meant that speed by itself was a rather poor predictor of the animals' stopping behavior for the majority of the memory period length, making it very unlikely that it could be used as cue to avoid the need for memory maintenance. Mice were thus solving the task as they were intended to: keeping a WM, through a task relevant cue free memory period, and using it to perform the appropriate action when asked for by a specific trigger - in our case the stopping area. This is comparable to other delayed response tasks commonly used to study WM [13] [16].

Minute monitoring of the mice's speed also allowed us to explore its representation in the neural activity and its relation to WM encoding (see *Chapters 2 and 3*). The nature of the memory signal during the delay period and how much it is influenced by motor signals has been a constant source of preoccupation and discussion [3] [7]. Moreover, tough we don't explicitly pursue it here, we think that having access to the movement of the animals in a trial by trial basis might also provide helpful insights about questions like the nature of mistakes, the timing and confidence of decisions and changes of mind. For that to be possible an increase in task difficulty, like mentioned before, would also be beneficial.

Finally it is worth mentioning that, although we have proved that our task is, in essence, comparable to a traditional delayed response task, maintaining a memory between sound and area is not the only problem the mice are solving. Looking at their speed strategies it is possible to see that the animals are trying to optimize their behavior in order to achieve their goals in the most efficient way. Such generally means to: 1- slow down after trial start waiting for the tone to determine their future action plan; 2- speeding

up and continue to run, as fast as possible, until after the area, minimizing the time before the next possibly rewarded trial, in no stop trials, *OR*, speeding up after the tone but then slowing down, just enough, when approaching the area, this way trying an optimal compromise between minimizing the time until the reward and maximizing the possibility of stopping, in stop trials. The execution of these deliberate strategies is not trivial, given that the mice are running in the dark and there are no obvious cues to inform them of their location on the belt. To achieve their purposes animals have thus to, at every moment, compute an estimation of their position in the belt and, according to an internally represented goal (WM), minutely select, and time, their speed strategies.

References

[1] J. J. Bolhuis, S. Bijlsma, and P. Ansmink. "Exponential decay of spatial memory of rats in a radial maze." In: *Behavioral and neural biology* 46 (2 Sept. 1986), pp. 115–122 (cit. on p. 73).

[2] O. Buresova et al. "Radial maze in the water tank: An aversively motivated spatial working memory task". In: *Physiology & Behavior* 34.6 (June 1985), pp. 1003–1005 (cit. on p. 36).

[3] S. L. Cowen and B. L. McNaughton. "Selective delay activity in the medial prefrontal cortex of the rat: contribution of sensorimotor information and contingency." In: *Journal of neurophysiology* 98 (1 July 2007), pp. 303–316 (cit. on p. 75).

[4] P. A. Dudchenko. "An overview of the tasks used to test working memory in rodents." In: *Neuroscience and biobehavioral reviews* 28 (7 Nov. 2004), pp. 699–709 (cit. on p. 36).

[5] P. A. Dudchenko. "How do animals actually solve the T maze?" In: *Behavioral neuroscience* 115 (4 Aug. 2001), pp. 850–860 (cit. on p. 73).

[6] A. Ennaceur and J. Delacour. "A new one-trial test for neurobiological studies of memory in rats. 1: Behavioral data." In: *Behavioural brain research* 31 (1 Nov. 1988), pp. 47–59 (cit. on p. 37).

[7] D. R. Euston and B. L. McNaughton. "Apparent encoding of sequential context in rat medial prefrontal cortex is accounted for by behavioral variability." In: *The Journal of neuroscience* 26 (51 Dec. 2006), pp. 13143–13155 (cit. on p. 75).

[8] C. R. Fetsch. "The importance of task design and behavioral control for understanding the neural basis of cognitive functions". In: *Current Opinion in Neurobiology* 37 (Apr. 2016), pp. 16–22 (cit. on p. 35).

[9] P. S. Goldman-Rakic. "Cellular basis of working memory." In: *Neuron* 14 (3 Mar. 1995), pp. 477–485 (cit. on p. 37).

[10] A. Gomez-Marin et al. "Big behavioral data: psychology, ethology and the foundations of neuroscience." In: *Nature neuroscience* 17 (11 Nov. 2014), pp. 1455–1462 (cit. on p. 34).

[11] Z. V. Guo et al. "Procedures for Behavioral Experiments in Head-Fixed Mice". In: *PLoS ONE* 9.2 (Feb. 2014). Ed. by Sidney Arthur Simon, e88678 (cit. on p. 72).

[12] C. D. Harvey, P. Coen, and D. W. Tank. "Choice-specific sequences in parietal cortex during a virtual-navigation decision task." In: *Nature* 484 (7392 Mar. 2012), pp. 62–68 (cit. on p. 74).

[13] C. D. Kopec et al. "Cortical and Subcortical Contributions to Short-Term Memory for Orienting Movements." In: *Neuron* 88 (2 Oct. 2015), pp. 367–377 (cit. on pp. 36, 75).

[14] J. W. Krakauer et al. "Neuroscience Needs Behavior: Correcting a Reductionist Bias." In: *Neuron* 93 (3 Feb. 2017), pp. 480–490 (cit. on p. 35).

[15] D. A. Levitis, W. Z. Lidicker, and G. Freund. "Behavioural biologists do not agree on what constitutes behaviour". In: *Animal Behaviour* 78.1 (July 2009), pp. 103–110 (cit. on p. 34).

[16] N. Li et al. “Robust neuronal dynamics in premotor cortex during motor planning.” In: *Nature* 532 (7600 Apr. 2016), pp. 459–464 (cit. on pp. 36, 75).

[17] D. Liu et al. “Medial prefrontal activity during delay period contributes to learning of a working memory task.” In: *Science (New York, N.Y.)* 346 (6208 Oct. 2014), pp. 458–463 (cit. on pp. 36, 37).

[18] R. G. Morris, J. J. Hagan, and J. N. Rawlins. “Allocentric spatial learning by hippocampectomised rats: a further test of the "spatial mapping" and "working memory" theories of hippocampal function.” In: *The Quarterly journal of experimental psychology. B, Comparative and physiological psychology* 38 (4 Nov. 1986), pp. 365–395 (cit. on p. 36).

[19] D. S. Olton and R. J. Samuelson. “Remembrance of places passed: Spatial memory in rats.” In: *Journal of Experimental Psychology: Animal Behavior Processes* 2.2 (1976), pp. 97–116 (cit. on p. 36).

[20] T. Otto and H. Eichenbaum. “Complementary roles of the orbital prefrontal cortex and the perirhinal-entorhinal cortices in an odor-guided delayed-nonmatching-to-sample task.” In: *Behavioral neuroscience* 106 (5 Oct. 1992), pp. 762–775 (cit. on p. 36).

[21] M. J. Pontecorvo, A. Sahgal, and T. Steckler. “Further developments in the measurement of working memory in rodents.” In: *Brain research. Cognitive brain research* 3 (3-4 June 1996), pp. 205–213 (cit. on p. 35).

[22] J. Qian et al. *Glmnet for Matlab*. 2013. URL: http://www.stanford.edu/~hastie/glmnet_matlab/ (cit. on p. 47).

[23] L. A. Rothblat and L. L. Hayes. "Short-term object recognition memory in the rat: nonmatching with trial-unique junk stimuli." In: *Behavioral neuroscience* 101 (4 Aug. 1987), pp. 587–590 (cit. on p. 36).

[24] H. D. Schlinger. "Behavior analysis and behavioral neuroscience". In: *Frontiers in Human Neuroscience* 9 (Apr. 2015) (cit. on p. 35).

[25] H. Shoji et al. "T-maze forced alternation and left-right discrimination tasks for assessing working and reference memory in mice." In: *Journal of visualized experiments : JoVE* (60 Feb. 2012) (cit. on p. 36).

[26] N. Tinbergen. *The Study Of Instinct*. Oxford Univ Pr (T), 1991 (cit. on p. 34).

[27] S. Walter. *The delayed reaction in animals and children [by] Walter S. Hunter. Pub. at Cambridge, Boston, Mass.* H. Holt & company, 1913 (cit. on p. 36).

[28] K. G. White, A. C. Ruske, and M. Colombo. "Memory procedures, performance and processes in pigeons." In: *Brain research. Cognitive brain research* 3 (3-4 June 1996), pp. 309–317 (cit. on p. 37).

[29] Y. Yang and R. B. Mailman. "Strategic neuronal encoding in medial prefrontal cortex of spatial working memory in the T-maze." In: *Behavioural brain research* 343 (May 2018), pp. 50–60 (cit. on p. 74).

Chapter 3

Electrophysiology, Single Cell and Population Analysis

Chapter Authors

João Afonso and Alfonso Renart

Authors' Contributions

Performed the surgical procedures: *João Afonso*

Performed the electrophysiology recordings: *João Afonso*

Conceived and designed the neural data analysis: *João Afonso and Alfonso Renart*

Wrote the code and analysed the neural data: *João Afonso*

Acknowledgements

We thank the staff of the Champalimaud Centre for the Unknown Vivarium for assistance and support in mice care related issues. We are also in debt to the Histology Platform for slicing and processing the mice brain samples and the Bioimaging Platform for support with the microscopy used in the identification of the recorded regions.

3.1 Abstract

The PFC as since long been implicated in WM dependent behaviors. PFC neurons with stimulus selective elevated activity during the delay period of WM tasks is still the most influential mechanistic model for WM storage. Recent studies, however, have questioned such scenario and, taking advantage of technological advances in brain activity monitoring and analysis, focused the attention on WM encoding and representation in the joint activity of prefrontal neural ensembles. Here we recorded the simultaneous activity of neurons, in the mice mPFC, during a WM dependent task. From the cells mixed-selectivity response profiles, and using a targeted dimensionality reduction technique, dPCA, we were able to demix WM representations of both the tone played and the decision made by the animals. Moreover, dPCA also revealed a strong, tonic like, signal, seemingly related to the mice engagement in the task, and a significant influence of the speed behavior of the animals on the neural activity.

3.2 Introduction

The prefrontal cortex seats at the apex of a cortical hierarchy ascending from areas involved in specific sensory and motor functions to progressively more integrative ones [15]. Despite controversy about its nature and exact homology with the primate one [25][46] [4] the rat and mice prefrontal cortices have been extensively studied as models of prefrontal function [8].

In general terms the PFC is thought of as responsible for guiding behavior in a adaptive manner, representing goals and orchestrating complex sequences of behavior to achieve them, according to context specific events and rules [9], what is regularly designated as executive [14] or cognitive [31] control. To do so it needs to be able to represent externally generated and internally retrieved information, keep it active and use it in the service of multiple processes like planning, rule learning and decision making [22]. The strong context dependence, with no universal tunning to specific stimuli or behaviors, and the ability to represent multi-domain information interlinked in cognitive processes is a big culprit of the unknowns still surrounding the PFC.

Complex forms of behavior unfold in space and time. To learn associations between temporally separated features, or orchestrate sequences of discontiguous actions, the brain needs to be able to maintain active representations of events, rules and future goals or actions. This process, investigated as WM, is central and subjacent to the PFC function described before and its implementation mechanism has been one of the main focus of prefrontal research.

The association between the PFC and WM was steadily established through several decades by lesion studies in non-human primates performing delay dependent tasks [7]. From the late 70s on this results were supported, at the mechanism level, by the finding in the primate's PFC of neurons with tonic elevated activity during the memory period. This delay period activity showed stimulus selectivity, was prolonged or shortened depending on the length of the delay and was only present in correct trials, making it an ideal candidate to be the neural substrate of WM [13]. Impairments in WM dependent tasks in lesioned subjects [47] [20], and cells with persistent activity during the delay period [3] [1], have also been consistently reported in rodents.

Recently, however, different lines of evidence have emerged challenging the role of fixed selectivity sustained activity as the mechanism responsible for WM [38]. Central to these new perspectives are: 1. the implausibility of existence in the PFC of seemingly as many specialized groups of neurons as the types of WM representations already observed [35]; 2. the possibility that some of the WM related deficits and activity could in fact be accounted by other cognitive processes [45] or motor behaviors ; 3. the unreliability between the presence or absence of cells with delay period elevated activity and the WM demandings of the task [42] ; 4. the fact that WM information can be decoded from ensembles without selective delay period neurons [1] and the accumulating evidence suggesting an important role for distributed dynamic population coding in the stable maintenance of representations in the PFC [30] [2]. These don't necessarily question the involvement of the PFC in executive processes mediating sequences of actions performed in time

but doubt that single neuron delay activity per se corresponds to the actual information storage mechanism [44].

Interpreting the precise meaning of delay period selective firing, and prefrontal function in general, is more complex than understanding the representations in lower hierarchical areas where the activity is more tightly linked to behavioral and environmental manifestations. The information being represented and the way it is represented seems to be more categorical [11] and context dependent [19] and many of the cells often exhibit complex and varied response properties that are not organized anatomically and reflect, simultaneously, different parameters. In fact, even in seemingly simple tasks, individual neurons' responses can be frustratingly complex [28] being correlated with several task aspects. The existence of such mixed selectivity, a characteristic of brain areas involved in cognitive processes across model organisms [39] [36], brings computational advantages, as the multiple pieces of information can be interpreted by downstream regions according to their functional relevance, but also demands a shift of focus from clearly tuned individual cells to mixed selectivity and neural populations.

The remarkable capabilities of the brain are a product of the interaction between interconnected populations of neurons. The latest recording, computational and algorithmic advances have given scientists access to study the simultaneous activity of progressively larger numbers of cells. Dimensionality reduction techniques [6] produce low dimensional representations of high dimensional data sets by exposing a set of latent variables, along which the original data covaries, that can be used to explore, produce and test hypotheses with population data. When approaching mixed selectivity

dimensionality reduction techniques that take into account the task parameters are particularly useful [24].

Here we used multi-electrode silicone probes to record the activity of neurons from the mPFC of mice solving a head-fixed delayed response task (see *Chapter 1*). As a model organism the mouse has been proved to be capable of executing simple WM dependent tasks [27] [17][21], is amenable to the recording technique we wanted to use [41] and allows for an high yield of animals. Also, tough that is not explored in the work here presented, by choosing the mouse as model animal we opened the door to, in the future, take advantage of the existing genetic tools to further dissect and deepen our observations.

In all sessions our probes targeted the PRL, IL and MO regions of the mouse mPFC, considered to be part of the same mPFC complex and all previously involved in WM and executive behaviors [8] [22]. From here on we'll use the term mPFC to refer interchangeably to all areas that are considered to be part of it (PrC, ACG, PRL, IL, MO), and will make no distinctions about function between them. As in previous recordings from the same area in similar vein tasks, both in non-human primates [28] and rodents [36], the neurons we observed evidenced heterogeneous response profiles, with a considerable proportion showing trial type selectivity during the memory period and being modulated by task relevant events, an indication that the behavior the animals were performing engaged the part of the brain we focused on. Because of the small amount of error trials we just calculated, and analysed, the individual neuron's TSHs for hits and correct rejections.

Using dPCA we found that it was possible to demix, from the activity

of the population, dimensions across which it was possible to differentiate, through the memory period, the tone played and the response selected by the animals. This means that in a period where no external cue could inform the mice about these variables the neurons encoded information about both. Interestingly, the dimension explaining the biggest proportion of the variance was one that separated correct (hits and correct rejections) from incorrect (misses and false alarm) in a tonic-like way, which might be interpreted as a signal of task engagement. Moreover, dPCA also revealed a strong influence of the mice speed patterns in the neural activity, pointing to a previously observed significant modulation of the area's neurons by motor behavior [5].

3.3 Methods and Materials

3.3.1 Extracelular Electrophysiology

3.3.1.1 Craniotomy Surgery

The day before the first electrophysiology session on a given hemisphere a surgical intervention was performed to open a hole in the skull and dura-mater of the animals on top of the brain location we wanted to record from. Mice were put to sleep in an induction chamber connected to the isoflurane delivery system (RWD Life Sciences) and, when stably anesthetized, moved to the stereotaxic apparatus (RWD Life Sciences), their snout covered by the isoflurane delivery mask, their eyes protected with eye ointment and the skull immobilized through a custom made piece attaching the stereotaxic arm to the head-implant. After, the layer of protective silicone adhesive (World Precision Instruments - Kwik Sil) was peeled, exposing the dental cement covered skull with the AP extremities of the stereotaxic coordinates of interest marked. Using an electric drill, with a 0.5 mm drill bit, a line was then gently drilled, between both marks, until all bone had been removed, exposing the dura. A 30 gauge needle, with the tip slightly bent, was used to puncture the dura, cut it along the length of the craniotomy and expose the surface of the brain. To protect the exposed brain the craniotomy was filled with phosphate-buffered saline solution (PBS) and the interior of the head-implant covered with a 1.5% concentration agar solution. When the later solidified it was sealed with a layer of silicone adhesive. Mice were then given one IP injection of antibiotic (Enrofloxacin) and one of analgesic

(Buprenorphine). With the surgery finished mice were gently returned to their home-cage and allowed to wake up in an heated environment.

3.3.1.2 Recording Session

Recording days were, for the mice, as any normal training day with the exception that, before session start, the recording probe was lowered to the intended recording coordinates. Before putting the animals in the setup everything was prepared so that probe insertion went as smoothly and fast as possible. The animals were used to a 20 minutes period between being head-fixed in the setup and the actual session start, ideally probe insertion shouldn't take much more.

After head-fixation the light-source was turned on, pointing to the head-plate hole on top of the implant, and the microscope was positioned providing a clear view of the center of the head-implant. The layers of Kwik Sil and agar were then peeled off and the craniotomy cavity re-filled with PBS. Using bregma as a reference the probe would then be placed above the craniotomy position, on the exact Ml and AP coordinates, and very slowly (approximately 1mm per minute) lowered until the desired DV coordinates.

With the probe in position a lukewarm drop of 1.5 % agar was dropped in the implant cavity, when solid this formed a shallow layer that prevented the brain from drying out and the probe from moving with the mice's movement. The electrophysiology acquisition software would then be started followed by the behavioral task.

In the end of the session the probe was gently pulled out of the brain, the craniotomy re-filled with PBS and the interior of the implant covered

with a layer of 1.5 % agar and sealed with Kwik Sil.

3.3.1.3 Electrophysiology Equipment and Spike Sporting

All electrophysiology recordings were performed with 64 channels silicone probes (Neuronexus, Buzsaki 64sp), connected through an adapter to an analog to digital amplifier headstage (Intan, RHD2164), and an open source electrophysiology multichannel acquisition board (OpenEphys) [43]. The channels' voltage signal was sampled at 30 kHz.

To extract action potentials from the raw neuronal voltage signal, cluster them and assigned them to a specific neuron we used the integrated spike sorting framework KiloSort [33]. Clusters of potential cells were posteriorly manually curated using the open source neurophysiological data analysis package Phy [40], given that the nature of our questions was not crucially dependent on individual cell isolation we allowed for a 15% refractory period contamination relative to the neuron mean firing rate (FR).

3.3.1.4 Histology

Before each recording session the tip of the shanks of the recording probe, where the recording sites were situ, was dipped in a orange-red lipophilic membrane stain (diI, ThermoFisher Scientific). The shanks' tips were submerged for 30 seconds and then pulled out and allowed to dry for another 30 seconds. This process was repeated 3 times.

After the recording sessions were over all mice were perfused and their brains fixed and sliced - this was done by an in-house platform. Using a fluorescent microscope (Zeiss AxioImager M2) we were then able to use the

fluorescent tracts of the DiI covered shanks, together with physical penetration marks, to approximately identify the area we recorded from.

3.3.1.5 Recording Sessions Overview

All neural data here presented came from 16 recording sessions performed in 5 different animals:

Session 1 *bM67*- Right hemisphere, 109 recorded neurons.

Session 2 *bM69*- Left hemisphere, 88 recorded neurons.

Session 3 *bM73*- Left hemisphere, 114 recorded neurons.

Session 4 *bM73*- Left hemisphere, 106 recorded neurons.

Session 5 *bM73*- Left hemisphere, 119 recorded neurons.

Session 6 *bM73*- Left hemisphere, 119 recorded neurons.

Session 7 *bM74*- Left hemisphere, 112 recorded neurons.

Session 8 *bM74*- Left hemisphere, 137 recorded neurons.

Session 9 *bM74*- Left hemisphere, 121 recorded neurons.

Session 10 *bM74*- Right hemisphere, 77 recorded neurons.

Session 11 *bM74*- Right hemisphere, 92 recorded neurons.

Session 12 *bM74*- Right hemisphere, 93 recorded neurons.

Session 13 *bM76*- Right hemisphere, 96 recorded neurons.

Session 14 *bM76*- Right hemisphere, 77 recorded neurons.

Session 15 *bM76*- Left hemisphere, 79 recorded neurons.

Session 16 *bM76*- Left hemisphere, 105 recorded neurons.

3.3.2 Neuronal Data Analysis

3.3.2.1 Trial Space Histograms and Delay Period Selectivity

To produce the trial space histogram (TSH) we divided all trials in space bins, counted for each neuron the number of spikes in each bin and then divided this spike count by the amount of time the animal took to transverse each bin. This way the TSHs were binned in space but had FR in spikes per second. TSHs were used throughout this thesis, in different analyses, as our standard way of looking at neural activity. For different analyses different length bins were used.

To get a quantitative coarse measure of the individual neurons' selectivity during the memory period we followed the following procedure: 1. in each hit and correct rejection trial we calculated the firing rate of the neuron in three linearly spaced distance bins starting 5 cm after sound end and ending 5 cm before area start; 2. for each bin we calculated the difference between the mean FRs of both trial types and accessed its significance via a shuffle test in which we computed the probability, P *value*, of obtaining a mean difference, at least as extreme as the original one, through an iterative process, in which we obtained a distribution of difference of means calculated after shuffling the trials' identity label. Here we performed 10000 shuffling iterations.

In the context of this analysis being selective to one of the conditions just means that that is the one with a higher FR when there's a significant statistical difference between the two.

3.3.2.2 Peri Event Time Histograms and Events Modulation

Peri-event time histogram (PETH) were produced by calculating the FR of each neuron in 0.025 seconds bins in a 2 seconds window centered at the event.

Significance of events related FR change was determined by means of a shuffle test, as described for delay period selectivity, comparing the mean FR in the 0.15 seconds period before the event with the mean FR 0.05 to 0.2 seconds after the event.

3.3.2.3 demixed Principal Components Analysis

For a complete and thorough description of dPCA please refer to the original paper [24]. To implement the dPCA algorithm we used the Matlab package provided by the method authors [23].

Briefly: For all N recorded neurons in one session the binned FR in any given trial was labeled in terms of the sound that was played s (out of $S = 2$) and the decision the mice made d (out of $Q = 2$). Each bin corresponded to a trial position p out of P and, ideally, for each SQ condition we would have the same K number of trials. Because in the large majority of our sessions we didn't have, or had very few, trials of the conditions corresponding to mistakes (misses and false alarms), we opted to pool together data from all sessions that met our requirements and treated our neurons as if they had been sequentially recorded . For that, instead of using single trial data, we average the activity of each neuron across the the trials of each SQ condition. This way our data can be thought of as SQ time-dependent

neural trajectories in a *N-dimensional* space and could be organized in a $\tilde{\boldsymbol{X}}$ matrix of size NxSQP.

The average activity of each Neuron across conditions (each row of $\tilde{\boldsymbol{X}}$) was then decomposed into a set of averages (or *marginalizations*) over various combinations of parameters. By applying this marginalization procedure to every neuron we split the Matrix $\tilde{\boldsymbol{X}}$ into parts

$$\tilde{\boldsymbol{X}} = \tilde{\boldsymbol{X}}_p + \tilde{\boldsymbol{X}}_{ps} + \tilde{\boldsymbol{X}}_{pd} + \tilde{\boldsymbol{X}}_{psd} + \tilde{\boldsymbol{X}}_{noise} = \sum_\theta \tilde{\boldsymbol{X}}_\theta + \tilde{\boldsymbol{X}}_{noise}$$

where $\tilde{\boldsymbol{X}}$ was centered and *p, ps, pd* and *psd* were labels, with *p* - condition independent (averaging across all conditions); *ps* - sound depedent (averaging across conditions with same sound being played after subtracting $\tilde{\boldsymbol{X}}_p$); *pd* - decision dependent (averaging across conditions where the animal made the same decision after subtracting $\tilde{\boldsymbol{X}}_p$); *psd* - sound-decision interaction (average across all SQ condition combinations after subtracting $\tilde{\boldsymbol{X}}_p + \tilde{\boldsymbol{X}}_{ps} + \tilde{\boldsymbol{X}}_{pd}$). The new marginalized matrices were made the same size (NxSQP) as the original $\tilde{X}$ by, for instance in the case of p, replicating the resulting average SQ times.

Given the above explained decomposition the loss fuction of dPCA was given by

$$L = \sum_\theta L_\theta$$

with

$$L_\theta = ||\tilde{\boldsymbol{X}}_\theta - \boldsymbol{F}_\theta \boldsymbol{D}_\theta \tilde{\boldsymbol{X}}||^2$$

where each $\boldsymbol{F}_\theta$ was an encoder matrix with q_θ columns and each $\boldsymbol{D}_\theta$ a

decoder matrix with q_θ rows. Matrix norm was $||\tilde{\boldsymbol{X}}||^2 = \sum_i \sum_j \tilde{\boldsymbol{X}}_{ij}^2$. The loss function penalized the difference between the marginalized data $\tilde{\boldsymbol{X}}_\theta$ and the reconstructed full data $\tilde{\boldsymbol{X}}$, the full data projected with decoders $\mathbf{D}$ onto a low-dimensional latent space and then reconstructed with the encoders $\mathbf{F}$. This loss functions was a linear regression problem with an additional rank constraint on the matrix of regression coefficients. A problem known as reduced-rank regression. When running the algorithm a regularized version of the loss function was used

$$L_\theta = ||\tilde{\boldsymbol{X}}_\theta - \boldsymbol{F}_\theta \boldsymbol{D}_\theta \tilde{\boldsymbol{X}}||^2 + \mu ||\boldsymbol{F}_\theta \boldsymbol{D}_\theta||^2$$

For this analysis we pooled neurons from all sessions with at least 5 trials in each SQ condition. This meant 6 sessions, from 3 different animals, and 615 neurons.

3.3.2.4 Explained Variance Calculations

The variance explained by each dPCA component, shown on and used to order *Figures 3.9,12,13 a*, was defined as

$$R^2 = \frac{||\tilde{\boldsymbol{X}}||^2 - ||\tilde{\boldsymbol{X}} - \boldsymbol{f}\boldsymbol{d}\tilde{\boldsymbol{X}}||^2}{||\tilde{\boldsymbol{X}}||^2}$$

with $\mathbf{f}$ and $\mathbf{d}$ being the specific component's encoder and decoder.

The cumulative fraction of variance in *Figures 3.9,11,12 b* was obtained using the same formula and stacking the components' encoders and decoders. The same process was used for the principal components analysis (PCA) cumulative variances, shown in the same figures, but now with just one set

of projection axis - **U**, instead of **F** and **D** used in dPCA.

Given the decomposition $\tilde{\boldsymbol{X}} = \sum_\theta \tilde{\boldsymbol{X}}_\theta$, the fraction of explained variance could be split into the sum of the contributions from the different marginalizations

$$R^2 = \sum_\theta \frac{||\tilde{\boldsymbol{X}}_{\boldsymbol{\theta}}||^2 - ||\tilde{\boldsymbol{X}}_{\boldsymbol{\theta}} - \boldsymbol{F}\boldsymbol{D}\tilde{\boldsymbol{X}}_{\boldsymbol{\theta}}||^2}{||\tilde{\boldsymbol{X}}||^2}$$

This was used to produce the bar plots in *Figures 3.9,11,12 c*

3.3.2.5 Clustering of Session Speeds

To cluster individual trials, based on their speeds, in an unbiased way we applied PCA to the speeds of every session organized in a matrix where columns were different trials and rows the speed bins from trial start to trial end. The loadings of the first PC were strongly bi-modal and clustered almost perfectly in hit and correct rejection trials. To further separate trials belonging to each trial type we divided the two distributions in 3 by binning the loadings of hits and correct rejection trials between the 0, 33, 66 and 100 percentiles.

3.3.2.6 dPCA on Speeds

In *Figure 3.11* and *Figure 3.12* we used the same dPCA method already described applied in separate to hit and correct rejection trials. Importantly, as parameter, instead of the sound played and the decision made, we used the three speed clusters obtained from the PCA loadings (described above) as the conditions.

For this aplication of dPCA we used all recording sessions as all conditions had a sufficient number of trials in every session.

3.4 Results

3.4.1 Acute Recordings Preparation

Our head-fixed task allowed us to perform acute extra-cellular electrophysiology recordings, using silicone probes, in awake behaving animals. Using this preparation we recorded the simultaneous activity of large dozens of neurons per session.

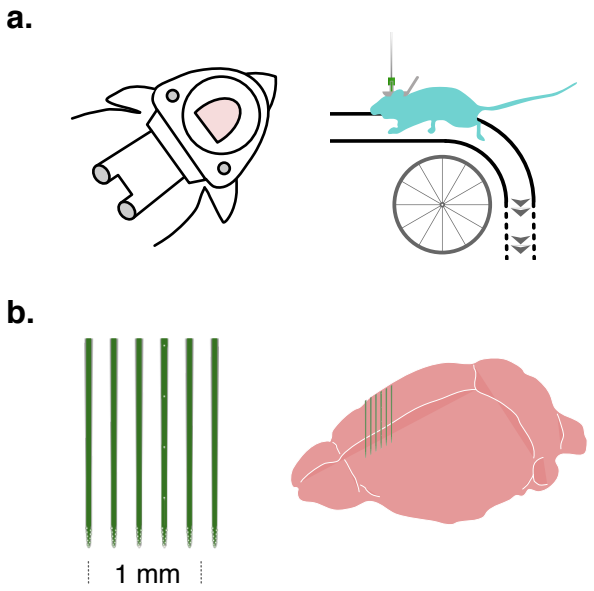

Figure 3.1: Acute Recordings on Awake Behaving Mice: (a) Left: Detail of head implant with central well allowing for easy access to the skull in recording sessions. Right: Scheme of a mouse behaving during a recording session. The session is as any other with the exception of the probe being stereotaxically lowered into the brain after the animal being head-fixed (b) Left: Detail of Buzsaky A64sp silicone probe, with 10 channels in the tip of each shank plus 4 more along the 4th shank from the left. Distance between shanks is 0.2mm. Right: Recording probe is inserted parallel to the midline, at a 17° *angle, spanning 1 mm in the AP axis of the mouse mPFC centered at the PRL area.*

The head-fixing implant (*Figure 3.1 a*) allowed easy access to the mice's

skull, both for the craniotomy surgery and the recording sessions. Additionally, it also created a stable environment for positioning and stabilizing the recording probe, optimizing the quality of the signal obtained. The day before the first recording session, in each of the hemispheres, animals underwent a surgery in which a craniotomy and durotomy were performed on top of the desired AP and ML recording coordinates. Recording days were as any normal training day (*Figure 3.1 b*) with the exception of the operations needed for probe insertion and extraction. See *methods section* for more information about the recording procedure.

Our targeted recording area was centered in the PRL region of the mice mPFC, an area traditionally implicated in WM and cognitive guided behavior (see chapter's *Introduction*). In the *Mouse Brain in Stereotaxic Coordinates* [34] the PRL is an elongated structure extending from aproximately 1.5 to 3 mm anterior of bregma and stretching to both sides of the midline by about 0.65 mm. In its most posterior end the PRL starts at 2.25 and goes to 2.75 mm, from bregma, in the DV axis. In its most anterior part it starts at 1 and ends at 1,8 mm, also from bregma.

In our recordings we aimed to place the probe in the sagittal plane (*Figure 3.1 c*) with its most posterior shank at 1.5 mm AP / 0.25 mm ML / 2.4 mm DV from bregma. Due to the proximity to the midline, and the difficulty of performing a craniotomy very close to the superior sagittal sinus, the surface penetration ML coordinate was 1 mm from it, but the probe was inserted at a 17° angle, this way targeting the 0.25 mm ML coordinate when the desired depth was reached.

Before each recording session we stained the shanks of the probe with

the lipophilic membrane stain DiI. The tracts left by the shanks, identifiable both through the staining and the penetration lesions, allowed us to identify the approximate location of the probes' shanks tips (*Figure 3.2 a*). Given

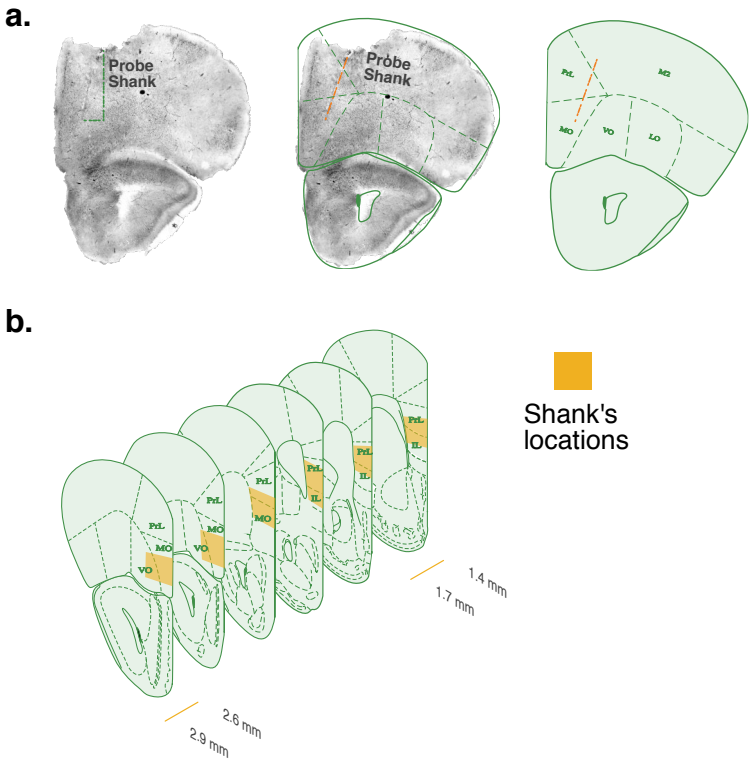

Figure 3.2: Recording Locations: (a) Location of one example probe's shank from one of the recording sessions. (b) Approximate recording areas of the six shanks of the probe along the AP axis. Values are for mean +/- standard deviation of the locations of the most anterior and posterior shanks across sessions. Remaining shanks position was estimated by linearly spacing them between the mean values of the most anterior and posterior shanks in all sessions. Areas legend in a and b: PrL - PreLimbic area; VO - ventral Orbital area: MO - medial Orbital area; IL - Infralimbic area.

that we performed at least two, but some times four, penetrations per hemisphere and that variability on exact probe placement was inevitable, identifying the position of each shank on each recording was impossible. The

approach we followed to visualize an estimate of the area we recorded from, in each mice's hemisphere, was to take the most anterior and posterior shank marks in it and linearly space the remaining 4 shanks between these. In *Figure 3.2 b* we follow an equivalent approach and use the mean positions of the most anterior and posterior shanks, across all recorded hemispheres of all animals, as the points between which the remaining shanks were linearly spaced.

3.4.2 Delay Period Selectivity

High order frontal areas have access to information from several modalities and representations of these can be find mixed in the activity of its neurons. As in a collection of previous works, that recorded the activity of neurons from frontal areas of different mammals [16] [28], also here we found neurons with diverse and complex responses to the task events.

Trial length in our task was determined by the speed of the animals running on the treadmill. To be able to examine and compare the mean trial activity of each neuron, particularly during the memory period, we computed TSHs (see *Methods Section* for a detailed description) in which spike counts were taken in length bins and then divided by the time the animal took to transverse each bin. In *Figure 3.3* we show the TSHs of 4 example neurons for trials from three different sound start locations. The mean trial activity of the different neurons was modulated in different ways by different task event or events, a modulation that was consistent, if slightly different, for trials with memory periods of different length.

Particularly interesting for us were neurons, like the ones in the three

bottom rows of *Figure 3.3*, in which the activity in the memory period was clearly different between the two conditions: hit and false alarm trials. These were evidence that, overall, the population of recorded neurons carried signals that allowed to differentiate conditions during the cue free memory period, and thus could be used by the mice to decide what to do upon reaching the stopping area.

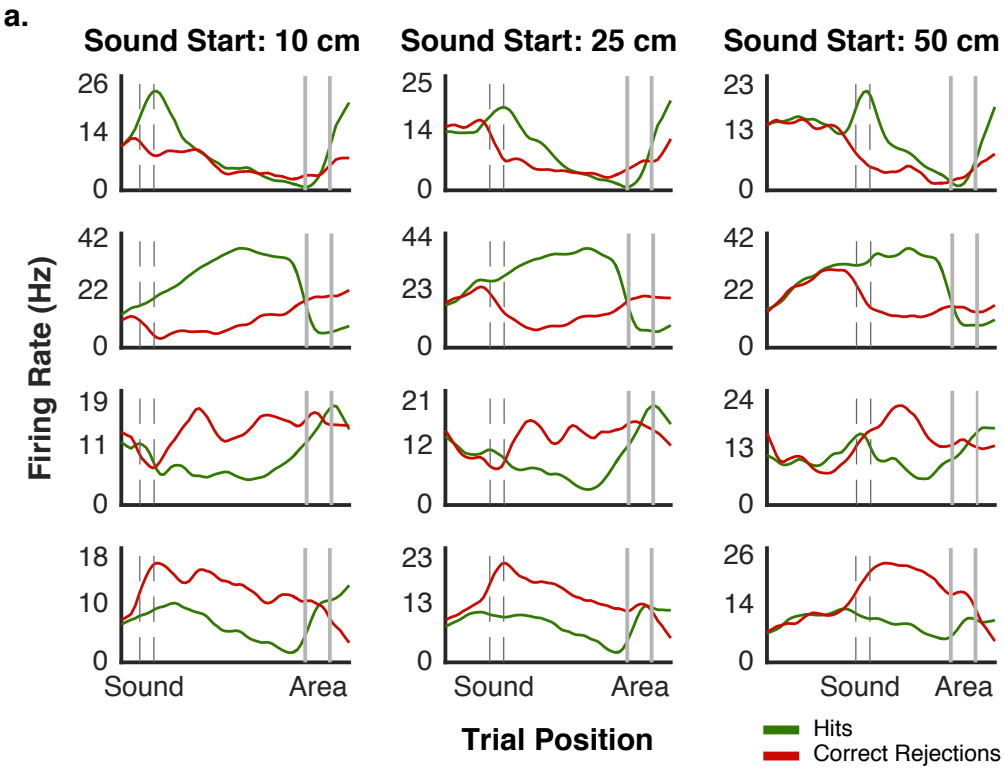

Figure 3.3: Trial Space Histograms of Firing Rates: (a) Rows: Example Neurons ; Columns: Three different sound start locations. TSHs are calculated by, in each trial, counting the number of spikes in 2 cm bins and dividing it by the time the animals took to transverse that bin.

A total 0.59 of the neurons recorded in all sessions showed a significant

mean activity difference (*Figure 3.4 a*), between hit and correct rejection trials, during at least one of three segments in which we partitioned the memory period (*Figure 3.4 c* upper y axes value). The proportion of neurons

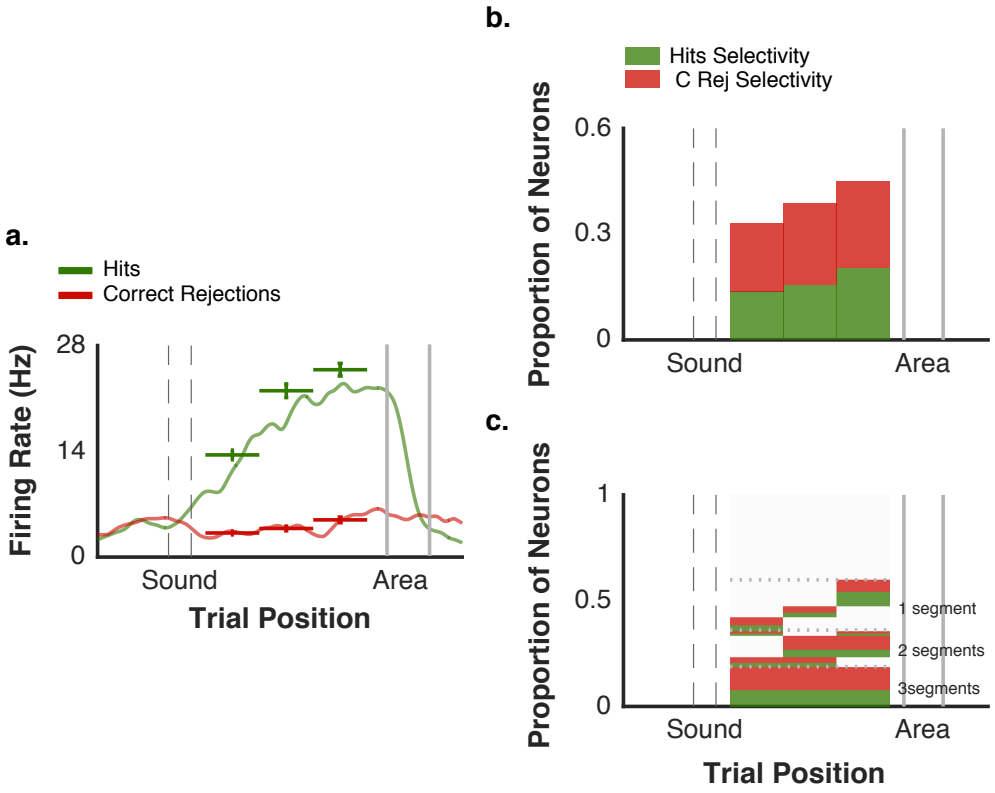

Figure 3.4: Firing Rate Selectivity in the Memory Period : (a) Example neuron with hit trials selectivity in the initial middle and final segments of the memory period. Errorbars are for the SEM. (b) Proportion of neurons with selective FR for each of the conditions in the three memory period segments. (c) Proportion of neurons with selective FR for each of the conditions grouped by in how many, and which, segments were they selective. Neurons with segments with different condition selectivity (0.024 of the total) were not included. In all three figures selectivity was accessed with a difference of means shuffle test ($p<0.05$) and defined has the condition in which the FR was higher.

with a significantly different FR between trial types was not constant in all the three segments (*Figure 3.4 b*): 0.34, 0.39 and 0.45 of the neurons

showed trial type selectivity in the beginning, middle and end of the delay period respectively. Also, 0.185, 0.165 and 0.24 were selective during the three segments, only in two or one of them, respectively. For the neurons in which the mean activity between trial type was significantly different only in one or two segments, these segments were, for the majority, the ones closer to the area (0.75 of the two segments selective neurons and 0.52 of the one segment selective ones). What seems to indicate a stronger representation of the action to be made comparatively to the sound played.

Overall, as can be seen in *Figure 3.4 b* and *Figure 3.4 c* there was a higher proportion of neurons with correct rejection (0.6) than hit trials selectivity (0.4). In the context of our analysis selectivity just meant which trial type had a higher mean FR in neurons showing a significant difference and could arise from an excitatory response to one trial type, an inhibitory response to the other or a conjunction of both.

3.4.3 Firing Rate Modulation by Task Events

The different running speeds and the fact that events were determined by the mice's position made it impossible to fully align task events in time. Nevertheless, assuming than in a small window of time around the event activity in all trials should be fairly aligned, we were able to compute raster plots and PETHs for the response of each neuron to specific task events.

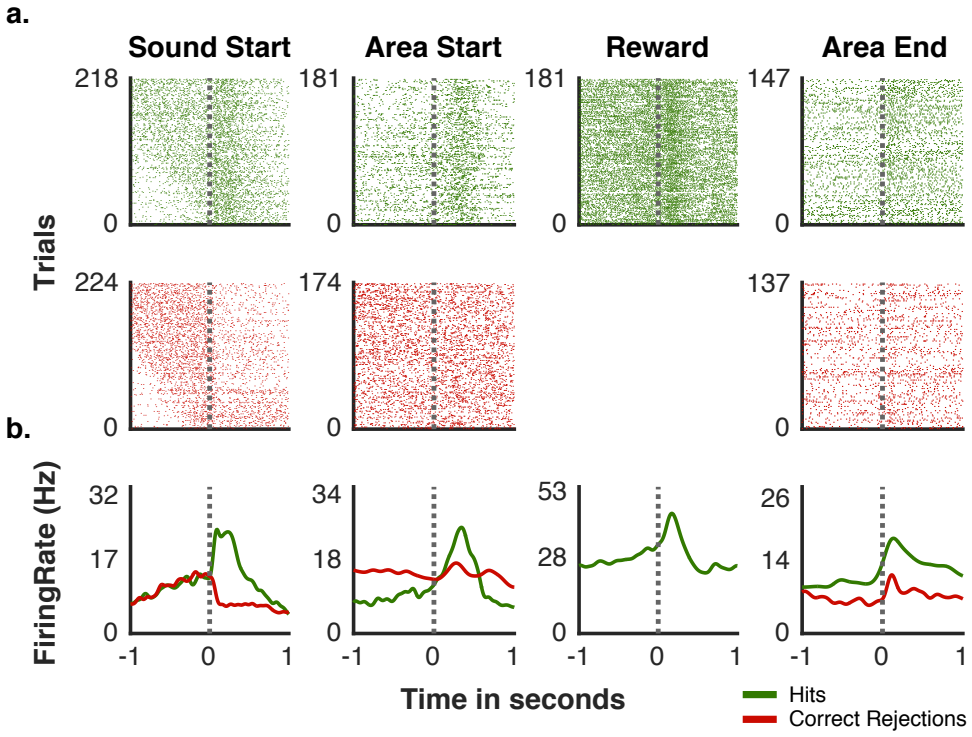

Figure 3.5: Peri Event Raster Plots and Time Histograms: (a) Session raster plots of four example neurons aligned to specific task events. Top: Stop Trials , Bottom: No Stop Trials . (b) Average PETHs of four example neurons aligned to specific task events.

Using this approach we were able to coarsely quantify how the activity of individual neurons was modulated (*Figure 3.6 a*) by specific task events and acquire a notion of how task engaged was the population we recorded from. We found that 0.58 of the total recorded neurons were modulated by at least one task event, with 0.2 modulated just in hit trials, 0.14 in correct rejection trials and 0.24 in both (*Figure 3.6 b*). From all recorded neurons 0.46 were modulated by one, 0.21 by two and 0.07 by three events in at least one of the trial types. There was also a small proportion of neurons modulated by four or five events. Consequence of the way we quantified it

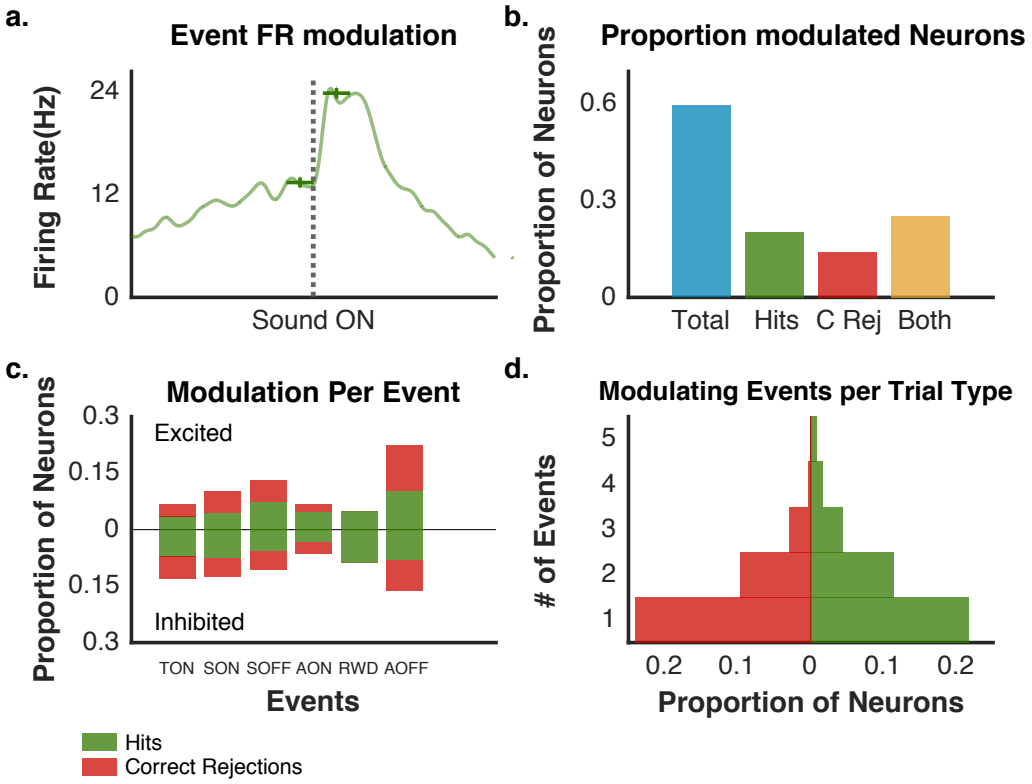

Figure 3.6: Significant FR Modulation by Task Events: (a) PETH of an example neuron with FR significantly modulated by the stop sound onset. (b) Proportion of neurons with significant FR modulation in at least one event, in hit, correct rejections or both types of trials. (c) Proportion of neurons with FR significantly modulated by each of the task events grouped by trial type and direction of modulation. (d) Proportion of neurons with FR significantly modulated by different number of events in each of the trial types. Modulation accessed with a difference of means shuffle test between the difference of the mean activity of each neuron 150 ms before the event and 50 - 200ms after the event ($p<0.05$).

(see *Methods Section*), but also of the continuous and dynamic nature of the task, with a limited ITI and the mice constantly running and stopping, the modulations we captured might not correspond to an abrupt triggered response to an event but be the product of slower FR dynamics. Such is much likely the case for neurons modulated by 5, 4 or even three separate

events.

Overall the event that modulated more neurons was the end of the stopping area (AOFF in *Figure 3.6 c*), 0.4 of all neurons. The exact meaning of this is impossible to apprehend in the context of our task. In hit trials the end of the stopping area coincides with a period in which the animals are speeding up just after being stopped collecting reward. In correct rejection trials it signals the end of the period where animals must remember not to stop. Also mPFC neurons have been implicated in retrospectively encoding trial outcome [29] [36]. All these might be partially responsible for our observation.

Surprisingly both area start (0.16) and reward (0.185) modulated a relative small percentage of neurons. Trial start, sound start and sound end modulated about the same proportion of neurons (0.21, 0.26 and 0.28 respectively) but exhibited an upward trend in terms of the proportion of those that were excited or inhibited. These events cover a period in which mice enter a new trial, signaled by light off, tend to slow down waiting for the tone and speed up again after tone hearing it. The modulation pattern probably reflects both the neurons' response to the specific events (light off, tone on, tone off) and the associated movement variations.

3.4.4 Low Dimensional Representations of Task Parameters

dPCA extracts from the population activity one dimensional principal components that are associated to specific task parameters (e.g. stimuli and decision), this way exposing the dependencies that explain the observed

neural activity (*Figure 3.7*). Due to the very few mistakes committed by the mice it was impossible to apply dPCA, at the single trial level, in the majority of the sessions. Because of such, in the analysis here shown, we pooled data from all our recordings that met the method criteria (see *Methods Section* and original dPCA paper [24]) and used the cells' trial averaged, instead of individual trial, activity. Also, to maximize the amount of input

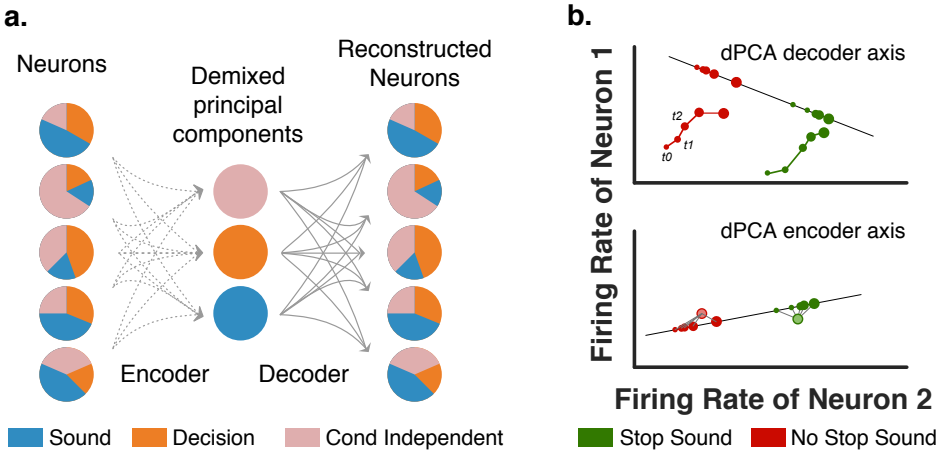

Figure 3.7: Demixed Principal Component Analysis (dPCA) : (a) In the Example scheme dPCA finds the latent variables that best explain the data while exposing their dependencies on the sound being played, the decision of the animal and condition independent factors. This is achieved through two linear transformations that compress and decompress the data both minimizing the reconstruction error and imposing a demixing constraint on the latent dimensions . (b) At any moment the firing rate of a population of N neurons can be represented in a N dimensional space. In this N = 2 example the response in time to two different Sounds is plotted as a trajectory of dots. Top: by projecting the data on the dPCA decoder axis one manages to separate the responses to the different stimuli while approximately preserving the geometry of the original data. Bottom: the projection on the decoder axis is mapped onto a different axis (encoder axis), allowing for the reconstruction of the sounds class means. Together, the encoder and decoder axis minimize the reconstruction error between the original data and the stimulus class means. Both (a) and (b) adapted from Koback et.al, 2016 [24].

data available, we grouped together all trials independently of the sound

start location in each. For that we built aligned TSHs in which the memory periods (the trial segment which length varied) were transformed to have the same number of different size bins (see *Methods Section* for clarification). The procedure didn't introduce significant artifacts in our data as original and aligned TSHs were qualitatively similar (*Figure 3.8*).

dPCA was able to almost perfectly demix, from the joint activity of all neurons, components independent and dependent of the task parameters (sound and decision) and the interaction between them (*Figure 3.9 c bottom*), in a way that captured most of the variance in the data (*Figure 3.9 b*).

Projecting the full data (hit, miss, correct rejection and false alarm trials) onto the first couple of components associated with sound and decision (*Figure 3.9 a* first two top rows, left column) revealed, for both parameters, a clear separation between the trials where the same sound had been presented or decision made. This showed that neurons possessed, at the population level, throughout the memory period, linearly decodable information about the sound played and the decision (stop or not) made by the mice. Curiously, for both parameters' first PCs, these representations were still separable in and after the stopping area, which might be attributed to the previously discussed involvement of the mPFC in keeping time sustained representations of previous actions and task relevant stimuli [29].

Also in the projections onto the second PCs of both sound and decision it was possible to separate different sound and response representations during the memory period. Here, though, the separation collapsed and the projections associated with both sounds and decisions crossed at area start. This

provides an indication that the stopping area has a task meaning attached to it, as it sharply modulates the projections, and so that, upon reaching it, the recorded neurons are still involved in some decision (or commitment to decision) process.

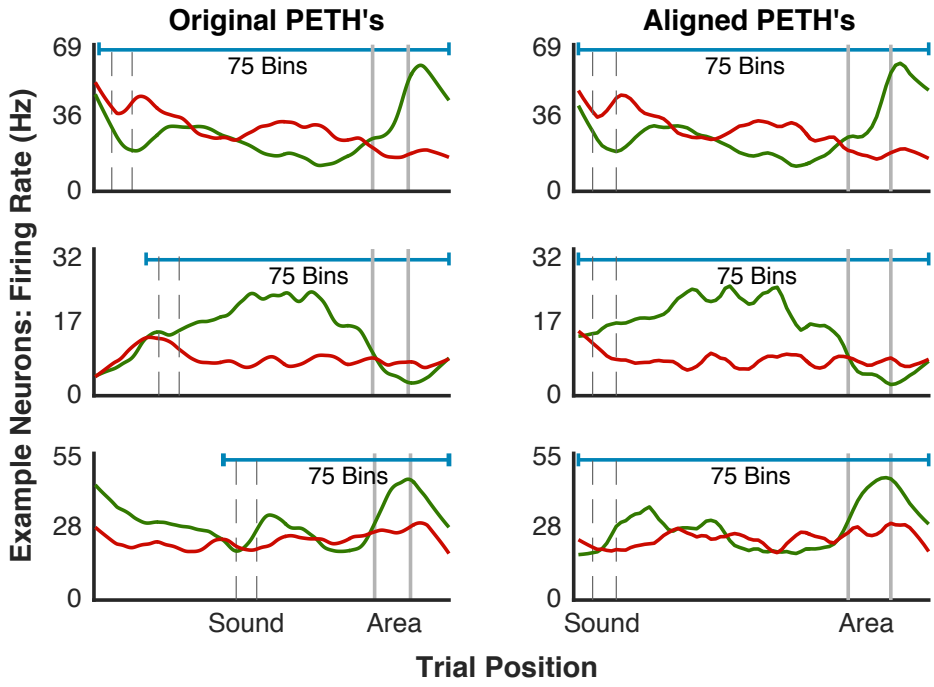

Figure 3.8: dPCA Input Trial Space Histograms: (a) To take full advantage of dPCA, and feed the algorithm as much data as possible, trials with different delay lengths were aligned by cutting them shortly before sound start and re-sampling the memory period data with the same number of different size space bins. Each row is an example neuron with the original TSH on the left and the aligned TSH on the right. The procedure doesn't alter the basic TSHs shapes.

On other behavioral tasks condition independent factors were normally responsible for explaining the majority of the variance in the data [24]. If one thinks that the experimenters are trying to explain the total variance in the neural activity using just a few parameters of the sensory space they

control and few behavioral manifestations they monitor (even when actively trying to prevent others), such observation is not surprising. In our task,

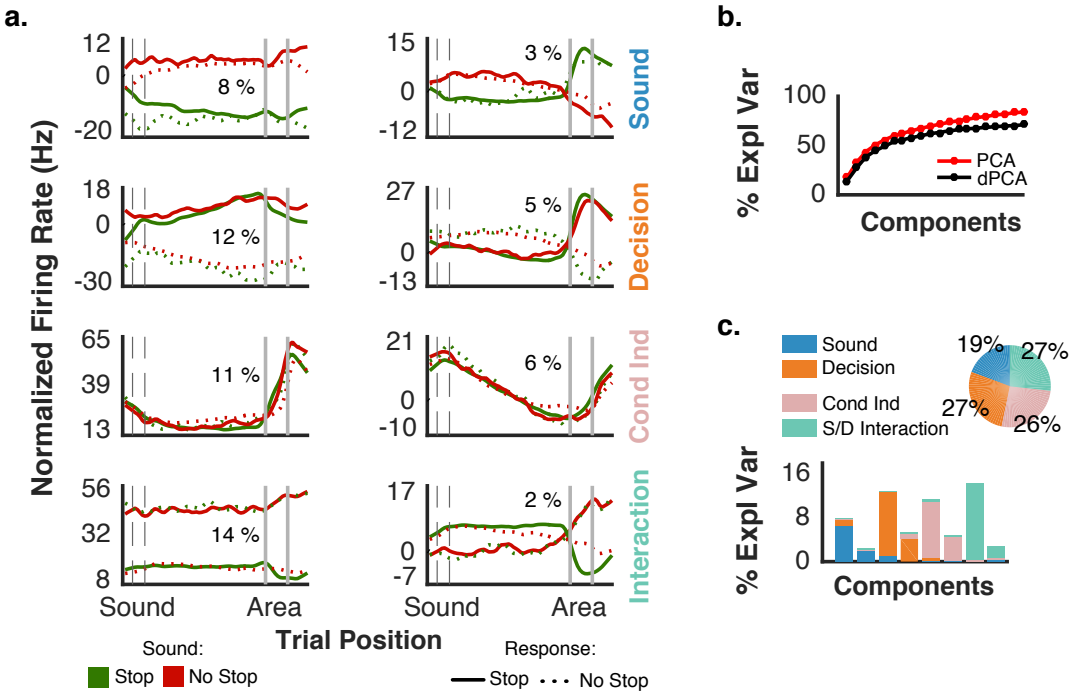

Figure 3.9: dPCA Results for Sound and Decision as Parameters : (a) Demixed principal components. Each subplot is the projection of the full data on a specific decoder axis. From top to bottom the rows depict the first and second sound, decision, condition independent and sound/decision interaction components. Overall variance explained by each component is shown as a percentage. (b) Cumulative variance explained by dPCA and PCA. Dashed line is an estimate of the fraction of 'signal variance' in the data (see Methods). (c) Top: Total signal variance split among parameters. Bottom: Variance of the individual demixed principal components. Each bar shows the proportion of total variance, and is composed out of four stacked bars, of different color, corresponding to condition-independent variance, sound variance, decision variance and variance due to stimulus-decision interactions. Each bar appears to be single-colored, which signifies nearly perfect demixing.

though, the condition independent components, which captured the variance associated with unaccounted task parameters, explained, in total, only

26% (*Figure 3.9 c top*) of the variance, with its most explanatory principal component being only the third overall (*Figure 3.9 a* third row left column). One possible explanation for this difference might be the influence of speed in the neural activity, as speed and motor responsive neurons have been found in the mPFC before [10] [18] [36].

Because of its continuous nature the speed of the animals can't be used as a parameter in dPCA, but we know, from the nature of our task and the behavioral analysis on *Chapter 1*, that movement is how animals expressed themselves in the task with speed varying greatly both within and between trials. We also know that, despite single trial variability, there were speed patterns that covaried with both the to be performed response of the animals (stop or not) and the sound played. The influence of speed in the variance of the neural data is thus probably masked in the sound and decision parameters variance explained. It's worth remembering here that, unlike in a saccade or a reaching movement, in our task speed was the result of a whole body coordinated effort.

Another unexpected finding was that the component that explained the most variance on the data, 14%, was the one that accounted for the interaction between sound and decision. When projecting the data onto this component we saw a trial long, seemingly constant, separation between correct (hits and correct rejections) and incorrect trials (misses and false alarms). Such hints to a relation of the neural activity in the mPFC with the engagement of the mice in the task.

We knew that, due to the nature of our recording method, with the probe being inserted in the beginning of each session, and a need to start the task

as soon as possible to not compromise the mice's behavior, an overall slight increase in FR was seen during each session (*Figure 3.10 b*). We also knew

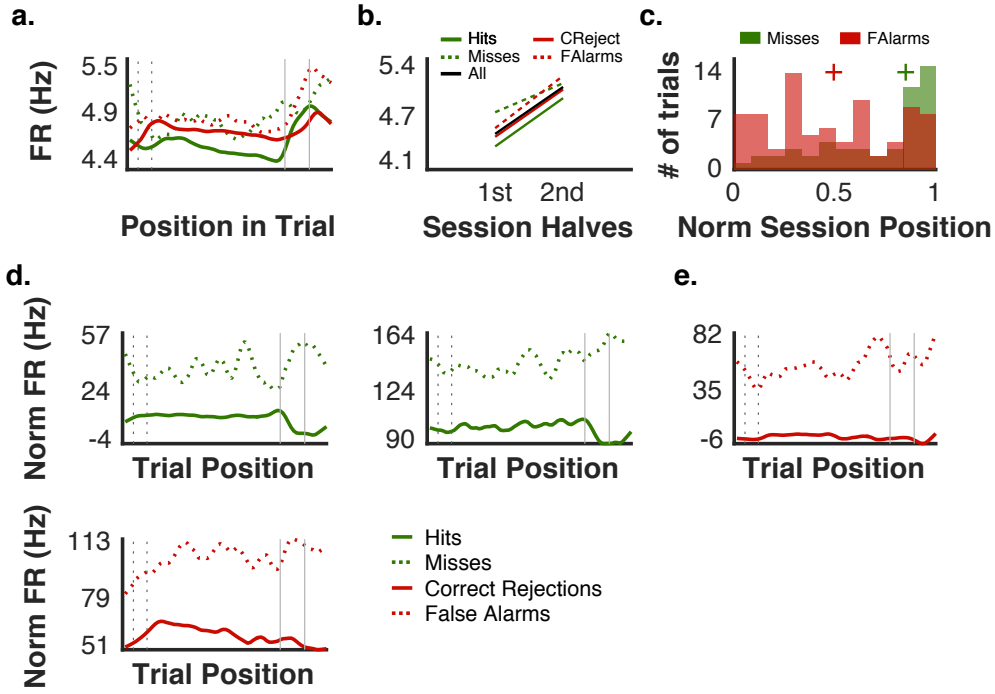

Figure 3.10: Differences Between Correct and Incorrect Trials: (a) Average TSHs of all neurons in all recording sessions grouped by trial type. (b) Average FR, across all neurons, in the first and second half of all sessions. (c) Histogram of the normalized session position (trial / number of trials in session) for false alarm and miss trials. Colored + signs are the medians of both distributions. (d) Left: projection of the stop sound trials in the first 0.7 portion of the session onto the first sound-decision interaction component. Right: projection of the stop sound trials in the last 0.3 portion of the session onto the first Sound/Decision Interaction component. (e) Top Right: projection of the no stop sound trials in the first 0.5 portion of the session onto the first sound-decision interaction component. Bottom Left: projection of the no stop sound trials in the last 0.5 portion of the session onto the first sound/decision interaction component.

that the distribution of incorrect trials was not even throughout the sessions, particularly for miss trials, that tended to occur more towards the end of the session (*Figure 3.10 c*). Looking at the mean firing rate of all recorded

neurons grouped by trial type we could observe a difference between hits and misses (*Figure 3.10 a*), but not so much between correct rejection and false alarms, which made us think that the interaction between the location of incorrect trials in the session and the increase in FR could be, at least partially, responsible by what we were observing in the dPCA interaction parameter.

The fact that in *Figure 3.10 b* the increase in FR affected all trial types in a quasi equal manner was an indication against it, but still we projected the neural data coming from the first and second halves of each session onto the first sound/decision interaction demixed principal component and observed the same result as in the whole session data, confirming the existence of a tonic-like separation between correct and incorrect trials of both trial types.

3.4.5 Low Dimensional Representations of Speed

As discussed before the movement of the animals on the treadmill, measured as speed, had the potential to be responsible for a fair degree of the variability observed in the neural data. Because dPCA doesn't deal with continuous variables we devised a way to get a notion of that influence. We grouped together trials that shared some speed related characteristics and employed these as input conditions to dPCA. To group the trials, avoiding imposing some arbitrary criterion (e.g. tresholding max or mean speed), we used the loadings resulting from applying PCA to the speeds of all trials in each session.

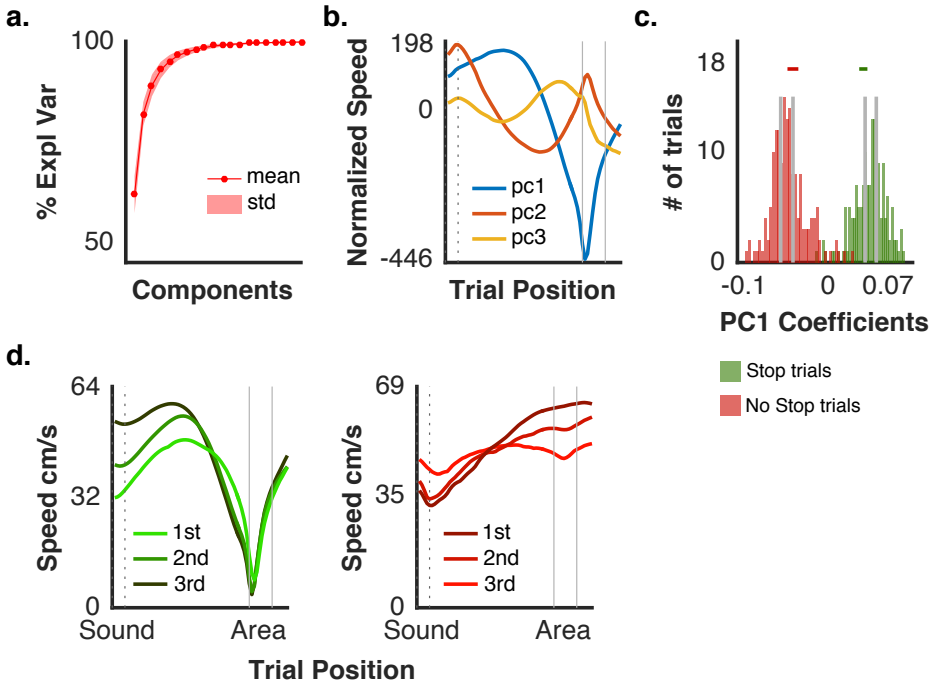

Figure 3.11: PCA on Session Speeds: (a) Cumulative explained variance of the PCA components. Dots are the components mean across all recording sessions, shaded area is the standard deviation. Note that, on average, the first component explains around 60 % of the variance on the trials speeds. (b) First 3 Principal Components on an example session. (c) Histogram of the loadings of the first PC color coded by trial type for an example session. Grey vertical bars are the 33 and 66 percentile of the loadings distributions for both trial types in which the mice stopped or didn't. Color bars on top are the mean +/- SD of the two trial-types loadings-means across all recording sessions. (d) Mean speeds of hit (left) and correct rejection (right) trials grouped by the loadings' percentiles showed in (c).

Speed data was very low dimensional with the first three principal components (*Figure 3.11 b*) explaining 87% of the total variance (*Figure 3.11 a*). The distribution of the loadings of the first PC was binomial, almost perfectly clustering the trials into the ones in which the mice stopped or didn't (*Figure 3.11 c*). We took advantage of that to divide each of the clusters (stop and no stop trials) in three groups (grey vertical bars in *Figure 3.11*

c) using their 0, 33, 66 and 100 percentiles. Mean speeds of the different groups in stop and no stop trials are shown in *Figure 3.11 d.*

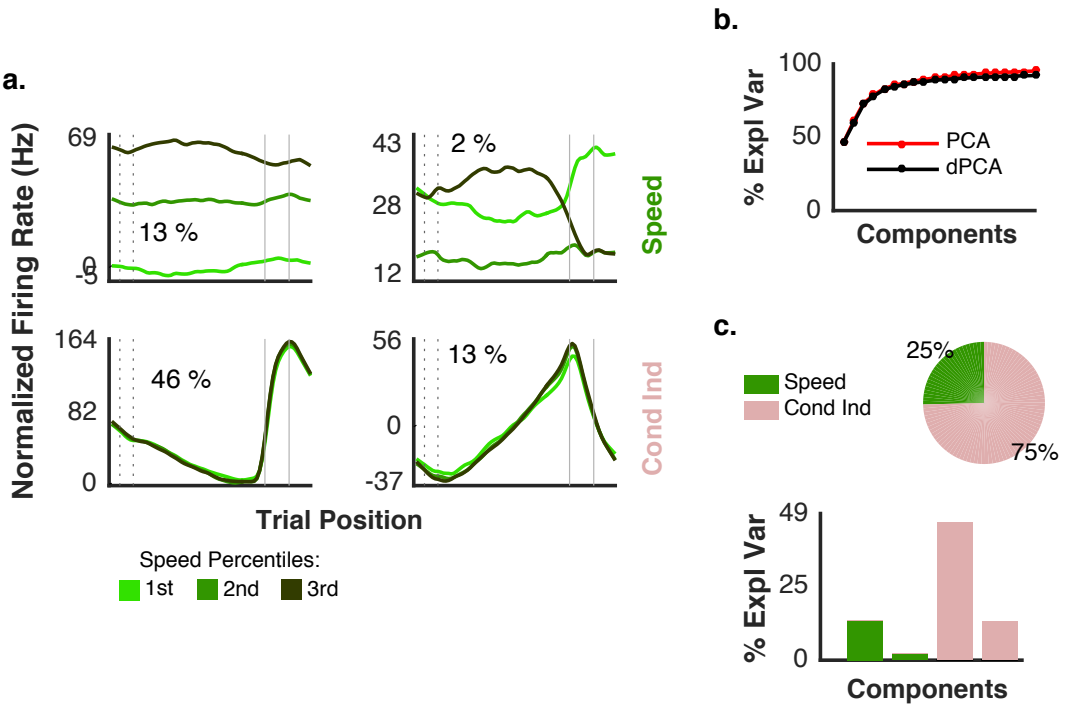

Figure 3.12: dPCA Results Stop Trials Speeds: (a) Demixed principal components. Each subplot is the projection of the full data on a specific decoder axis. From top to bottom the rows depict the first and second speed and condition independent components. Overall variance explained by each component is shown as a percentage. (b) Cumulative variance explained by dPCA and PCA. (c) Top: Total signal variance split among parameters. Bottom: Variance of the individual demixed components. Each bar shows the proportion of total variance and is made of two stacked bars of different color: one for speed and one for condition independent variance. The graph shows the first two components for speed and condition independent in this order. The almost complete dominance of one color in each bar shows the effectiveness of the demixing.

We found that this simple segmentation of trials according to their speeds accounted for 25% of overall variance in neural activity during stop trials, with 13% coming from the first component alone (*Figure 3.12 a top right*

plot and *Figure 3.12 c*). The influence was even bigger for trials where the mice didn't stop with our grouping accounting for an impressive 48% of the variance, with 18% in the first component (*Figure 3.13 a top right plot* and *Figure 3.13 c*). The difference in the variance explained by our grouping procedure in stop and no stop trials probably arises from the fact that speed trajectories in stop trials were more stereotyped, having less trial to trial and group to group variability, thus being better captured by the condition independent components. This highlights that the condition independent components are also capturing speed associated variance, particularly the one related with intra-trial mean speed trajectories common to all our groups.

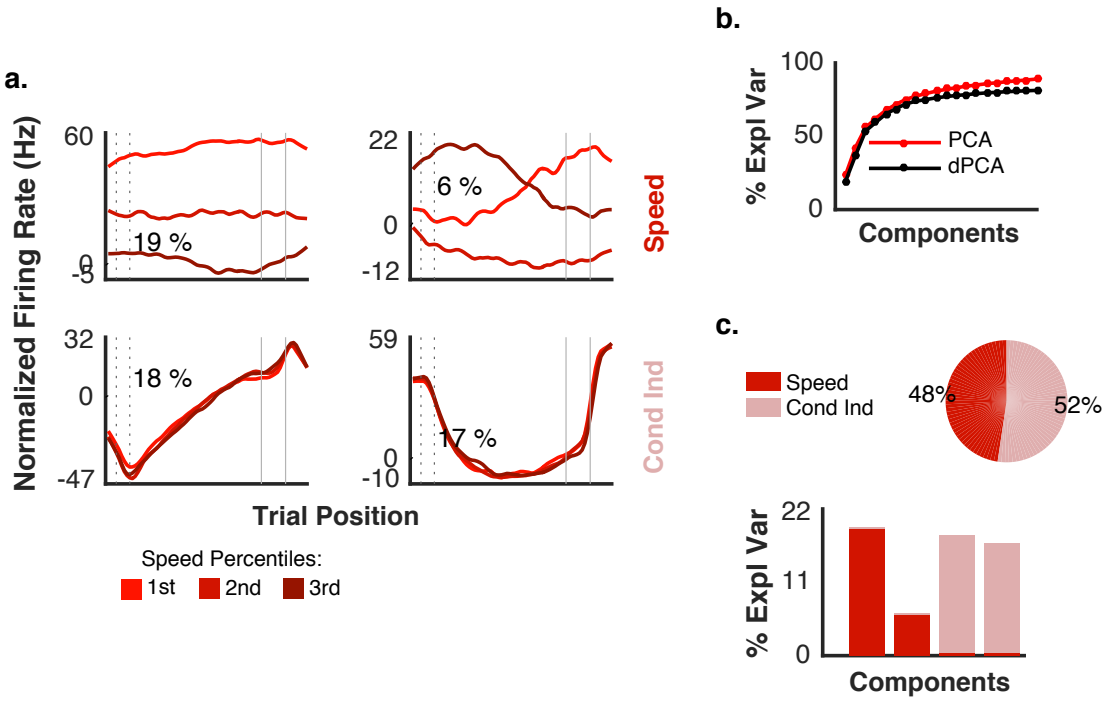

Figure 3.13: dPCA Results No Stop Trials Speeds: As in figure 12 but for trials in which the mice didn't stop.

The fact that such a crude partition of trials, according to their speed characteristics, is able to explain the aforementioned values of variance in the recorded neural data attests to the influence motor aspects have on it in the context of our task.

3.5 Discussion

To investigate the mPFC's involvement in guiding behavior in a WM dependent delayed response task on a treadmill we recorded (*Figure 3.1*) the simultaneous activity of populations of neurons centered at the ventral part of the prelimbic area (*Figure 3.2*).

In a coarse analysis, to better understand how the task engaged the recorded area, we found that the neurons evidenced trial type memory period selectivity, with around 0.59 showing a mean FR that was different between hit and correct rejection trials for at least one third of it (*Figure 3.4 c*). These were not all classic WM-like neurons, with condition specific elevated activity in the memory period, such as the one in *Figure 3.4 a*, as the FR differences could be due to different combinations of excitation and inhibition in each of the trial types. Nevertheless, this selectivity (see *Figure 3.3* bottom three rows) was a strong indication that the area contained signals, during the cue free memory period, that could be used to generate appropriate behavior later on.

Neurons seemed to care more about the response, stopping or not, than the tone played with the proportion of selective cells increasing closer to the stopping area area (*Figure 3.4 b and c*). It's noteworthy that the mean TSHs of 0.185 of the selective neurons encoded trial type for the entire duration of the memory period, a different scenario from what it was observed in the same area in similar tasks (e.g. *Fujisawa et.al, 2008* [12]) in which different neurons encoded different segments of it. Even considering that it might be partially explained by inhibition in hit trials, the fact that 0.39 of the

neurons were selective for correct rejection trials (see *Figure 3.3 bottom two rows* and *Figure 3.4 b bottom two rows*) also indicates that, contrary to what might have been thought, these were not "passive" trials in which the mice just ran to reach the next one.

Neurons' FR was also modulated by specific occurrences with 0.58 of the cells changing their response with at least one task event. Some neurons were modulated by events of just one trial type while others responded in both trial types *Figure 3.6 b* and to more than one event *Figure 3.6 d.* Interestingly, the event that modulated more neurons, both in hit and correct rejection trials was the end of the stopping area: 0.4. If in the case of the hit trials some of this can possibly be related with a motor signal resulting from animals accelerating after reward consumption, in correct rejection trials there is no significant change in speed associated with the end of the reward area *Figure 2.6.* The prefrontal as been previously implicated in monitoring functions, including outcome [37], the strong modulation induced by the end of the stopping area might be related with this. An interesting situation is raised by such scenario given that in trials where the no stop sound is played mice never receive feedback about the correctness of their choice so any signal related with outcome in those trials is necessarily taking in account an internal expectation. Another possible interpretation is that, given the coincidence of the end of the area with the ITI signaling lights being turned on, the modulation might reflect a perception of transition between trials or contexts.

Our single neuron analysis, even if broad and descriptive in nature, revealed a population of neurons with heterogeneous response profiles, able

to encode trial identity during the memory period and being modulated by one or more events from both trial types. The nature of our task was highly dynamic with the animals constantly accelerating and decelerating to navigate from event to event and trial to trial, without clear baseline periods to allow neural activity to stabilize (the ITIs were very short). Given these and the relevance of movement as the mean to solve the task it was to be expected, even if not directly captured by this analysis, for the neural activity to also reflect motor components. The way dynamic movement related activity strongly modulates, throughout the cortex, the response of neurons to task related events has been recently extensively analysed [32].

Using a targeted dimensionality reduction technique, dPCA, we were able to demix, from the joint activity of the neurons, low dimensional representations of the sound played, the response executed by the mice and interactions between these. Strikingly the most salient feature encoded in the data was a difference between correct (hits and correct rejections) and incorrect (misses and false alarms) trials (*Figure 3.9 a* bottom left) covering the entire trial in a tonic-like manner. The fact that the difference was present from trial start to end, and was poorly modulated by any task event, seems to suggest that it reflects some sort of task independent internal state of the mice, like engagement or awareness. The PFC is known to operate in a context dependent manner, with internal states being part of what forms the context in which a behavior is selected [9], it's possible that in error trials the animals were more disengaged which impacted the activity. Such could explain why the animals made mistakes, as looking at the first demixed principal components for sound and decision (*Figure 3.9*

a first two rows left column) doesn't reveal any marked difference between the way these variables were encoded in correct versus error trials, and so no obvious WM-related reasons for the mistakes committed.

As discussed before, a delayed response task doesn't determine the identity of the information animals have to remember to solve the task. Subjects could keep a memory of the played tone until the reward area or upon hearing the tone they could immediately decide what to do and keep a memory of the decision. Our analysis reveals that, in the context of our task, the neurons in the mPFC encode, from sound onset, in both correct and error trials, a retrospective memory of the task cue and a prospective memory of the to be made response (*Figure 3.9 a* first two rows left column). It's noteworthy that sound encoding remains pretty much constant between sound and area, but decision encoding becomes stronger as the animals approach the area and the moment of decision commitment. Contrary to what happened in classical delay period neurons, this selective representations didn't collapsed with the trigger cue, and the animals response, but kept active into the ITI and the end of the trial, similar to what was described by Maggi et.al,2018 [29], and agreeing with PFC involvement in behavior and environment tracking. Modulations associated with the beginning of the stopping area were, however, present in other components (e.g second demixed components of both sound and decision and first condition independent demixed component), an indication that the area effectively acts as some sort of trigger signal and that not everything is decided after cue presentation. These modulations are not simply explained by the animals stopping or receiving reward, given that they happen both in trials in which the mice stop, or

don't, and receive, or not, reward.

Given the reductionist nature of behavioral tasks the total variance of neural activity explained by its parameters is normally low, with the majority of the variance being captured by the catch all condition independent parameter [24]. The scenario we observed was different, with the variance explained being more uniformly spread between the parameters, and condition independent factors explaining just 26% of the variance (*Figure 3.9 c*). Movement is a crucial feature of our task, with the animals pursuing their objectives while running at high speed, an exercise that involves a full body coordinated effort. This is not what happens in a good proportion of the behavioral assays used in neuroscience in which body movement is normally purposefully restrained or the animals are confined to small behavioral boxes. The possible influence of the speed and speed variations of the mice in the neural activity are not directly captured by any of the task features used in the dPCA analysis, but we know that in different moments of the task speed covaries both with the tone played and the response made. It's thus possible that our task parameters explain more variance than normally observed because they are inheriting movement associated variance with them correlated. Movement has been shown before to explain a good degree of the variance present in neural activity [32]

In favor of such hypotheses, and confirming the big influence movement had on the recorded activity, are the results we obtained when using speed as the parameter input to dPCA. For such we divided the stop and no stop trials in three groups clustered in an unbiased way based on the mice speed strategies(*Figure 3.11*). This simple division accounted for 13% of

the explained variance in stop trials and for an impressive 48% in no stop trials,*Figures 3.12-13* . Bear in mind that given the stereotypical nature of the speed trajectories some of the speed related variance is captured by the condition independent parameter, especially in stop trials, and so that this is an underestimation of the real impact movement has on the neural activity. A strong presence of motor behavior representation in the mPFC neural activity had previously been described [5] [26].

Taken together all these reveal that the heterogeneous activity of neurons in the mice mPFC encodes several task features spanning the sensory to cognitive to motor arch. These multidimensional representations and the ability to sustained them in time linking intra-trial events, but presumably also different trials, its evidence of the area's putative involvement in coordinating and orchestrating behavior.

References

[1] E. H. Baeg et al. "Dynamics of population code for working memory in the prefrontal cortex." In: *Neuron* 40 (1 Sept. 2003), pp. 177–188 (cit. on p. 85).

[2] O. Barak, M. Tsodyks, and R. Romo. "Neuronal Population Coding of Parametric Working Memory". In: *Journal of Neuroscience* 30.28 (July 2010), pp. 9424–9430 (cit. on p. 85).

[3] A. S. Batuev, N. P. Kursina, and A. P. Shutov. "Unit activity of the medial wall of the frontal cortex during delayed performance in rats." In: *Behavioural brain research* 41 (2 Dec. 1990), pp. 95–102 (cit. on p. 85).

[4] V. J. Brown and E. M. Bowman. "Rodent models of prefrontal cortical function." In: *Trends in neurosciences* 25 (7 July 2002), pp. 340–343 (cit. on p. 84).

[5] S. L. Cowen and B. L. McNaughton. "Selective delay activity in the medial prefrontal cortex of the rat: contribution of sensorimotor information and contingency." In: *Journal of neurophysiology* 98 (1 July 2007), pp. 303–316 (cit. on pp. 88, 124).

[6] J. P. Cunningham and B. M. Yu. "Dimensionality reduction for large-scale neural recordings." In: *Nature neuroscience* 17 (11 Nov. 2014), pp. 1500–1509 (cit. on p. 86).

[7] C. E. Curtis and M. D'Esposito. "The effects of prefrontal lesions on working memory performance and theory." In: *Cognitive, affective & behavioral neuroscience* 4 (4 Dec. 2004), pp. 528–539 (cit. on p. 85).

[8] J. W. Dalley, R. N. Cardinal, and T. W. Robbins. "Prefrontal executive and cognitive functions in rodents: neural and neurochemical substrates." In: *Neuroscience and biobehavioral reviews* 28 (7 Nov. 2004), pp. 771–784 (cit. on pp. 84, 87).

[9] D. R. Euston, A. J. Gruber, and B. L. McNaughton. "The role of medial prefrontal cortex in memory and decision making." In: *Neuron* 76 (6 Dec. 2012), pp. 1057–1070 (cit. on pp. 84, 121).

[10] D. R. Euston and B. L. McNaughton. "Apparent encoding of sequential context in rat medial prefrontal cortex is accounted for by behavioral variability." In: *The Journal of neuroscience* 26 (51 Dec. 2006), pp. 13143–13155 (cit. on p. 112).

[11] D. J. Freedman et al. "A comparison of primate prefrontal and inferior temporal cortices during visual categorization." In: *The Journal of neuroscience : the official journal of the Society for Neuroscience* 23 (12 June 2003), pp. 5235–5246 (cit. on p. 86).

[12] S. Fujisawa et al. "Behavior-dependent short-term assembly dynamics in the medial prefrontal cortex." In: *Nature neuroscience* 11 (7 July 2008), pp. 823–833 (cit. on p. 119).

[13] S. Funahashi. "Prefrontal cortex and working memory processes." In: *Neuroscience* 139 (1 Apr. 2006), pp. 251–261 (cit. on p. 85).

[14] J. M. Fuster. “Prefrontal neurons in networks of executive memory”. In: *Brain Research Bulletin* 52.5 (July 2000), pp. 331–336 (cit. on p. 84).

[15] J. M. Fuster. “The Prefrontal Cortex—An Update”. In: *Neuron* 30.2 (May 2001), pp. 319–333 (cit. on p. 84).

[16] R. de Haan et al. “Neural Representation of Motor Output, Context and Behavioral Adaptation in Rat Medial Prefrontal Cortex During Learned Behavior.” In: *Frontiers in neural circuits* 12 (2018), p. 75 (cit. on p. 101).

[17] C. D. Harvey, P. Coen, and D. W. Tank. “Choice-specific sequences in parietal cortex during a virtual-navigation decision task.” In: *Nature* 484 (7392 Mar. 2012), pp. 62–68 (cit. on p. 87).

[18] V. Hok et al. “Coding for spatial goals in the prelimbic/infralimbic area of the rat frontal cortex.” In: *Proceedings of the National Academy of Sciences of the United States of America* 102 (12 Mar. 2005), pp. 4602–4607 (cit. on p. 112).

[19] J. M. Hyman et al. “Contextual encoding by ensembles of medial prefrontal cortex neurons.” In: *Proceedings of the National Academy of Sciences of the United States of America* 109 (13 Mar. 2012), pp. 5086–5091 (cit. on p. 86).

[20] Y. Izaki et al. “Effects of rat medial prefrontal cortex temporal inactivation on a delayed alternation task.” In: *Neuroscience letters* 315 (3 Nov. 2001), pp. 129–132 (cit. on p. 85).

[21] J. B. Kahn et al. "Medial prefrontal lesions in mice impair sustained attention but spare maintenance of information in working memory." In: *Learning & memory (Cold Spring Harbor, N.Y.)* 19 (11 Oct. 2012), pp. 513–517 (cit. on p. 87).

[22] R. P. Kesner and J. C. Churchwell. "An analysis of rat prefrontal cortex in mediating executive function." In: *Neurobiology of learning and memory* 96 (3 Oct. 2011), pp. 417–431 (cit. on pp. 84, 87).

[23] D. Koback and W. Brendel. *demixed Principal Component Analysis*. 2016. URL: https://github.com/machenslab/dPCA (cit. on p. 94).

[24] D. Kobak et al. "Demixed principal component analysis of neural population data". In: *eLife* 5 (Apr. 2016) (cit. on pp. 87, 94, 108, 110, 123).

[25] M. Laubach et al. "What, If Anything, Is Rodent Prefrontal Cortex?" In: *eNeuro* 5 (5 2018) (cit. on p. 84).

[26] A. J. Lindsay et al. "How Much Does Movement and Location Encoding Impact Prefrontal Cortex Activity? An Algorithmic Decoding Approach in Freely Moving Rats." In: *eneuro* 5 (2 2018) (cit. on p. 124).

[27] D. Liu et al. "Medial prefrontal activity during delay period contributes to learning of a working memory task." In: *Science (New York, N.Y.)* 346 (6208 Oct. 2014), pp. 458–463 (cit. on p. 87).

[28] C. K. Machens, R. Romo, and C. D. Brody. "Functional, But Not Anatomical, Separation of "What" and "When" in Prefrontal Cortex". In: *Journal of Neuroscience* 30.1 (Jan. 2010), pp. 350–360 (cit. on pp. 86, 87, 101).

[29] S. Maggi, A. Peyrache, and M. D. Humphries. "An ensemble code in medial prefrontal cortex links prior events to outcomes during learning". In: *Nature Communications* 9.1 (June 2018) (cit. on pp. 107, 109, 122).

[30] E. M. Meyers et al. "Dynamic Population Coding of Category Information in Inferior Temporal and Prefrontal Cortex". In: *Journal of Neurophysiology* 100.3 (Sept. 2008), pp. 1407–1419 (cit. on p. 85).

[31] E. K. Miller and J. D. Cohen. "An integrative theory of prefrontal cortex function." In: *Annual review of neuroscience* 24 (2001), pp. 167–202 (cit. on p. 84).

[32] S. Musall et al. "Movement-related activity dominates cortex during sensory-guided decision making". In: (Apr. 2018) (cit. on pp. 121, 123).

[33] M. Pachitariu et al. "Kilosort: realtime spike-sorting for extracellular electrophysiology with hundreds of channels". In: *bioRxiv* (June 2016) (cit. on p. 91).

[34] G. Paxinos and K. B. J. Franklin. *mouse brain in stereotaxic coordinates*. 2nd ed. Vol. 232. San Diego: Academic Press, 2001, pp. 885–895 (cit. on p. 99).

[35] B. R. Postle. "Working memory as an emergent property of the mind and brain." In: *Neuroscience* 139 (1 Apr. 2006), pp. 23–38 (cit. on p. 85).

[36] N. J. Powell and A. D. Redish. "Complex neural codes in rat prelimbic cortex are stable across days on a spatial decision task." In: *Frontiers*

in behavioral neuroscience 8 (2014), p. 120 (cit. on pp. 86, 87, 107, 112).

[37] K. R. Ridderinkhof et al. "Neurocognitive mechanisms of cognitive control: the role of prefrontal cortex in action selection, response inhibition, performance monitoring, and reward-based learning." In: *Brain and cognition* 56 (2 Nov. 2004), pp. 129–140 (cit. on p. 120).

[38] A. C. Riggall and B. R. Postle. "The relationship between working memory storage and elevated activity as measured with functional magnetic resonance imaging." In: *The Journal of neuroscience* 32 (38 Sept. 2012), pp. 12990–12998 (cit. on p. 85).

[39] M. Rigotti et al. "The importance of mixed selectivity in complex cognitive tasks". In: *Nature* 497.7451 (May 2013), pp. 585–590 (cit. on p. 86).

[40] C. Rossant. *Phy Project*. URL: https://github.com/kwikteam/phy (cit. on p. 91).

[41] S. Royer et al. "Control of timing, rate and bursts of hippocampal place cells by dendritic and somatic inhibition." In: *Nature neuroscience* 15 (5 Mar. 2012), pp. 769–775 (cit. on p. 87).

[42] M. Shafi et al. "Variability in neuronal activity in primate cortex during working memory tasks." In: *Neuroscience* 146 (3 May 2007), pp. 1082–1108 (cit. on p. 85).

[43] J. H. Siegle et al. "Open Ephys: an open-source, plugin-based platform for multichannel electrophysiology." In: *Journal of neural engineering* 14 (4 Aug. 2017), p. 045003 (cit. on p. 91).

[44] K. K. Sreenivasan, E. K. Curtis, and M. D'Esposito. "Revisiting the role of persistent neural activity during working memory". In: *Trends in Cognitive Sciences* 18.2 (Feb. 2014), pp. 82–89 (cit. on p. 86).

[45] S. Tsujimoto and B. R. Postle. "The prefrontal cortex and oculomotor delayed response: a reconsideration of the "mnemonic scotoma"." In: *Journal of cognitive neuroscience* 24 (3 Mar. 2012), pp. 627–635 (cit. on p. 85).

[46] H. B. Uylings, H. J. Groenewegen, and B. Kolb. "Do rats have a prefrontal cortex?" In: *Behavioural brain research* 146 (1-2 Nov. 2003), pp. 3–17 (cit. on p. 84).

[47] T. Yoon et al. "Prefrontal cortex and hippocampus subserve different components of working memory in rats." In: *Learning & memory (Cold Spring Harbor, N.Y.)* 15 (3 Mar. 2008), pp. 97–105 (cit. on p. 85).

Chapter 4

Single Trial Decoding of Speed and Memory

Chapter Authors

João Afonso and Alfonso Renart

Authors' Contributions

Conceived and designed the neural data analysis: *João Afonso and Alfonso Renart*

Wrote the code and analysed the neural data: *João Afonso*

4.1 Abstract

A distinctive characteristic of prefrontal areas, in both primates and rodents, is the predominance of neurons, with heterogeneous response profiles, that reflect in their activity the combination of external factors with the brain appraisal of these. This mixed selectivity has been associated with the PFC's ability to simultaneously encode all the different multimodal features needed to guide adaptive behavior. To be fully understood the relation between population encoded activity and behavior needs to be explored at a moment to moment level, particularly with cognitive and motor variables, which time varying characteristics are poorly described by averaged measures. Here, using simple linear models, we show that, in the context of our task, WM information about trial type and the ongoing speed strategy of the mice are simultaneously encoded, at the single trial level, in the joint activity of mPFC's neurons. Importantly, the variables can be decoded in a fairly independent way, with WM encoding not depending on behavior. Also, movement encoding neurons tendentiously reflect past changes in speed of the mice on the treadmill.

4.2 Introduction

At every moment distributed networks of neurons in the brain communicate and work together to represent the world and generate adapted behavior. The idea that the chances of understanding this process only get better by monitoring the simultaneous activity of the biggest possible number of cells is intuitive. Hence, despite the body of knowledge built on top of studies based on single neuron recordings and averaged repeated measures [6], a general agreement is forming that neural activity can only be completely understood at the ensemble and single trial level [5]. The simultaneous recording of populations of neurons gives access to how information is encoded in the spatiotemporal features of the ensembles' activity and allows access to the mechanisms behind phenomenons that are poorly captured or even disguised by averaging across presentations.

The issues arising from trial averaging are particularly pertinent in the case of motor behaviors - more difficult to constrain and systematize than stimuli in the sensory domain, and internal cognitive processes - many times not directly relatable to any external time-varying measurable quantity [3]. The relevance of population recordings grows, thus, with the distance from the periphery, being particularly relevant in high order cognitive areas, like the PFC. In these areas the activity of the neurons is more variable, being less reliably driven by specific external inputs and outputs and more by the activity of other neurons that convey the brain's own interpretation, and appraisal, of those same external features [2].

The integrative nature of the PFC's activity means that its neurons can

exhibit virtually any type of response profile, mixing influences from sensory, cognitive and motor aspects. Such mixed selectivity has been hypothesized to underlie the ability of the neurons to generate high dimensional representations of a significant amount of task-relevant aspects [26], this possibly explaining the impressive flexibility, and adaptability, of the encoding observed in the PFC [7], and facilitating the selective readout of information by downstream areas.

Accordingly, a growing number of studies, focused on how information is processed in the PFC, of both primates and rodents, by the evolving patterns of ensembles of neurons, have consistently revealed that multiple task relevant elements are simultaneously encoded in the neurons' joint activity. This multiplexed information commonly represents a diverse set of features, associated with guiding and controlling behavior in a task specific manner, such as cue or cues identity, location and direction, behavioral strategy and progress tracking, goals and trial outcome monitoring [29] [16] [28] [10] [15] [13] [1]. The decodable information tends to display temporal stability, being present in the absent of external drivers both when the task overtly demands for it, as in WM tasks [29] [16], or in passive task periods with no cognitive demands [1]. Passive representations of previous choices and outcomes were even found in the first time naive animals had contact with a given task, pointing for an innate role of the mPFC in linking certain phenomenons in time, or at least to a very fast ability in forming certain task specific representations [17]. The way given features are encoded by the populations has also been shown to be largely independent of the characteristics of the feature per se varying with different task rules and contexts [23] [11].

What is known about a given brain area depends on the questions asked when studying it. Traditionally, activity related with the animals' movements, or internal states, has been ignored, discarded, or controlled for, in an attempt to isolate information directly linked to variables of interest. Movement, nevertheless, seems to be broadly represented in the cortex, with its signals being deeply intertwined with task relevant features and possible serving computational purposes [20]. Running, for instance, is known to modulate the gain of visual inputs [22], visual motion [27] and predictive coding [12].

Prefrontal research has been traditionally concerned with high order cognitive functions, but, as was realized in the context of WM related activity investigation [4] [9], motor variables can also strongly impact the area's activity [14]. Movement and movement trajectories [9] [11], head position [4] and speed [10] [23] have been, for instance, identified has influencing mPFC's activity. Interestingly the way these motor variables are encoded in the area seems to also depend on the context in which they happen, and in particular in their relation to motivationally relevant outcomes [4].

In the context of our task, taking advantage of the dozens of simultaneously recorded neurons per session, we were able to decode, at the single trial level, both the centimeter by centimeter speed of the animals on the treadmill, during the entire trial, and a stable representation, during the memory period, of trial selective information that could be used to guide behavior. Speed, a low level motor variable, and trial identity, an internally generated and sustained cognitive variable, were simultaneously and seemingly independently encoded in the activity of the same population of neurons.

Moreover, the ensemble's activity tendentiously reflected the speed at which the mice were running, rather than determining it, and was more involved in encoding its changes than absolute values. The motivational context in which the behavior was performed also impacted how well speed could be decoded, with our model decoding better speed when the mice already knew they were going to receive reward.

The ability of the mPFC population's activity to encode, in a multiplexed way, both a categorical cognitive variable and a continuous and detailed representation of the ongoing animal behavior supports the area's role in integrating multimodal sources of information and using them to orchestrate and control behavior.

4.3 Methods and Materials

4.3.1 Predicting Speed

4.3.1.1 General Model

We used the Glmnet Matlab package [24] to fit the multivariate linear regression model we employed to predict speed in each session. The algorithm minimizes the penalized sum of squares

$$\frac{1}{2N}\sum_{i=1}^{N}(yi - \beta_0 - x_i^T\beta)^2 + \lambda[(1-\alpha)||\beta||_2^2/2 + \alpha||\beta||_1]$$

through cyclic gradient descent with $\lambda \geq 0$ as a complexity parameter and $0 \leq \alpha \leq 1$ as compromise between ridge and lasso (ridge:$\alpha = 0$; lasso: $\alpha = 1$).

As the response vector $\mathbf{Y}$ we used the concatenated speeds of all trials, in cms/s, calculated in 1 cm bins. As predictors we used the FRs of all recorded neurons organized in an input matrix $\mathbf{X}$ where the values in each row were used to predict the speed value in the correspondent row of the vector $\mathbf{Y}$. All rows of $\mathbf{X}$ had 21 columns per recorded neuron, with all columns containing the FR, in Hz, of the respective neuron, in a given 1 cm bin, organized in the follwoing way: the FR in the center column of each 21 columns' group corresponded, in trial position, to the speed in the same row of the target vector $\mathbf{Y}$, the 10 columns before and after contained the FRs of the neuron $10 * 1$ cm bins before and after that. This procedure amounted to convolve

a $21 * 1$ cm kernel with the FR of all neurons through each trial. The input matrix $\mathbf{X}$ was then $S * NK$ with S = number of speed bins being predicted; N = number of neurons; K = size of the predicting kernel.

All predictions were made on data not used for training, using 10 fold cross validation and the regularization parameter λ was fitted by the algorithm using an inner nest of cross validation, again with 10 folds.

4.3.1.2 Speed Prediction Performance Calculations

To access how well were our models predicting speed (*Figure 4.2* and *Figure 4.15*) we used R^2 defined here as

$$R^2 = 1 - \frac{\sum_{i=1}^{n}(y_i - \hat{y}_i)^2}{\sum_{i=1}^{n}(y_i - \bar{y})^2}$$

with y = real speeds; $\hat{y}$ = predicted speeds; $\bar{y}$ = mean of real speeds.

In *Figure 4.4* the performance of the models was compared through the residual sum of squares $\sum_{i=1}^{n}(y_i - \hat{y}_i)^2$.

4.3.1.3 Past-Future and Speed-Acceleration indices

The 21 coefficients predictive kernels, $\mathbf{K}$, of all neurons were attributed a past future index (PFI) according the following formula

$$PFI = \frac{|\frac{1}{N}\sum_{i=1}^{10} k_i| - |\frac{1}{N}\sum_{i=12}^{21} k_i|}{|\frac{1}{N}\sum_{i=1}^{10} k_i| + |\frac{1}{N}\sum_{i=12}^{21} k_i|}$$

where for neurons that influence speed the first 10 elements have a higher mean,$|\frac{1}{N}\sum_{i=1}^{10} k_i|$, and for neurons that reflect speed the last 10 elements have a higher mean$|\frac{1}{N}\sum_{i=12}^{21} k_i|$,

The same kernels were also attributed a speed acceleration index (SAI). For that, each kernel **K** was first normalized between 0 and 1 and then centered so that the first and last values of K were equidistant from 0 with the lower of them being made negative and the higher positive. After this transformation the following formula was used to calculate the SAI from the transformed kernel $\tilde{K}$

$$SAI = \frac{|\tilde{K}_{21} - \tilde{K}_1| - |\frac{1}{N}\sum \tilde{K}|}{|\tilde{K}_{21} - \tilde{K}_1| + |\frac{1}{N}\sum \tilde{K}|}$$

sigmoid shaped kernels, $\tilde{K}$, had an absolute mean, $|\frac{1}{N}\sum \tilde{K}|$ close to 0 and a big absolute difference between the last and first values,$|\tilde{K}_{21} - \tilde{K}_1|$. In gaussian shaped kernels the mean of $\tilde{K}$ was big and the absolute difference between the first and last values close to 0.

4.3.1.4 Speed Prediction with Past and Future Neuronal Activity

All linear regression models used to predict speed in *Figure 4.15* were fitted using the same algorithm described above in the *General Model* section, just the input matrix **X** and the response vector **Y** were different. **Y** was a vector with the concatenated speeds of all trials, in cms/s, calculated in 3 cm bins. The input matrix **X** had the same number of rows as **Y** with each column containing the FR, in Hz, of each of the recorded neurons, in the same trial position bin as the speed in the correspondent row of **Y**. Several models were fitted with the row correspondence of **X** and **Y** being shifted in relation to each other.

4.3.2 Predicting Trial Identity

4.3.2.1 General Model

To predict trial identity from the neural activity during the memory period of each trial we used logistic regression. For this we again used the Glmnet package [24] that uses cyclical gradient descent to minimize, in the case of logistic regression minimize

$$-\frac{1}{N}\sum_{i=1}^{N} y_i * (\beta_0 + x_i^T\beta) + \log(1 + e^{(\beta_0 + x_i^T\beta)}) + \lambda[(1-\alpha)||\beta||_2^2/2 + \alpha||\beta||_1],$$

with $\lambda \geq 0$ as a complexity parameter and $0 \leq \alpha \leq 1$ as a compromise between ridge and lasso (ridge:$\alpha = 0$; lasso: $\alpha = 1$).

The response vector $\mathbf{Y}$ had the same number of rows as the number of 1 cm bins between sound off and the end of each trial. All rows coming from hit trials were set to be equal to 1 and all coming from correct rejection trials equal to 0. The input matrix $\mathbf{X}$ was built as described above for the speed prediction general model.

4.3.2.2 Speed Prediction Performance Calculations

The performance of the trial identity prediction models (*Figure 4.9* and *Figure 4.13*) was accessed via the area under the receiver operating characteristic (ROC) curve. The ROC curve was created by plotting the hit rate (true positives) of the model against the false alarm rate (false positives)

at various threshold settings. Our thresholds went from 0 to 1 in 0.001 increments.

4.3.3 Speed and Trial Identity Predictions Comparison

In *Figures 3.12-14* the relation between each neuron's 21 coefficients prediction kernels, resulting from speed and trial identity predictions, was accessed via the Pearson correlation coefficient between the kernels.

To compare overall session decoding the Pearson correlation coefficient was taken between the full vector of coefficients fitted by each model (corresponding to the concatenation of all neurons' kernels).

4.4 Results

4.4.1 Decoding Speed, From Neural Activity, at the Single Trial Level

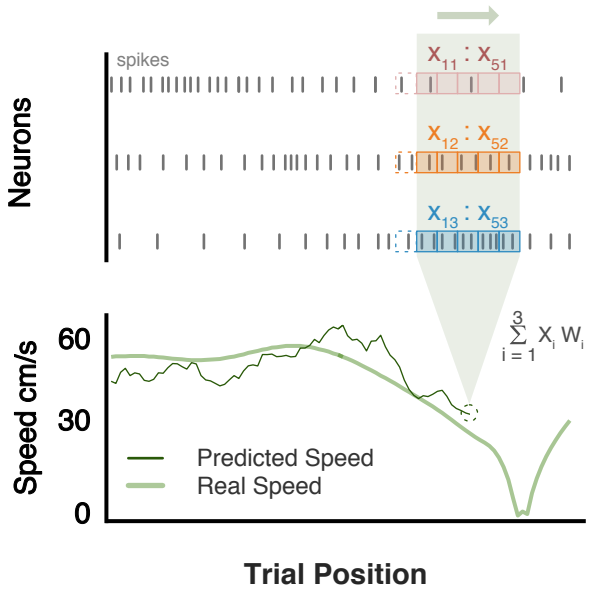

Figure 4.1: Predicting Mice Speed from Single Trial Neural Activity: To predict the speed of the mice in each cm of a given trial we used a sliding kernel to linearly combine the activity of all simultaneously recorded neurons a given number of cms into the past and into to future relative to the cm being predicted. In the figure toy example speed is predicted by combining the firing rates of three neurons over 5cm, averaged in 1 cm bins, and centered on the cm we want to predict. In reality we used a 21 cm sliding kernel extending 10 cm into the past and future of the speed bin being predicted. The coefficients associated with each firing rate bin were fitted using linear regression.

As we showed in the previous chapter (*Figure 3.12* and *Figure 3.13*) speed exerts a considerable influence in the neural activity observed in the mPFC of mice solving the task. To better characterize this influence, and

understand how speed was represented in the population activity, we took advantage of our simultaneously recorded neurons and tried to decode speed at the single trial level.

Using a cross validated linear regression model we predicted the speed of the mice, in each centimeter of each trial, from the linear combination of the activity of all neurons at and around the centimeter being predicted. In practice, we combined the FR of each neuron in 21 × 1 cm bins centered at the bin being predicted and extending 10 cm into the future and past of that bin (*Figure 4.1*).

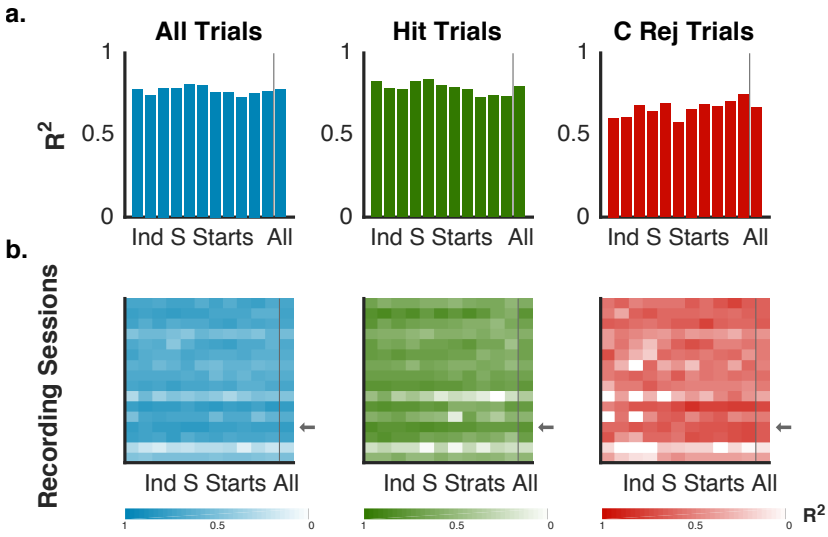

*Figure 4.2: Performance of the Speed Prediction Model: Speed in each cm of a trial was predicted by combining the firing rates of all neurons using a 21 * 1 cm bins kernel extending 10 cm into the past and the future of the position we wanted to predict (see Figure 4.1). The model was fitted using all hit and correct rejection trials from all sound start locations. (a) Performance of the model in one recording session, quantified as R^2, for all, hit and correct rejection trials. In all 3 cases the first 11 bars are for the R^2 calculated separately for the trials with the same sound start position and the last bar for the R^2 calculated with all trials grouped. (b) Model performance in each recording session. The X axis is the same as above and each row is one recording session. The arrows signal the session showed in (a).*

Our linear model was able to predict the speed of the animals on the treadmill consistently well across sessions and for all sound start locations (0.64 ± 0.13 SD mean session R^2 using both trial types and all sound start locations) (*Figure 4.2 a and b left*). Prediction was better, though, in hit than in correct rejection trials (0.63 ± 0.15 SD and 0.52 ± 0.15 SD mean session R^2, respectively) (*Figure 4.2 a and b middle and right*). Here we didn't fit different models for each trial type data, just calculated the R^2s separately from the true and predicted speeds grouped by trial type. The R^2 calculation is dependent not only in how close the model predictions are to the real speed values, but also in how close is the mean of those same values to them (see *Methods Section*). Given the difference in mean speed patterns, and in speed variability, inside each trial and between trials, comparing the R^2s calculated with all trials or with just the condition specific ones might have introduced distortions. Looking at the normalized error between the real and the predicted values, for the three situations, the results were, however, consistent with the obtained R^2s: when considering all trials together the mean error per speed value predicted was 8.32 ± 1.4 SD cm/s; in just hit trials the mean error was 8 ± 1.5 SD cm/s; and in just correct rejection trials 8.7 ± 1.3 SD cm/s.

To gain a clearer idea of the meaning of the R^2 values and the fidelity of the predictions we plotted the mean predicted and real values, in one example session, together. In *Figure 4.3* one can observe how well the mean predicted speeds track the mean real speeds along the entire trial, in both hits and correct rejections and for all sound start locations. Importantly, the prediction captures well the crossings and overlaps between the speed

patterns of the two trial types, evidence that it is not just reflecting a baseline difference between the two.

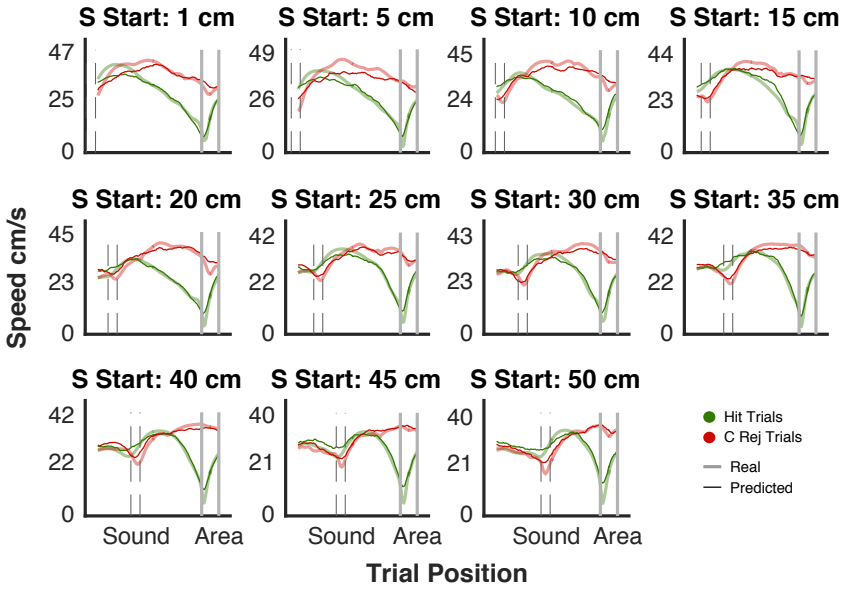

Figure 4.3: Real and Predicted Mean Speeds: Real and predicted mean speeds, grouped by sound start location and trial type, of an example session.

Because of the existence of clear stereotypical mean speed trajectories, in both trial types, it was not totally evident for us if the neurons were just encoding these mean modes of action or if they were, in fact, encoding speed in each trial. To address this question we fitted two new models, using the same data and procedure as before, but introducing two crucial manipulations: in one we shuffled the correspondence between the input FRs and the target speeds across all trials; in the other we shuffled the input-target correspondence just within trials of the same condition, hits and correct rejections, breaking single trial correspondence but preserving the means. By comparing the performance of the non shuffled original model

with the two new shuffled models we would be able to find what proportion of our original prediction power was explained from predicting the mean or trial specific speed.

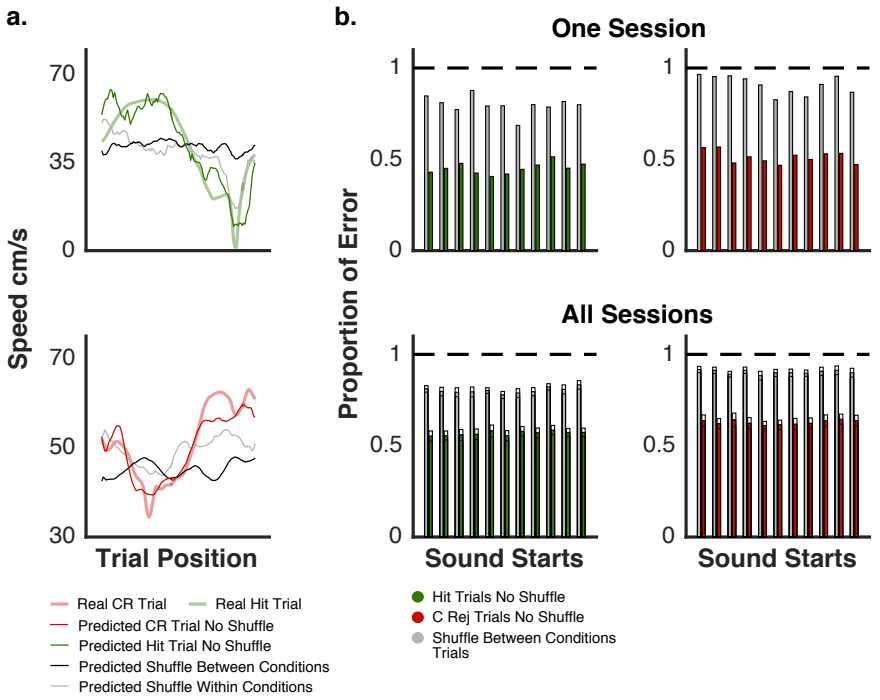

Figure 4.4: Trial to Trial Vs. Mean Trial type Speed Prediction : (a) Example trials: real and predicted speeds. 3 Different models were fitted: Black - shuffling neural and speed data between all trials; Grey - shuffling between trials of the same condition; Red and Green - no shuffle. (b) Proportion of RMSE, relative to the total shuffle model (dashed line), of the condition shuffle (grey bars) and no shuffle models (colored bars). Top: example session, Bottom: all sessions. Boxes on the bottom plots bars are for the SEM.

Introducing information about trial type specific mean speed (shuffling just within the same condition) improved our prediction, in comparison with the total shuffle model, for both hits and correct rejections (mean original error proportions of 0.8 $\pm$ 0.09 SD and 0.9 $\pm$ 0.08 SD, for hit and correct re-

jection trials respectively, across sound start locations). Although improved this prediction was still considerable worst than the achieved by the original, non shuffled, model which reduced the total shuffle model error even further (mean original error proportion of 0.56 ± 0.10 SD and 0.62 ± 0.11 SD, for hit and correct rejection trials respectively, across sound start locations) (*Figure 4.4*). Such showed us that at least half of our model performance was coming from actually predicting trial specific speed.

It was somewhat surprising that our predictions were so accurate given that we were fitting a single model to trial segments with different meanings and needs, from both trial types and in all sound start locations. The good performance of the model in these conditions implies that the mPFC, a non primary motor area, encodes, in each trial, a fairly universal representation of a low level motor feature: speed.

4.4.2 How are the Neurons Encoding Speed ?

We showed that the population activity in the mice's mPFC possesses information about the speed at which the animals run on the treadmill while solving the task. Because of the method we used to decode speed, linearly combining the activity of all neurons in 21 × 1 cm bins around the speed position being predicted, we could look at the coefficients the model attributed to each neuron's prediction kernel to gain an idea of when and how much was the activity of each neuron important for the prediction.

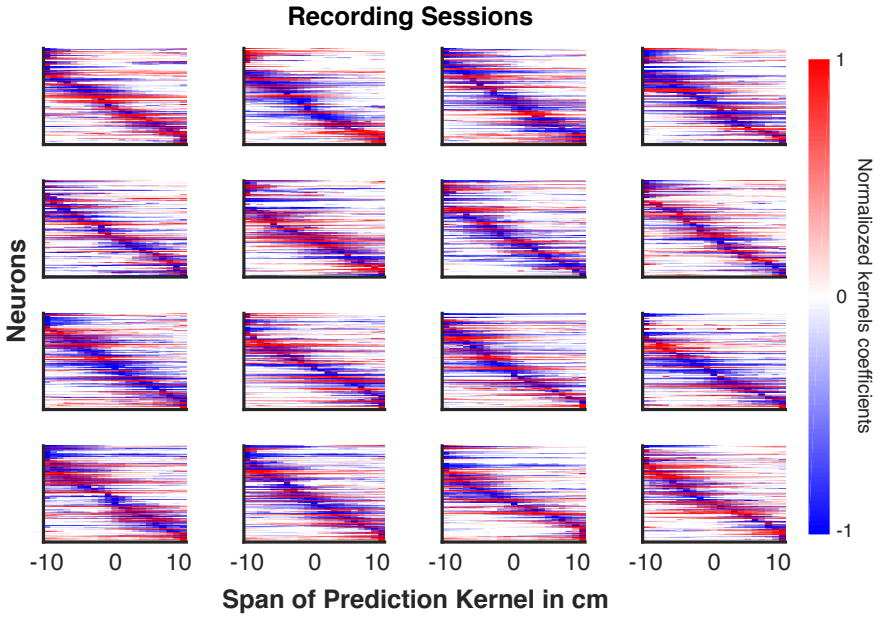

Figure 4.5: Speed Prediction Kernels Coefficients : Coefficients of the 21 bins sliding kernels, fitted when predicting speed, for all neurons in all sessions, sorted by position of their center of mass. For visualization purposes kernels were normalized so that all coefficients would be between -1 and 1 but maintained their original sign. Neurons with the center of mass in the past (negative values) reflect the speed at which the mouse was running. Neurons with the center of mass in the future influence the speed at which the mouse will be running.

Figure 4.5 shows, for all sessions, normalized between -1 and 1 and adjusted so that all coefficients maintained the same sign, each neuron's 21 bin coefficients prediction kernel sorted by their centers of mass. In all sessions the relation of the neurons' activity with speed was heterogeneous with cells that reflected, either by increasing or decreasing their FR, the speed at which the animals were running some distance into the past and others that were predictive, again in both directions, of the speed at which the mice would be running some centimeters into the future.

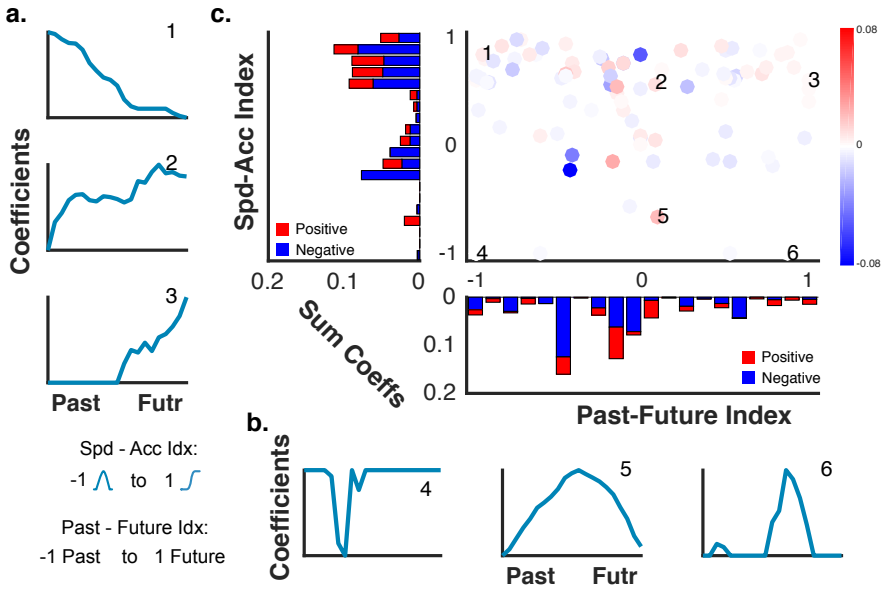

Figure 4.6: Speed-Acceleration and Past-Future Indices : Speed prediction kernels can be classified using a Speed-Acceleration index (-1 if the kernel as a gaussian like shape being involved in predicting a constant speed or 1 if the kernel as a sigmoid like shape being involved in predicting a change in speed) and a Past-Future index (-1 if the neuron activity reflects the speed of the animal 1 if it contributes to it). (a) examples of kernel shapes with positive Spd-Acc index. (b) examples of kernel shapes wit negative Spd-Acc index. (c) Spd-Acc Vs. Past-Fut indices plot of all neurons from one example session. Neurons are color code according to the mean value of their kernel coefficients. Bar plots show the sum of the kernel coefficients means (positive and negative) in each 0.1 bin of both indices.

For every session the information contained in *Figure 4.5* could be summarized by characterizing each neuron's kernel in terms of its past-future (kernel's center of mass location) and speed-acceleration (kernel's shape) relation with speed prediction (*Figure 4.6*). Plotting the classification, along this two axes, of the kernels of all neurons, across all sessions, revealed that the biggest contribution to the predicted speed values came from sigmoid like kernels, involved in encoding changes in speed (*Figure 4.7* center and

left, and a mean 0.74 ± 0.06SD of neurons per session with a positive Spd-Acc index) that had their center of mass in the past (*Figure 4.7* center and bottom, and a mean 0.57 ± 0.03SD of neurons with negative PFI index) this way reflecting, rather than influencing, speed. Curiously, neurons with gaussian shaped kernels, particularly the ones associated with larger coefficients, had a closer to zero PFI and so encoded speed in the present or at least in a balanced way between past and future.

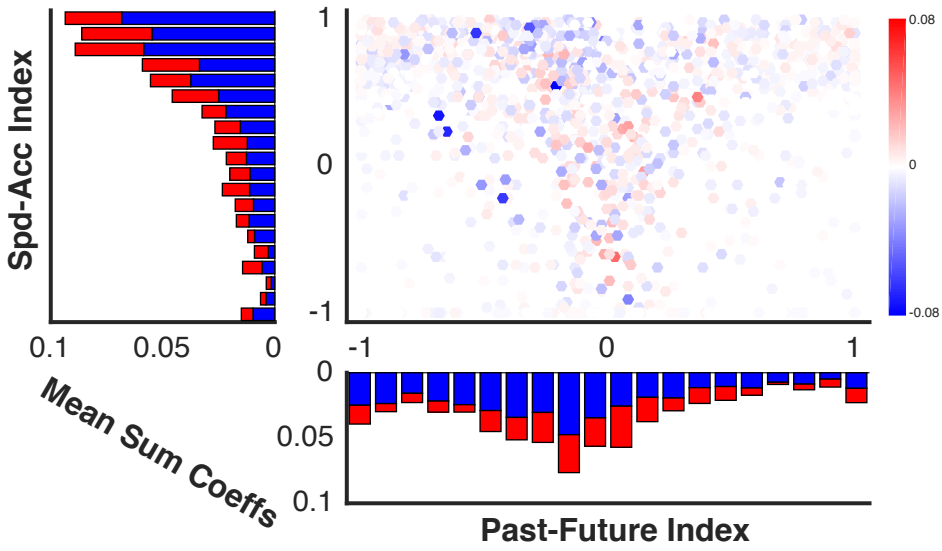

Figure 4.7: Speed-Acceleration and Past-Future Indices All Sessions : Same as (c) in Figure 4.6 but now for all neurons from all recording Sessions.

To get a more direct handle on the important question of whether mPFC activity reflected, or was being reflected, in the mice's speed we used a different modeling approach: speeds and FRs in each trial were calculated in 3 cm bins and then the bins alignment was systematically shifted, into the past and the future, relative to each other, with a different speed predicting

model fitted in each shift (*Figure 4.8 a*). The same procedure was followed using all trials or just hit or correct rejection trials.

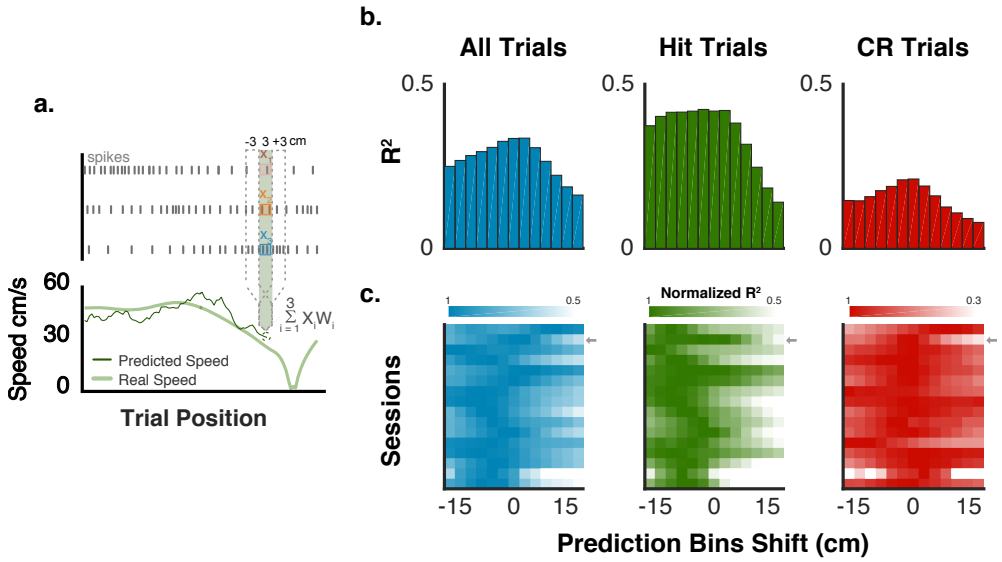

Figure 4.8: Predicting Speed with Past and Future Neural Activity : (a) Speed, in 3 cm bins, is predicted by linearly combining the FR of all neurons calculated over same length bins. Different models were fitted shifting the alignment of the speed and FR bins into the future and past in one bin (3 cm) shifts. 13 Models were fitted: one aligned plus six 3 cm shifts into the past and six into the future. (b) Performance of each model in one example session for: both types of trials predicted together - left; hit trials predicted separately - center; correct rejection trials predicted separately - right. For all 3 plots 0 corresponds to present and each bar into the past (negative X axis) and future (positive X axis) corresponds to a 3 cm shift. ***(c)*** *Same as above above but now color mapped for all sessions. Arrows indicate the example session in (b).*

Using this approach we were still able to decode speed information from the mPFC's population activity but the performance of the models was worst. This was somewhat to be expected as we were predicting speed in one bin using the FR in another individual same size bin, instead of pulling information from several bins around the predicted one, as we did before. Also, overall, the performance was better in the models applied to all and

hits than to correct rejection trials (mean session R^2s of 0.35 ± 0.13SD, 0.38 ± 0.12SD and 0.29 ± 0.08SD, for the best shifted position models in all, hit and correct rejection trials, respectively) (*Figure 4.8 b and c*), in line with the results obtained when predicting speed with the sliding kernel approach (*Figure 4.2*).

By fitting a different model with each bin shift we found that, as the coefficient kernels' analysis had already suggested, information in the mPFC allow us to predict better speed to the past than to the future of the neural activity (*Figure 4.8 b and c*). A tendency that was stronger in hit trials (sum of R^2s of models in negative bins representing in average 0.75 ± 0.12SD of the total R^2s sum across sessions) but also true for the models fitted to all trials together (0.6 ± 0.08SD) and, to less extent, correct rejections (0.54 ± 0.15SD).

All together these results demontrate that it's possible to decode, from the simultaneously recorded activity of neurons in the mPFC, the speed at which the mice run on the treadmill while solving the task. Moreover, that the FRs encode more changes than stable values of speed and that these representations tend to be retrospective, relating more to past than future speeds.

Until now we worked under the assumption that the mPFC encodes speed in the same way independently of trial type and position on the trial. Given that the mPFC is not a primary motor area and has been found to represent the same feature, and behavior, differently depending on the context [10] [4], we were aware that our assumption was, with great probability, simplistic. To test broadly how decoding speed in a trial type, or trial position, specific

manner would compare with predicting speed in a general way, we fitted new models, separately, to the entire trial, or just after the sound, in hit and correct rejection trials (*Figure 4.15 a*).

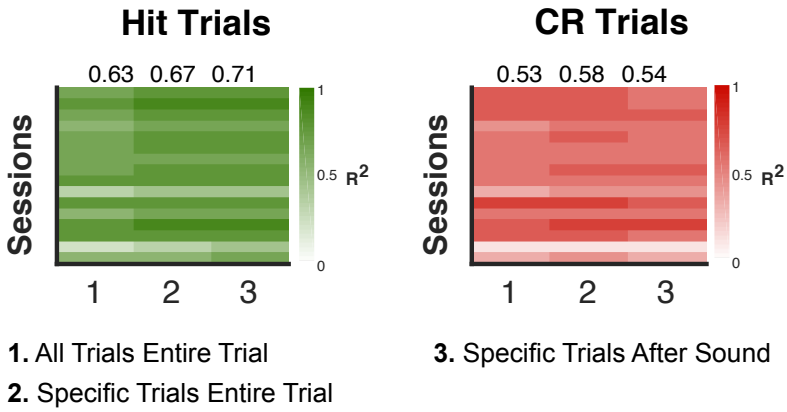

Figure 4.9: Predicting Speed in a Condition Specific Manner : Speed prediction model performance for hit and correct rejection trials: predicted together in the entire trial - 1; Predicted separately in the entire trial - 2; Predicted separately from sound onset to trial end - 3.

For both hit and correct rejection trials fitting a model specifically to each trial type improved our speed prediction performance, even if not in a dramatic fashion (mean session R^2 of 0.63 $\pm$ 0.15SD and 0.67 $\pm$ 0.12SD in hit trials and 0.53 $\pm$ 0.15SD and 0.58 $\pm$ 0.14SD in correct rejection trials for general and trial type specific model). In hit trials our prediction performance was still further increased when we limited our analysis to period of the trial after the sound (mean session R^2 of 0.71 $\pm$ 0.12SD), this is the period where the speed behavior becomes more relevant and where the mice already have an expectation that they are going to receive reward. The same doesn't happen in correct rejection trials where, when one restricts the analysis to the portion of the trial after the sound, the mean performance

of the model drops to an R^2 of 0.54 ± 0.11SD.

The performance of our model improved when we tried to predict speed in a condition specific manner and also, in the case of the hits, in a particularly relevant part of the the trial. Despite these, the improvement was not dramatic, and although a more refined analysis would be necessary to fully address this issue, it is possible to say that speed in the mPFC is encoded in a way that can be read out by a same linear model in fairly universal, not radically context dependent, way.

4.4.3 Decoding Trial Identity, From Neural Activity, at the Single Trial Level

We learned that neurons in the mice mPFC encode speed in a single trial basis, but what about the memory needed for the animals to know what action to perform upon reaching the stopping area? Was it possible to decode, from the population activity, in every trial and throughout the entire memory period, information that would allow to classify the type of trial the mouse was in? To answer this question we used logistic regression, and the same 21 × 1 cm bins sliding kernel approach, to predict the probability, at each memory period centimeter, of an animal being in a hit trial (*Figure 4.9*). Importantly, due to the small amount of mistakes committed by the mice, we only used correct trials in these predictions and so it was impossible to disambiguate if the representation we were decoding was from the sound played or the decision made by the animals.

Our model was able to decode very well (*Figure 4.10*), from the population activity, throughout the memory period, the identity, hit or correct

rejection, of a given trial, for all different sound start locations (mean AUC of 0.94 ± 0.08SD , across all sessions, for predicting the identity of all trials together).

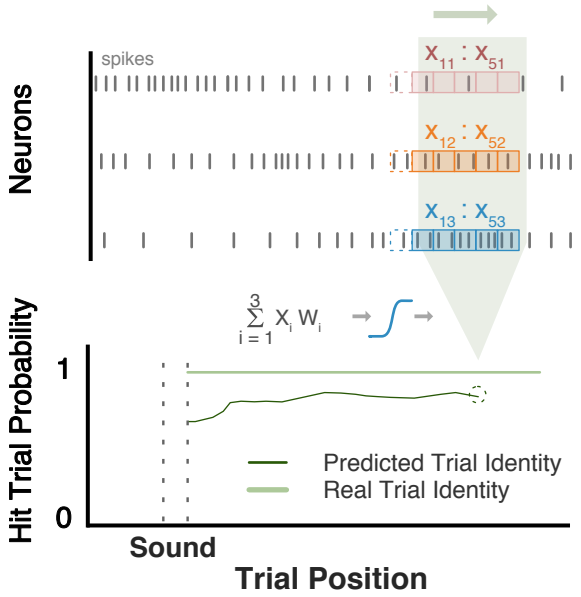

Figure 4.10: Predicting Trial Identity from Single Trial Neural Activity: To predict the identity of a given trial (hit or correct rejection) we followed the same procedure described in Figure 4.1 but used logistic, instead of linear regression, to fit the model and predict the probability of the mice being in a hit trial at each cm between sound off and trial end.

These representations were quite stable along the the entire memory period, as can be seen in the predictions for all centimeters of the memory period averaged across same sound start location trials (*Figure 4.11*). Hence, in each trial, for the entire delay period between the end of the sound and the action trigger signal provided by the area, it was possible to decode, from the mPFC, information that could guide the behavior of the mice. Such stability was also an indication that our ability to decode trial identity was

not dependent on the fact that we could also predict speed: speeds, in hit and correct rejection trials, are markedly different close to the area, but are overlapping just after the sound.

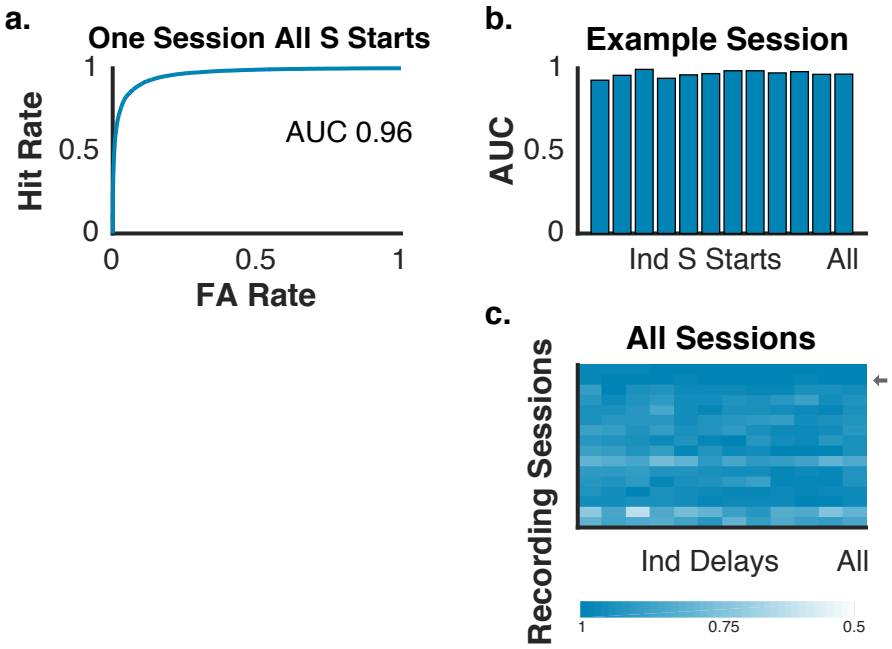

*Figure 4.11: Performance of the Trial Identity Prediction Model : Trial identity of each cm of a trial is predicted by combining the firing rates of all neurons using a 21 * 1 cm bins kernel extending 10 cm into the past and the future of the position we wanted to predicted (see Figure 4.9). The model is fitted with all correct trials from all delays grouped. (a) Performance of the model in one recording session, quantified as AUC, for all different sound start location trials grouped. (b) Same session as in (a) but now with the performance of the model in all sound start locations individually (first 11 bars) and together (12th bar). (c) Model performance in each recording session. The X axis is the same as above and each row is one recording session. The arrows signal the example session in (a) and (b).*

Despite this observation we were still interested in understanding if and how was our ability to predict speed and trial identity, from the same population of neurons, related. In an extreme situation, where speed between

trial types was different in the entire memory period, predicting speed and trial identity would be effectively the same and trial type representation could be solely due to motor and not cognitive differences. Functionally, if both pieces of information, a stable WM and a evolving representation of behavior, would have to be used to aid the mice during the task, it would be important if they could be retrieved independently and unequivocally.

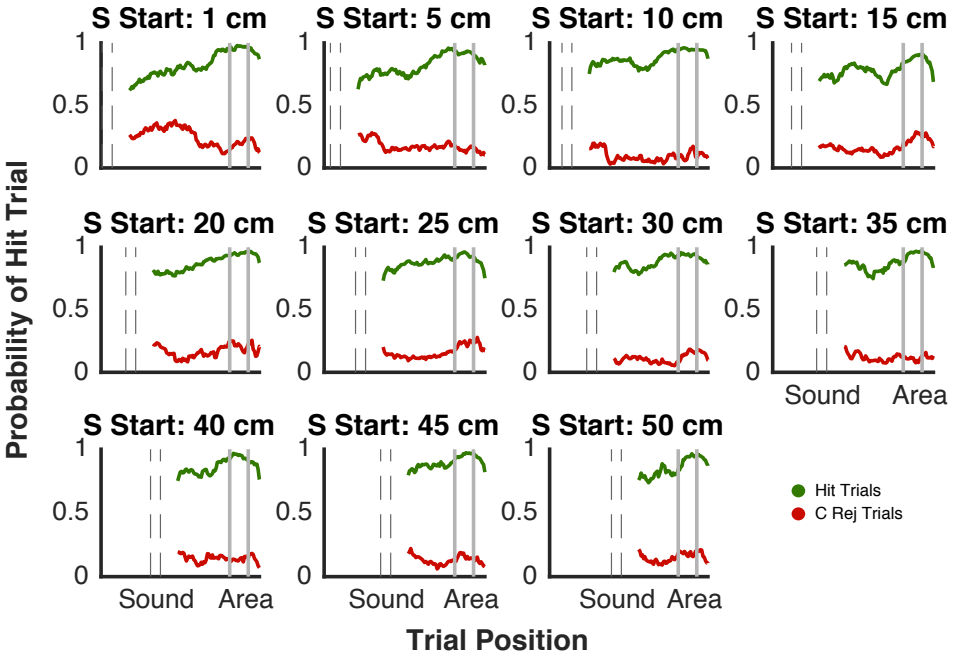

Figure 4.12: Real and Predicted Mean Trial Identity : Real and predicted mean trial identity, grouped by sound start location and trial type, of an example session.

To clarify the relation between our speed and trial identity prediction models we calculated the correlation between the coefficients kernels of each neuron resulting from predicting the former (*Figure 4.5*) and the later (*Figure 4.12*). Note that in the context of trial identity prediction it doesn't

make sense to classify the kernels like we did for speed (*Figure 4.6*) as we were basically predicting the same value throughout the entire memory period.

Taking the correlation between each neuron's kernels we calculated for each recording session an histogram of kernel correlations (*Figure 4.13 a and b*). Doing so we found that, for the majority of the neurons in all sessions, the kernels were negatively correlated (0.63 ± 0.08SD mean session proportion of neurons with negative correlation coefficient between both kernels). Taking the correlation between the full vectors of coefficients (not split into each neuron's kernel) yielded consistent results (*Figure 4.13 c*) with a mean correlation coefficient of -0.39 $\pm$ 0.16SD across all sessions. The sign of the correlation doesn't have a biological meaning here, as it is dependent on the values used to encode both trial types when predicting trial identity, the relevant fact was if they were, or not, correlated.

Even in the trials with a shorter memory period, where there was less space for the speeds to diverge, as the animal sped up or slowed down, depending on if they were in a correct rejection or hit trial, there was a clear speed difference between the two trial types in the portion of the memory period closer to the stopping area (*Figure 2.6*). In this segment of the trial one should have been able to discern trial identity quite well just by being able to predict the speed at which the mice were running. The correlation observed between the coefficients of our models, when predicting speed and trial identity, were much probably related with this correlation between speed and trial type, which, as we've showed in *Chapter 2*, serves no necessary behavioral function.

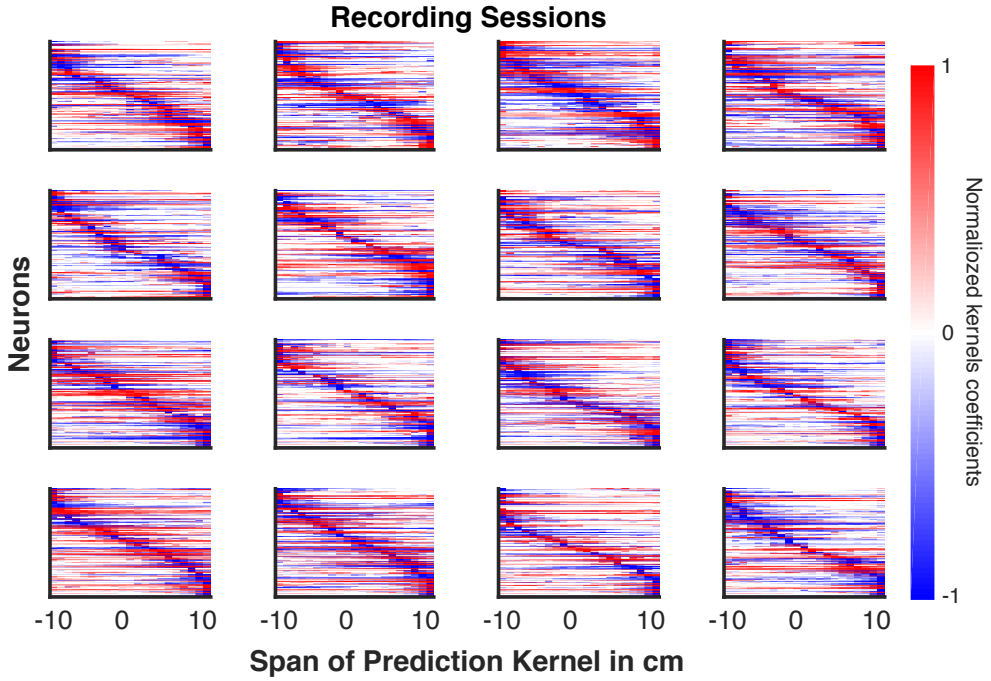

Figure 4.13: Trial Identity Prediction Kernels Coefficients : Coefficients of the 21 × 1 bins trial identity prediction sliding Kernels for all neurons, in all sessions, sorted by position of their center of mass. For visualization purposes kernels were normalized so that all coefficients would be between -1 and 1 but maintained their original sign. Neurons with the center of mass in the past (negative X axis values) can be think of as retrospectively encoding an estimation of trial identity. Neurons with the center of mass in the future (positive X axis values) can be think of as prospectively encoding an the estimation of trial identity.

How much of our ability to predict trial identity was derived from predicting speed? Did the neurons carry independent representations of both variables, with our models picking up an existent but unnecessary correlation, or was our ability to decode speed and trial identity inextricably related? To further investigate this we predicted speed and trial identity in three different 15 cm trial segments, in the beginning, middle and end of the memory period (*Figure 4.14 a*), with the objective of comparing the

coefficient kernels in stretches of the memory period where the extent of the separation between the speed trajectories in the two trial types was different.

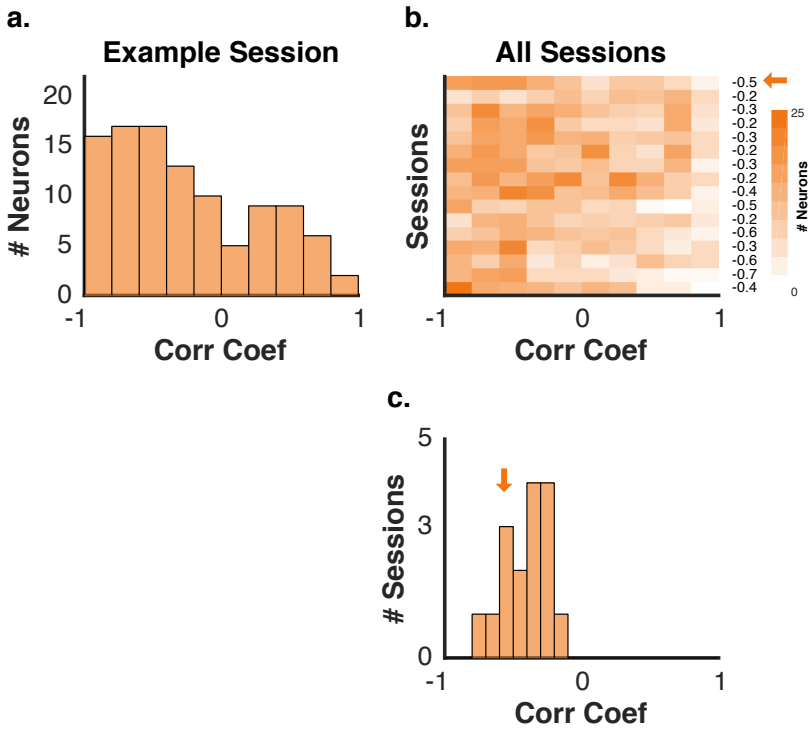

Figure 4.14: Speed and Trial Identity Prediction Kernels Comparison : (a) Histogram of the cross correlation coefficients between each neuron speed and trial identity prediction sliding kernel for a given example session. (b) Same as in (a) but now color coded for all sessions. Numbers on the right of the plot are the cross correlation coefficients between each session full vector of coefficients for speed and trial identity prediction. (c) Histogram of the cross correlation coefficients between each session full vector of coefficients for speed and trial identity prediction.

By doing so we first found that our ability to predict speed and trial identity was maximal at segment 3, the one closest to the stopping area (*Figure 4.14 b*), but that we were still able to predict both quite well in the the first and intermediate segments (mean session R^2 of 0.49 $\pm$ 0.1SD , 0.49

± 0.12SD and 0.67 ± 0.08SD for segments 1,2 and 3, respectively; mean AUC of 0.91 ± 0.11SD, 0.93 ± 0.1SD and 0.96 ± 0.09SD for segments 1,2 and 3, respectively).

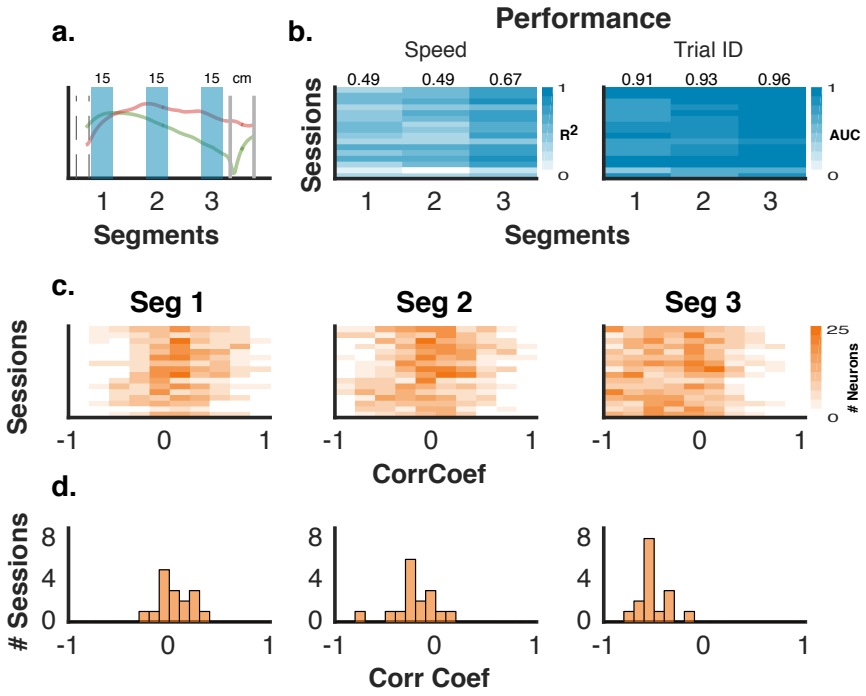

Figure 4.15: Speed and Trial Identity Prediction in Different Segments of the Trial : (a) Using the same sliding kernel approach speed and trial identity were predicted independently for three different 15 cm segments of the trials. (b) Left: Speed prediction model performance in the three different segments quantified as R^2. Right: trial identity prediction model performance in the three different segments quantified as AUC. For both the number on top of the plots are the mean performances of the model across sessions in each segment. (c) Same as in (b) of Figure 4.12 but now for the three different segments. (d) Same as in (c) of Figure 4.12 but now for the three different segments.

Importantly, we also found that the correlation between the speed and trial identity models' coefficients covaried with the separation between both trial types speed trajectories (*Figure 4.14 c and d*). From segment 1 to seg-

ment 3 the way our models decoded, from the population activity, speed and trial identity went from being largely uncorrelated to becoming negatively correlated (mean proportion of neurons per session with kernel correlations between -0.2 and 0.2 of 0.43 ± 0.07SD, 0.4 ± 0.07SD and 0.32 ± 0.07SD and mean sessions coefficients' vectors correlations of 0.04 ± 0.15SD, - 0.2 ± 0.2SD and -0.5 ± 0.13SD for segments 1, 2 and 3, respectively), following the increase in difference between the speeds in hit and correct rejection trials.

It is thus possible to decode, from the simultaneous activity of an ensemble of neurons in the mouse mPFC, a stable cognitive representation that is not being driven by sensory stimuli nor overt motor actions: there is no task relevant sensory cue in the memory period and trial identity can be decoded, in a fairly independent way, from the speed of the animals, a motor variable that reflects an whole body engagement and leaves little room for other memory bridging behaviors.

4.5 Discussion

As we saw in *Chapter 3* (*Figure 3.9*, *Figure 3.12* and *Figure 3.13*) motor activity, measured as the speed at which the mice ran on the treadmill, had a substantial influence in the neural activity we recorded. Speed was freely determined by the animals at every moment of every trial and so, even if mean trial specific patterns existed, it was only possible to completely understand how it was being encoded in the neural activity by looking at the relation of the two variables continuously in a single trial basis. We were able to do so by leveraging on the simultaneous activity of the neuron ensembles we recorded in each session.

Applying a rather simple linear model (*Figure 4.1*) to all the trials of each session we were able to decode the speed at which the animals were running for the total trial length (*Figure 4.2* and *Figure 4.3*). The performance of our model wasn't just related with distinguishing the speeds coming from the two different trial types, as can be seen from the R^2s calculated separately for hit and correct rejection trials, nor with predicting the mean patterns of activity in each of the trials, demonstrated by the shuffle controls in *Figure 4.4*. Activity in the mPFC possessed, thus, enough movement related information for it to be possible to decode the speed of the mice at each cm of each trial.

The presence of motor neural correlates in the mPFC has been documented before (e.g *Cowen and McNaughton, 2007* [4] and *Euston and McNaughton, 2006* [9]), but speed related neurons or activity, though found, are normally discarded or controlled so not to act as confounds for other

variables of interest like location [10] or strategic decisions and prospective direction choice [23]. *Lindsay et.al, 2018* [14] didn't find strong representations of velocity when specifically looking at the influence of motor patterns in the mPFC. Crucially, though, their observations took place in small and closed environment and in the context of spontaneous behavior, with the animals not being engaged in a particular task. Considering that the mPFC is an high order area, involved in combining meaningful streams of information to guide behavior [8], it should be expected for it to encode information important in the context of solving a specific problem or exercise. In our task forward linear movement was the only behavior through which mice could navigate the environment and speed modulation the way to implement different goal oriented strategies. It makes then sense for speed related information to be found in the mPFC of the animals.

The functional significance of such representation cannot be established in the context of our work here, but given what is known about the area and what we observed in our data some hypotheses might be discussed. The mPFC has been implicated more in monitoring and controlling than directly generating behavior [21] [19], maintaining representations of past behavioral and environmental features [17], accordingly our neurons seem to preferentially encode information about the past rather than of the future movements of the animals (*Figure 4.7* and *Figure 4.8*). These online representation of the behavior might be useful in terms of keeping track of a set of necessary actions leading to a desired goal [15] or in providing a feedback signal that can be used for state estimation, if we look at it in the context of a motor control problem [30].

We also found that the neurons cared more about changes than constant values of speed (*Figure 4.7*). If one thinks about what the animals have to accomplish accelerations and decelerations are the *de facto* actions they have at their disposal to implement selected strategies. Looking at the speed patterns, in average or at the single trial level (*Figure 2.4* and *Figure 2.6*), what defines them, in each condition, are not so much the actual values of speed at which their are completed but their specific shapes, determined by the acceleration - deceleration patterns of the animals. If the mPFC is keeping track of the mice's behavior, in order to situate it in the context of a general strategy being implemented, it makes sense for it to represent its actual purposeful actions, and not just the speed at which they are being executed.

In the context of its general role in cognitive control [18] [25] the mPFC has been studied in situations where automatic and impulsive behaviors have to be modulated. To anticipate these scenarios, and intervene when necessary, activity in the area has, presumably, to keep a representation of what the subject is doing in the context of a given task or problem. Our task is simple and it's not clear, given what it's hypothesized to be the area's function, if its demands would engage it. One way to start addressing this question would be to zoom in around specific trial segments and verify if neurons shift from retrospective to prospective encoding of the mice behavior, signaling an involvement of the mPFC in generating behavior. Candidate segments would be when the tones are played (particularly the stop sound, where animals have to withhold the licking response and continue running) and the stopping area where, in the case of hit trials, animals have to com-

mit to stopping and, in correct rejections, inhibit the attractive pull of this behavior (the reward associated response). We plan to perform this analysis in the near future.

We fitted the coefficients associated with the bins of the sliding kernel used to predict speed at each cm of each trial (*Figure 4.1*), consequently, all speed values were decoded the same way. This assumed that speed encoding in the mPFC was universal and didn't depend on contextual factors, something to be more expected from a primary motor area. Our model performs better in hit than correct rejection trials (*Figure 4.2*). Such observation might mean that neurons in the area are more engaged by trials to which the prospect of reward confers added importance, akin to what was observed by *Cowen and McNaughton, 2007* [4]. Another possibility is for the enhanced performance to be related to the fact that hit trials have more acceleration - deceleration periods than correct rejections, with these, as described before, being better represented by the neurons. Predicting speed separately for each of the conditions yielded consistent results and showed that even with a dedicated model speed is less decodable in correct rejection than in hit trials (*Figure 4.9*).

The mPFC has been described to encode the same features in a different way depending in the context in which they are encountered [11]. Our results, concerning the encoding of speed, show that while fitting separate models to different trials types, and different segment sections, improves our results(*Figure 4.9*), thus pointing to some context dependency, such improvements are not dramatic, with a fair degree of speed related information seemingly present in the same format through different task contexts. Our

exploration of this issue is coarse, especially in what concerns different task epochs, a better description of how speed encoding varies with context would need a more detailed analysis.

Apart from the behavioral strategy followed by the mice the other outstanding feature of our task was its memory guided component. Using an analogous approach to the one used to decode speed (*Figure 4.10*) we were able to classify, at each cm of each trial after the sound, the identity of the respective trial (*Figure 4.11 and Figure 4.12*). Because we just used correct trials in our analysis it was not possible to discern what information was used to differentiate between trial type (sound or decision) but, irrespective of the memory content, its representation was stably decodable, in the same way, during the entire memory period.

As when using dPCA, also here the WM representations continued active past the moment in which the mice stopped to collect reward (in hit trials) or successfully crossed the area without stopping (in correct rejection trials). Such indicates that the mPFC is not just involved in keeping information within the scope of one trial, but also in carrying it past its most immediate usefulness, bridging temporally dissociated contexts (or trials, in the case of the task).

In our task, and after the presentation of the auditory cue, neurons in the mPFC simultaneously encoded, in each trial, the speed at which the mice were running on the treadmill and the identity of the respective trial. Multiplexed encoding of task variables by ensembles of neurons in the mPFC has been consistently reported [1][23][17] before. In both trial types (hits and correct rejections) mice adopted different speed strategies that became more

and more different as the animals approached the area and prepared to stop. When we decoded trial type were we really decoding a cognitive internally sustained representation or, as it as been described before [9] [4], were we merely picking up neural signals reflecting different behavioral patterns? The relation between mean condition speed strategies was not constant, varying in signal and amplitude throughout the trial (*Figure 2.6*), despite so we were able to decode trial identity in a stable way, which seemed to indicate that the former was not crucially dependent on the later. Looking at the correlations between both the kernels of individual neurons and the vectors of coefficients from each session, resulting from predicting speed and trial identity, we confirmed this first indication (*Figure 4.15*). Hence, although the behavioral differences could in fact be picked up by the model, leading to a correlation between predicting speed and trial identity (*Figure 4.14* and *Figure 4.15*), this was not a necessary condition for successful prediction of the later. It was possible to predict trial identity, in a way that was largely uncorrelated with predicting speed, in a trial segment (just after the sound) where speed strategies were similar between hit and correct rejection trials.

Taking advantage of our simultaneous ensemble recordings to relate neural activity to behavioral and cognitive variables we discovered that neurons in the mice mPFC encoded, in each trial and in a multiplexed way, both an ongoing representation of its momentaneous behavior (speed) and a stable internally generated representation that could be used to guide behavior (trial identity). Both variables could be decoded in uncorrelated way, which provides evidence that trial identity representation was not anchored on differences in speed behavior and suggests that they can be read, independently

from each other, by other brain regions or networks.

References

[1] E. H. Baeg et al. "Dynamics of population code for working memory in the prefrontal cortex." In: *Neuron* 40 (1 Sept. 2003), pp. 177–188 (cit. on pp. 137, 170).

[2] G. Buzsáki. "Large-scale recording of neuronal ensembles." In: *Nature neuroscience* 7 (5 May 2004), pp. 446–451 (cit. on p. 136).

[3] M. M. Churchland et al. "Techniques for extracting single-trial activity patterns from large-scale neural recordings." In: *Current opinion in neurobiology* 17 (5 Oct. 2007), pp. 609–618 (cit. on p. 136).

[4] S. L. Cowen and B. L. McNaughton. "Selective delay activity in the medial prefrontal cortex of the rat: contribution of sensorimotor information and contingency." In: *Journal of neurophysiology* 98 (1 July 2007), pp. 303–316 (cit. on pp. 138, 155, 166, 169, 171).

[5] S. A. Deadwyler and R. E. Hampson. "The significance of neural ensemble codes during behavior and cognition." In: *Annual review of neuroscience* 20 (1997), pp. 217–244 (cit. on p. 136).

[6] R. J. Douglas and K. A. Martin. "Opening the grey box." In: *Trends in neurosciences* 14 (7 July 1991), pp. 286–293 (cit. on p. 136).

[7] J. Duncan. "An adaptive coding model of neural function in prefrontal cortex." In: *Nature Reviews. Neuroscience* 2 (11 Nov. 2001), pp. 820–829 (cit. on p. 137).

[8] D. R. Euston, A. J. Gruber, and B. L. McNaughton. "The role of medial prefrontal cortex in memory and decision making." In: *Neuron* 76 (6 Dec. 2012), pp. 1057–1070 (cit. on p. 167).

[9] D. R. Euston and B. L. McNaughton. "Apparent encoding of sequential context in rat medial prefrontal cortex is accounted for by behavioral variability." In: *The Journal of neuroscience* 26 (51 Dec. 2006), pp. 13143–13155 (cit. on pp. 138, 166, 171).

[10] V. Hok et al. "Coding for spatial goals in the prelimbic/infralimbic area of the rat frontal cortex." In: *Proceedings of the National Academy of Sciences of the United States of America* 102 (12 Mar. 2005), pp. 4602–4607 (cit. on pp. 137, 138, 155, 167).

[11] J. M. Hyman et al. "Contextual encoding by ensembles of medial prefrontal cortex neurons." In: *Proceedings of the National Academy of Sciences of the United States of America* 109 (13 Mar. 2012), pp. 5086–5091 (cit. on pp. 137, 138, 169).

[12] G. B. Keller, T. Bonhoeffer, and M. Hfffdfffdbener. "Sensorimotor mismatch signals in primary visual cortex of the behaving mouse." In: *Neuron* 74 (5 June 2012), pp. 809–815 (cit. on p. 138).

[13] C. C. Lapish et al. "Successful choice behavior is associated with distinct and coherent network states in anterior cingulate cortex." In: *Proceedings of the National Academy of Sciences of the United States of America* 105 (33 Aug. 2008), pp. 11963–11968 (cit. on p. 137).

[14] A. J. Lindsay et al. "How Much Does Movement and Location Encoding Impact Prefrontal Cortex Activity? An Algorithmic Decoding Ap-

proach in Freely Moving Rats." In: *eneuro* 5 (2 2018) (cit. on pp. 138, 167).

[15] L. Ma et al. "Tracking Progress toward a Goal in Corticostriatal Ensembles". In: *Journal of Neuroscience* 34.6 (Feb. 2014), pp. 2244–2253 (cit. on pp. 137, 167).

[16] C. K. Machens, R. Romo, and C. D. Brody. "Functional, But Not Anatomical, Separation of "What" and "When" in Prefrontal Cortex". In: *Journal of Neuroscience* 30.1 (Jan. 2010), pp. 350–360 (cit. on p. 137).

[17] S. Maggi, A. Peyrache, and M. D. Humphries. "An ensemble code in medial prefrontal cortex links prior events to outcomes during learning". In: *Nature Communications* 9.1 (June 2018) (cit. on pp. 137, 167, 170).

[18] E. K. Miller. "The prefrontal cortex and cognitive control." In: *Nature reviews. Neuroscience* 1 (1 Oct. 2000), pp. 59–65 (cit. on p. 168).

[19] E. K. Miller and J. D. Cohen. "An integrative theory of prefrontal cortex function." In: *Annual review of neuroscience* 24 (2001), pp. 167–202 (cit. on p. 167).

[20] S. Musall et al. "Movement-related activity dominates cortex during sensory-guided decision making". In: (Apr. 2018) (cit. on p. 138).

[21] N. S. Narayanan and M. Laubach. "Top-Down Control of Motor Cortex Ensembles by Dorsomedial Prefrontal Cortex". In: *Neuron* 52.5 (Dec. 2006), pp. 921–931 (cit. on p. 167).

[22] C. M. Niell and M. P. Stryker. "Modulation of visual responses by behavioral state in mouse visual cortex." In: *Neuron* 65 (4 Feb. 2010), pp. 472–479 (cit. on p. 138).

[23] N. J. Powell and A. D. Redish. "Complex neural codes in rat prelimbic cortex are stable across days on a spatial decision task." In: *Frontiers in behavioral neuroscience* 8 (2014), p. 120 (cit. on pp. 137, 138, 167, 170).

[24] J. Qian et al. *Glmnet for Matlab*. 2013. URL: http://www.stanford.edu/~hastie/glmnet_matlab/ (cit. on pp. 140, 143).

[25] K. R. Ridderinkhof et al. "Neurocognitive mechanisms of cognitive control: the role of prefrontal cortex in action selection, response inhibition, performance monitoring, and reward-based learning." In: *Brain and cognition* 56 (2 Nov. 2004), pp. 129–140 (cit. on p. 168).

[26] M. Rigotti et al. "The importance of mixed selectivity in complex cognitive tasks". In: *Nature* 497.7451 (May 2013), pp. 585–590 (cit. on p. 137).

[27] A. B. Saleem et al. "Integration of visual motion and locomotion in mouse visual cortex." In: *Nature neuroscience* 16 (12 Dec. 2013), pp. 1864–1869 (cit. on p. 138).

[28] E. Spaak et al. "Stable and Dynamic Coding for Working Memory in Primate Prefrontal Cortex." In: *The Journal of neuroscience* 37 (27 July 2017), pp. 6503–6516 (cit. on p. 137).

[29] M. R. Warden and E. K. Miller. "The representation of multiple objects in prefrontal neuronal delay activity." In: *Cerebral cortex (New York, N.Y. : 1991)* 17 Suppl 1 (Sept. 2007), pp. i41–i50 (cit. on p. 137).

[30] D. M. Wolpert and Z. Ghahramani. "Computational principles of movement neuroscience." In: *Nature neuroscience* 3 Suppl (Nov. 2000), pp. 1212–1217 (cit. on p. 167).

Chapter 5

General Discussion

5.1 Objective

Functionally, WM refers to the general process through which the brain is able to maintain sustained in time active representations [14]. Such ability is the backbone of high level cognition, allowing subjects to "glue" events, contingencies, and sequences of actions in time, this way enabling planning and goal directed behaviors [15]. This pivotal role in complex behavior made establishing its neural basis a priority of neuroscience research.

Mechanistically WM is also an interesting process [9] [4] [29]. It's rather intuitive to imagine, and study, how and why neural activity is driven by immediate environmental input or body output, but its harder to conceptualize, and investigate, the means by which neurons keep an active representation in the absence of external direct influence.

Our project aimed to contribute to the ongoing effort of illuminating the subject by exploring how neural activity in the mice mPFC was involved in the completion of a WM guided task. By recording the simultaneous activity of populations of neurons, while, at the same time, minutely and precisely quantifying the animal behavior, we hoped to be able to disentangle, characterize and understand better the multivariate activity of the area and the way WM information and other relevant task variables were encoded and related.

5.2 Properties of Recorded Neurons

While the emphasis, when using multi-site electrodes to perform extracellular electrophysiology, is normally put on the ensemble based analysis the simultaneous recorded neurons allow, a necessary, but least recognized advantage, is the fast collection of a high yield of individual cells. A coarse description, and quantification, of the dozens of neurons we typically recorded from, in each session, revealed a scenario of heterogeneous response patterns and diffuse tunning to multiple task features. Such is not strange as it is the hallmark of areas in hierarchically high and integrative positions [22][1], like the primate dorsolateral PFC, an area heavily involved in WM dependent behaviors [15] [16], of which the mice mPFC is believed to be homologous [19], or at least share analogous functions[30].

The recorded neurons were typically engaged by the task, with a good proportion having their FR modulated by one or more events and/or showing condition selectivity during the memory period. Curiously, contrary to what others observed [12], almost one third of the neurons were selective for the entire memory period. It's important to note here, though, that these were not, in their majority, classic sustained elevated activity cells, with the selectivity, as we calculated it, simply representing significant difference in FR. It is also worth noting that both the response to specific events, and the memory period selectivity results, were influenced by the continuous dynamic modulation of activity produced by the temporal integration of the responses to specific task features with the mice movement: animals were constantly running and stopping, accelerating and decelerating, with seldom any time for the activity to stabilize.

5.3 Multiplexed Representations

Even if it was difficult to make sense of the averaged response profiles of the mPFC neurons recorded during the task, it was rather probable that mixed [27][28] on them were several layers of task and behavioral relevant information only decodable at the population level. Using both a targeted dimensionality reduction technique [6], dPCA[20], and simple linear models (linear and logistic regression [18]), we were able to decode, from the joint activity of the neurons, multiplexed representations of WM sustained information, the speed at which the mice ran on the treadmill and a signal seemingly related to their engagement while solving the task.

Because of the very few mistakes committed by the animals, it was not possible to run dPCA on the activity of the simultaneously recorded neurons in each session. Nevertheless, we were able to apply it to the averaged joint activity of neurons pooled from several sessions [20]. Also, due to the same reason, when decoding information, at single trial level, using linear and logistic regression, we applied the models only to correct trials (hits and correct rejections).

5.3.1 Working Memory

Even not taking advantage of the full potential of our data, dPCA revealed that, as necessary for an area presumed to be involved in using WM to organize and guide behavior, the mice mPFC encodes, in a stable way and during the entire memory period, both a retrospective representation of the sound played and a prospective representation of the to be performed action.

Using logistic regression we confirmed that, in each trial and throughout the entire memory period, it was possible to decode the identity of the trial the mice were performing (hit or correct rejection). However, because we only analysed correct trials it was not possible to identify what information and when was being encoded.

In delayed response tasks [8] the cue immediately reveals the to be performed response, consequently, it's not possible to discern which information, stimulus or decision, are the animals using to solve the task and it's not straightforward to understand what is being stored in the activity of the neurons [13]. In our task dPCA revealed that both are represented in a quite stable way for the entire length of the delay period, even decision, which representation, in delayed response tasks with a fixed duration memory period, has been described to, sometimes, only be reactivated closer to the response moment [31]. The fact that we don't observe the same might be related to our variable length memory periods, but might also be influenced by our decision to put together trials from all different sound start locations. Applying dPCA separately to the different sound start trials would, possibly, have revealed different patterns of decision encoding in WM.

What is the function and nature of these memory representations? We proved, to the extent that our data allowed us, that the mice were not using speed based behavioral strategies to bridge the cue free delay, and a cognitive representation was necessary for good task performance. In the mouse the mPFC is a good candidate for the place where such representations could be useful in guiding behavior [15][7] and, accordingly, we found that the joint activity of the area, both in average and that the single trial level,

contained trial type selective information during the delay. This ability to decode memory was seemingly not dependent on the activity of one, or a few, selective and reliable neurons as, per session, an average of 0.4 ± 0.04 SD of the recorded neurons was necessary to account for 0.8 of the total sum of the model loadings (data not shown). Also, the encoding didn't seem to be drastically dynamic as we were able to predict trial identity, with the same model, throughout the entire memory period. Our sliding kernel approach to decoding makes this conclusion not completely clear, however. Both mentioned questions would thus benefit from a more thorough analysis: such as fitting different models with an increasing numbers of cells and comparing the evolution of the performances, for the first, and checking how well could we decode trial type in one segment of the trial with a model fitted in a different segment, for the second.

The observed memory selectivity seemed to, effectively, represent a cognitive function and not be the product of behavioral differences in the memory period, as previously reported in the context of other delayed response tasks[5][11]. Different speed strategies existed between trial types in our task, but, the same way they were not necessary for the mice to solve the task, they were also not essential for our ability to decode environmentally absent information during the memory period. This was already suggested by the constant nature of the memory representations, both in the dPCA components as in the logistic regression prediction (by opposition to the dynamical nature of the difference between trial type specific speeds), but was confirmed by the fact that both speed and memory could be decoded from the neural activity, in a fairly independent way.

Despite of their nature, the function and need of the WM representations for task performance is not clear and further investigation would first need to test the whole area involvement by inactivating it chemically or optically. But even if we can only speculate about the necessity of the memory encoding we observed, one thing we can say, according to the dPCA results, is that its presence doesn't mean that animals won't make mistakes: both for sound and decision the representations, in correct and incorrect trials, are seemingly indistinguishable. The reason for the mice mistakes doesn't seem, thus, to lie in a lack of memory guidance.

When one thinks about WM it generally thinks about memorizing a piece of information between two defined points of interest, or maybe the putative underlying mechanism with a neuron that elevates its discharge rate between a cue and an action. But if we see WM as the underlying mechanism of keeping representations active in time and allowing reality to be bond together, there's no intrinsic reason for information to be discarded the moment it is used. Both in the first dPCA components, for sound and decision, as in the trial identity decoding, with logistic regression, the active representations didn't collapse with the mice stopping (or safely crossing the area) but continued through the ITI and presumably into the next trial. This has been showed before [26] and may serve several useful functions, like keeping track of previous outcomes, and courses of actions, and binding together events in causal chains [23].

5.3.2 Movement

Movement on the wheel was the way mice had to express their choices and strategies in the task. If a fundamental role of the PFC is to coordinate goal oriented behavior [15] [10] then, in the context of our task, movement was the most important variable it had to work with. Accordingly, speed on the wheel was strongly represented on the neural activity we recorded. Just by clustering trial types, according to specific speed strategies, we were able to explain a significant amount of the total variance of the data in both trials in which the animals stopped, or not. Also, movement related variance, picked up by the sound and decision components, is one of the possible explanations for why, in our task, and contrary to others [20], the variance explained, in the dPCA analysis, it's much more divided between all parameters, instead of mainly concentrated on the condition free one. Movement's relevance was further confirmed by our ability to decode speed at every point of each trial, which, given the trial to trial variability of the mice speed strategies, was the only way to understand its true relation with the neural activity [3].

As mentioned, changes of speed were the way mice had to express their actions on the wheel and their encoding in the mPFC might have been related to the region's role in organizing and controlling behavior. Recent evidence, however, has shown that movement related activity is pervasive in the mouse cortex during sensory-guided decision making [25], raising questions about the regional, and encoding, specificity of the speed signal we observed. In the current impossibility of directly comparing recordings from

distinct brain regions we can look at how the way speed is encoded in our recordings relates to the putative functions of the mPFC.

The facts are not conclusive. From what is known of the area one would hypothesize that, rather than a fine description of speed at every moment, the mPFC would encode more general action related information. Seemingly consistently we observed that the mPFC cares more about changes of movement, the actions mice had their disposal to shape their strategy. Also expected would be for the format and strength of speed encoding to be different in different contexts. The way features are encoded in the mPFC has been shown to be context dependent [17] and differences in the quality of the encoding have been observed with motor representations [5] in relation to different outcome contexts. We could decode speed better in rewarded than in non rewarded trials, which might be a reflection that the mPFC cares more about what the animal is doing when the possibility of reward exists. We also see an improvement, if not huge, in rewarded trials, when decoding speed just after the sound (moment when the identity of trial is given away) compared with decoding it in the entire trial. The same is not true, though, for non rewarded trials where, even if there is no reward involved, one might have expected a better encoding closer to the area, where the speed behavior becomes more relevant. Although we didn't compare it directly, the way speed is encoded in the different mentioned contexts doesn't seem to be radically different. We could decode it quite well, in both trial types, using the same model and decoding it in separate in specific contexts didn't lead to great differences in model performance.

The analysis we do here is coarse, though, and the clarification of these

questions would benefit from more detail: a finer compartmentalization of the contexts, a thorough comparison of the coefficients of the models specifically applied to each of them and cross predicting speed in specific segments with the models generated in others. In a larger scope it would also be quite interesting to compare the characteristics of the movement encoding that we observed in the mPFC with brain regions in different anatomical positions and with different functions.

Assuming a specificity of the speed information we are able to decode another open question is its functional relevance. Our analysis revealed that mPFC activity is tendentiously related with the past movement of the mice and so the region doesn't seem to be directly involved in driving the animals movement at every moment, which would be more expected from a primary motor area. By encoding past actions the mPFC representations might be useful in the context of keeping track of the ongoing behavior of the mice in order to situate in a determined plan or sequence of actions. The mPFC is known to keep representations of past behaviors and be involved in sequential behavior tracking [21]. An interesting possibility, given the proposed role of the PFC in cognitive control [24], is that, in particular task moments, like the vicinity of the area, the region would assume control of the behavior and start encoding the future actions of the animal. To test this hypothesis we plan to zoom in and verify if, in particular trial locations, the temporal relation we observed, between the neural activity and the speed of the animals, is inverted. For that we will need to change the way we bin the neural activity, as doing it in space completely blurs its dynamics when the animals stop in the crucial zone of the reward area.

Here we focused on how the behavior of the mice was encoded in the mPFC, but also important for understanding the region's function, given the spatial character of our task, would be to explore how the area represents space. One interesting future analysis would thus be to try to decode location in the belt from the neural activity.

5.3.3 Task Engagement

Corruption or lack of WM representations don't seem to be the reason why mice committed mistakes: in the memory period of error trials the animals seemingly possessed, based on the dPCA analysis, the same information, about the tone played and the to be performed action, as in correct trials. One possible explanation for the animals' behavior in error trials is that, despite possessing all the relevant information, mice disengaged from the task. Activity in the PFC is a combination of sensory and motor representations with the values and meanings the subjects endow them with [2]. These together form a specific context [10] and give rise to a state of neural activity needed for given behavior. Correct performance of the task is not only dependent on cue and action information but also on the mice internal state.

In our task the strongest signal present in the neural activity, quantified by the variance explained in the the dPCA analysis, was a seemingly tonic, whole trial length, difference between correct and incorrect trials. Such a signal can be interpreted as reflecting something about the mice internal state and being a correlate of behavioral engagement. Further analysis would be needed to understand more about the temporal dynamics of this signal,

such as when does it appear and if it is present in sporadic mistakes or just when the animals go through periods of bad performance. Particularly interesting would also be to decode speed in error trials and understand how the mice engagement affects speed encoding in the mPFC.

Also worth would be a deeper exploration of the comparison between the neural activity in correct and incorrect trials. *Rigotti et.al, 2013* [28], for instance, also found that the PFC of monkeys, in a WM task, encoded the same memory period information both in correct and incorrect trials, but that, during mistakes, the neural activity dimensionality collapsed.

5.4 Final Remarks

In this thesis we developed a new behavioral paradigm to investigate how the neural activity in a high order cognitive brain area, the mice mPFC, is involved in a goal directed, WM dependent, task. Through a careful, and thoughtful, analysis of the behavior we proved that the mice were not resorting to a low level, or automatic, behavioral artifice to solve the task, but actually needed a cognitive representation to guide their behavior. Additionally, we also discovered that the animals chose specific speed strategies in order to seemingly optimize their stop/no stop behavior and minimize the time to the next reward. Such knowledge paved the way for a more meaningful and informed interpretation of the recorded neural signals.

The population activity we recorded, through the use of multi-site silicone probes, showed qualitatively similar properties to equivalent data sets recorded both in primates an rodents. From an heterogeneous population of neurons, with mixed selectivity response profiles, it was possible to decode,

simultaneously, variables reflecting the WM maintenance of stimuli and decisions, the ongoing speed strategy of the animals and a measure of task engagement.

The precise functional relevance of these observations can not be established in the context of our work here but, given the information it encodes, what is known about the area and the problem the animals are solving in our task, it is possible to speculate that the observed mPFC's activity might serve two basic functions: 1. keep a stable WM representation of the present behavioral context or goal (stop, or no stop, trial); 2. monitor the ongoing behavior of the mice (speed) against a representation of the environmental context (location on the belt) with the possibility of intervening, in specific task moments, shifting from reflecting to directly influencing the behavior. The also observed engagement signal can be thought of as an activity background, reflecting internal state, that interacts with other encoded features.

The work laid out here, and the data-set that supports it, can now serve as the base of a deeper, and more precise, investigation. Some of the questions raised can, and should, be further explored, as suggested throughout, with variations, and improvements, of the analysis here performed.

References

[1] C. D. Brody et al. “Timing and neural encoding of somatosensory parametric working memory in macaque prefrontal cortex.” In: *Cerebral cortex (New York, N.Y. : 1991)* 13 (11 Nov. 2003), pp. 1196–1207 (cit. on p. 179).

[2] G. Buzsáki. “Large-scale recording of neuronal ensembles.” In: *Nature neuroscience* 7 (5 May 2004), pp. 446–451 (cit. on p. 187).

[3] M. M. Churchland et al. “Techniques for extracting single-trial activity patterns from large-scale neural recordings.” In: *Current opinion in neurobiology* 17 (5 Oct. 2007), pp. 609–618 (cit. on p. 184).

[4] A. Compte et al. “Synaptic mechanisms and network dynamics underlying spatial working memory in a cortical network model.” In: *Cerebral cortex (New York, N.Y. : 1991)* 10 (9 Sept. 2000), pp. 910–923 (cit. on p. 178).

[5] S. L. Cowen and B. L. McNaughton. “Selective delay activity in the medial prefrontal cortex of the rat: contribution of sensorimotor information and contingency.” In: *Journal of neurophysiology* 98 (1 July 2007), pp. 303–316 (cit. on pp. 182, 185).

[6] J. P. Cunningham and B. M. Yu. “Dimensionality reduction for large-scale neural recordings.” In: *Nature neuroscience* 17 (11 Nov. 2014), pp. 1500–1509 (cit. on p. 180).

[7] J. W. Dalley, R. N. Cardinal, and T. W. Robbins. "Prefrontal executive and cognitive functions in rodents: neural and neurochemical substrates." In: *Neuroscience and biobehavioral reviews* 28 (7 Nov. 2004), pp. 771–784 (cit. on p. 181).

[8] P. A. Dudchenko. "An overview of the tasks used to test working memory in rodents." In: *Neuroscience and biobehavioral reviews* 28 (7 Nov. 2004), pp. 699–709 (cit. on p. 181).

[9] D. Durstewitz, J. K. Seamans, and T. J. Sejnowski. "Neurocomputational models of working memory." In: *Nature neuroscience* 3 Suppl (Nov. 2000), pp. 1184–1191 (cit. on p. 178).

[10] D. R. Euston, A. J. Gruber, and B. L. McNaughton. "The role of medial prefrontal cortex in memory and decision making." In: *Neuron* 76 (6 Dec. 2012), pp. 1057–1070 (cit. on pp. 184, 187).

[11] D. R. Euston and B. L. McNaughton. "Apparent encoding of sequential context in rat medial prefrontal cortex is accounted for by behavioral variability." In: *The Journal of neuroscience* 26 (51 Dec. 2006), pp. 13143–13155 (cit. on p. 182).

[12] S. Fujisawa et al. "Behavior-dependent short-term assembly dynamics in the medial prefrontal cortex." In: *Nature neuroscience* 11 (7 July 2008), pp. 823–833 (cit. on p. 179).

[13] S. Funahashi. "Prefrontal cortex and working memory processes." In: *Neuroscience* 139 (1 Apr. 2006), pp. 251–261 (cit. on p. 181).

[14] S. Funahashi and J. M. Andreau. "Prefrontal cortex and neural mechanisms of executive function." In: *Journal of physiology, Paris* 107 (6 Dec. 2013), pp. 471–482 (cit. on p. 178).

[15] J. M. Fuster. *The Prefrontal Cortex*. Academic Press, 2008 (cit. on pp. 178, 179, 181, 184).

[16] P. S. Goldman-Rakic. "Cellular basis of working memory." In: *Neuron* 14 (3 Mar. 1995), pp. 477–485 (cit. on p. 179).

[17] V. Hok et al. "Coding for spatial goals in the prelimbic/infralimbic area of the rat frontal cortex." In: *Proceedings of the National Academy of Sciences of the United States of America* 102 (12 Mar. 2005), pp. 4602–4607 (cit. on p. 185).

[18] G. James et al. *An Introduction to Statistical Learning*. Springer-Verlag Gmb, Aug. 15, 2013 (cit. on p. 180).

[19] R. P. Kesner and J. C. Churchwell. "An analysis of rat prefrontal cortex in mediating executive function." In: *Neurobiology of learning and memory* 96 (3 Oct. 2011), pp. 417–431 (cit. on p. 179).

[20] D. Kobak et al. "Demixed principal component analysis of neural population data". In: *eLife* 5 (Apr. 2016) (cit. on pp. 180, 184).

[21] L. Ma et al. "Tracking Progress toward a Goal in Corticostriatal Ensembles". In: *Journal of Neuroscience* 34.6 (Feb. 2014), pp. 2244–2253 (cit. on p. 186).

[22] C. K. Machens, R. Romo, and C. D. Brody. “Functional, But Not Anatomical, Separation of "What" and "When" in Prefrontal Cortex”. In: *Journal of Neuroscience* 30.1 (Jan. 2010), pp. 350–360 (cit. on p. 179).

[23] S. Maggi, A. Peyrache, and M. D. Humphries. “An ensemble code in medial prefrontal cortex links prior events to outcomes during learning”. In: *Nature Communications* 9.1 (June 2018) (cit. on p. 183).

[24] E. K. Miller and J. D. Cohen. “An integrative theory of prefrontal cortex function.” In: *Annual review of neuroscience* 24 (2001), pp. 167–202 (cit. on p. 186).

[25] S. Musall et al. “Movement-related activity dominates cortex during sensory-guided decision making”. In: (Apr. 2018) (cit. on p. 184).

[26] N. J. Powell and A. D. Redish. “Complex neural codes in rat prelimbic cortex are stable across days on a spatial decision task.” In: *Frontiers in behavioral neuroscience* 8 (2014), p. 120 (cit. on p. 183).

[27] M. Rigotti et al. “Internal representation of task rules by recurrent dynamics: the importance of the diversity of neural responses.” In: *Frontiers in computational neuroscience* 4 (2010), p. 24 (cit. on p. 180).

[28] M. Rigotti et al. “The importance of mixed selectivity in complex cognitive tasks”. In: *Nature* 497.7451 (May 2013), pp. 585–590 (cit. on pp. 180, 188).

[29] M. G. Stokes et al. “Dynamic coding for cognitive control in prefrontal cortex.” In: *Neuron* 78 (2 Apr. 2013), pp. 364–375 (cit. on p. 178).

[30] H. B. Uylings, H. J. Groenewegen, and B. Kolb. "Do rats have a prefrontal cortex?" In: *Behavioural brain research* 146 (1-2 Nov. 2003), pp. 3–17 (cit. on p. 179).

[31] K. Watanabe and S. Funahashi. "Prefrontal Delay-Period Activity Reflects the Decision Process of a Saccade Direction during a Free-Choice ODR Task". In: *Cerebral Cortex* 17.suppl 1 (Aug. 2007), pp. i88–i100 (cit. on p. 181).

ITQB-UNL | Av. da República, 2780-157 Oeiras, Portugal
Tel (+351) 214 469 100 | Fax (+351) 214 411 277

www.itqb.unl.pt